JOURNAL OF MECHANICAL ENGINEERING

STROJNIŠKI VESTNIK

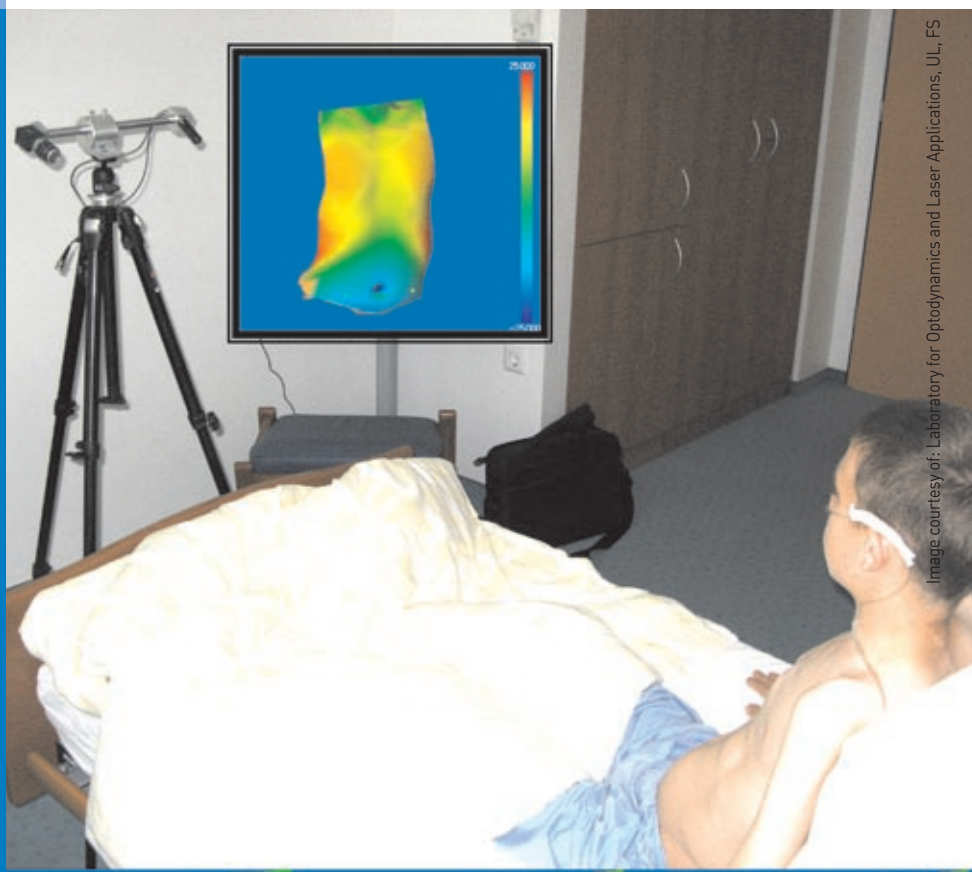

Image courtesy of: Laboratory for Optodynamics and Laser Applications, UL, FS

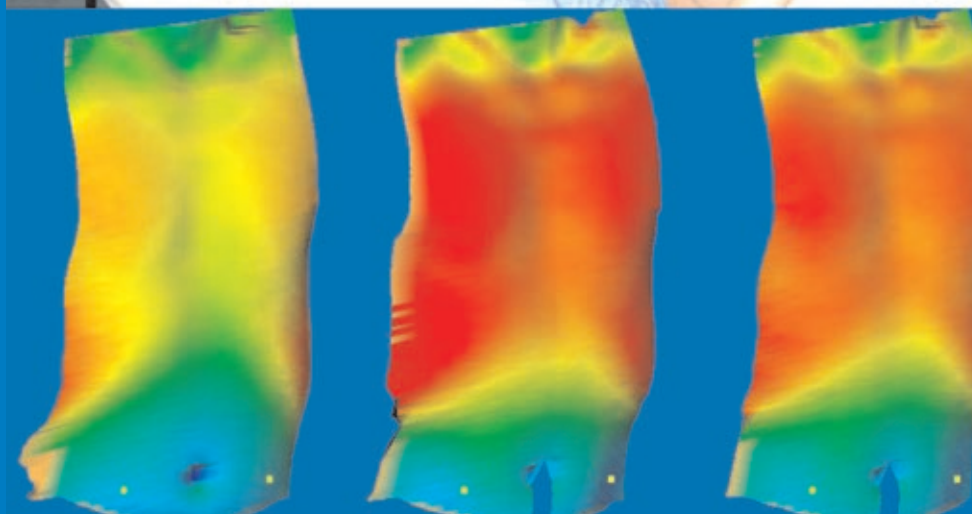

no. 7-8
year 2008
volume 54

Strojniški vestnik - Journal of Mechanical Engineering
ISSN 0039-2480

Editorial Office
University of Ljubljana
Faculty of Mechanical Engineering
Journal of Mechanical Engineering
Aškerčeva 6
SI-1000 Ljubljana, Slovenia
Phone: 386-(0)1-4771 137
Fax: 386-(0)1-2518 567
E-mail: info@sv-jme.eu
http://www.sv-jme.eu

Founders and Publishers
University of Ljubljana
- Faculty of Mechanical Engineering
University of Maribor
- Faculty of Mechanical Engineering
Association of Mechanical Engineers of Slovenia
Chamber of Commerce and Industry of Slovenia
- Metal Processing Association

Editor
Andro Alujevič
University of Maribor, Faculty of Mechanical Engineering
Smetanova 17, SI-2000 Maribor, Slovenia
Phone: +386(0)2-220 7790, E-mail: andro.alujevic@uni-mb.si

Deputy Editor
Vincenc Butala
University of Ljubljana, Faculty of Mechanical Engineering
Aškerčeva 6, SI-1000 Ljubljana, Slovenia
Phone: +386(0)1-4771 421, E-mail: vincenc.butala@fs.uni-lj.si

Technical Editor
Darko Švetak
University of Ljubljana, Faculty of Mechanical Engineering
Aškerčeva 6, SI-1000 Ljubljana, Slovenia
Phone: +386(0)1-4771 137, E-mail: info@sv-jme.eu

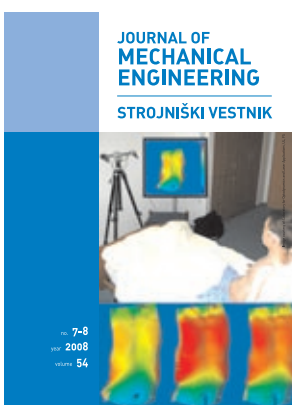

Cover plate: Laser multiple-line triangulation system for real-time 3-d monitoring of chest wall during breathing. The system will help to train the patient how to breath by observing the 3-d image of his chest. Bottom: An example of the rib-cage-dominant breathing pattern. Colors represent different amounts of the chest wall movement. (*Laboratory for Optodynamics and Laser Applications, UL, FS*)

Print
Littera Picta, Medvode, printed in 600 copies

Yearly subscription

companies	100,00 EUR
individuals	25,00 EUR
students	10,00 EUR
abroad	100,00 EUR
single issue	5,00 EUR

SV-JME is indexed in *SCI-Expanded*, *Compendex* and *Inspec*.
The journal is subsidized by the Slovenian Research Agency.

Strojniški vestnik - Journal of Mechanical Engineering is also available on http://www.sv-jme.eu, where you access also to papers' supplements, such as simulations, etc.

Contents

Strojniški vestnik -Journal of Mechanical Engineering
volume 54, (2008), number 7-8
Ljubljana, August 2008
ISSN 0039-2480

Published monthly

Papers

Strojniški vestnik - Journal of Mechanical Engineering 54(2008)7-8, 503-506
UDC 681.786
Paper received: 02.06.2008
Paper accepted: 07.07.2008

Laser Multiple Line Triangulation System for Real-time 3-D Monitoring of Chest Wall During Breathing

Matija Jezeršek[1,*], Matjaž Fležar[2], Janez Možina[1]
[1] University of Ljubljana, Faculty of Mechanical Engineering, Ljubljana, Slovenia
[2] University Clinic Golnik, Golnik, Slovenia

An optical system for 3-D chest wall measuring during breathing is described. The system is based on a laser multiple-line triangulation technique. It uses a CCD camera and a laser that simultaneously projects thirty-three light planes on the measured surface. The accuracy is ±0.5 mm, the measuring range is 400x600x500 mm and the frequency is 80 Hz. The system efficiency was tested by an adult volunteer, who was breathing in two regimes: rib-cage-dominant and abdomen-dominant. The results show the breathing pattern in a graphical and numerical way.

Keywords: breathing measurement, chest wall, laser triangulation, 3-D measurement

0 INTRODUCTION

The measurements of respiratory mechanics during tidal breathing are limited due to the invasiveness of devices used to measure flow of pressures at mouth. Since human breathing is involuntary, all devices which interfere with nasal or oral airway change the pattern of breathing and make tidal volume measurement inaccurate. Currently available devices, such as respiratory inductive plethysmographs, magnetometers, and stretching belts [1-2], are not accurate and produce a lot of artifacts when they are compared to mouth breathing recorded by flow meters. Approximately 10% of adult patients and all children below the age of 5 do not cooperate well with the standard lung function measurements in order to get true respiratory system performance.

The optical methods do not disturb the breathing pattern due to a noninvasive principle of measurement. All known optical methods are limited to measure the chest wall displacement at certain number of predefined points. They are mainly based on laser triangulation [3-4] or stereophotogrametry [5]. Their common drawback is the need to determine the measuring points before signal acquisition. This is done by positioning the measuring sensors or by sticking the photogrametrical markers on the patient's torso.

To avoid the above mentioned problems, we introduced a 3-D laser multiple-line triangulation method. Its novelty is in the measurement of the entire three-dimensional shape of the chest wall at the frequency which is in general limited with the camera frame rate (80 Hz in our case).

Non-invasive methods, such as laser multiple-line triangulation method, will contribute to regular medical work to obtain the lung volumes and changes in lung volumes in real-time without the need of invasive monitoring.

1 MEASURING PRINCIPLE

The main elements of the measurement setup are shown in Fig. 1. The system is based on the multiple-line laser triangulation principle [6]. It consists of a laser projector and a camera. The diode-type laser projector (Lasiris SNF-533L, 20 mW, 670 nm) generates a light pattern of 33 equally inclined light planes directed toward the measured surface, i.e. human chest. The camera records the illuminated surface from a different viewpoint, and consequently, the light pattern is distorted by the shape of the surface (Fig. 2). An ambient light is filtered by a narrow-band interference filter (10 nm FWHM, centered at 670 nm) which is placed between the lens and the camera's CCD sensor. The image contrast is improved consequently.

The measuring apparatus is designed to operate in two modes: high-speed and real-time. In the high-speed mode, the image sequence is acquired first, and the processing is done later. The maximum acquisition frequency is limited to 80 Hz by the camera. In the real-time measuring mode all the processing is done in between two consecutive measurements.

*Corr. Author's Address: University of Ljubljana, Faculty of Mechanical Engineering, Aškerčeva 6, SI-Ljubljana, Slovenia, matija.jezersek@fs.uni-lj.si

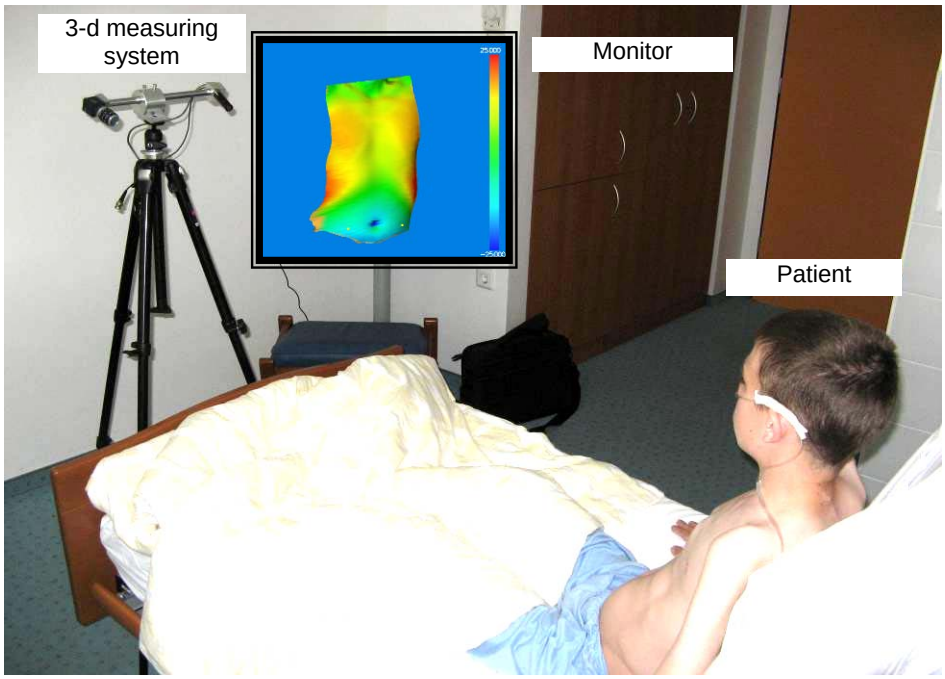

Figure 1: *The graphical breathing assistance based on the laser multiple-line 3-D measuring system*

The processing involves: image processing [7], three-dimensional surface reconstruction [8], shape analysis, and displaying in shaded and color mode, where colors represent different amounts of depth changes at each measurement point. The maximum measuring frequency is lower in the case of the real-time measurement. However, it is still high enough, approximately 25 Hz, if the processing is done on a 3-GHz Pentium processor.

1.1. Calibration and accuracy

The calibration of the apparatus is based on a reference sample: a groove-shaped plate that is measured at various heights. The parameters related to the optical geometry of the apparatus are then numerically optimized until the minimum deviation (the sum of the squared errors) between the measured points and the reference surface is found. The major advantage of this procedure is that all the transformation parameters can be determined in a single measuring step, i.e., the camera's internal parameters (focal length, central point and distortion), the projector's distortion, and the projector's position regarding the camera (rotation and translation). The accuracy of the calibrated apparatus is ±0.5 mm, which is calculated as a standard deviation between points of the measured and nominal reference surface. The measuring range depends on the camera's and projector's lens focal lengths, CCD sensor dimensions, the triangulation angle, and the distance between the laser projector and the camera. In our case, the range is approximately 400×600 mm in width and height and approximately 500 mm in depth.

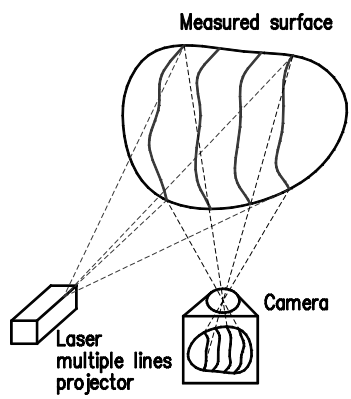

Figure 2: *The measuring principle is based on the laser triangulation with multiple-line illumination*

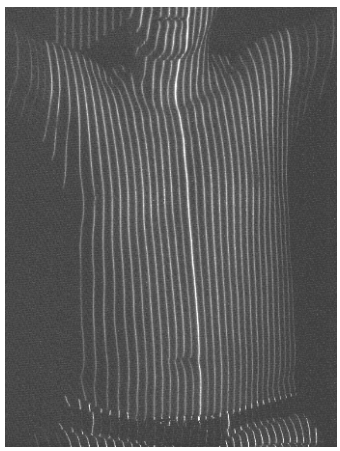

Figure 3: *The image of the volunteer's frontal torso illuminated by the laser multiple-line projector*

2 MEASUREMENT PROCEDURE

To test the monitoring efficiency of the breathing patterns, an adult male volunteer was studied. He was asked to take a normal breath out in the beginning of each measurement cycle. This pose was used as a reference shape for displacement calculation. After that, the rib-cage-dominant breathing and the abdomen-dominant breathing were performed several times.

The patient's chest must be located within the measuring range, which is in a distance between 1,200 mm and 1,700 mm from the apparatus. Its orientation is such that the laser light planes are directed vertically (see Fig. 3). Such orientation produces better visibility of the observed chest area. The adjustment of the right position of the apparatus according to the patient is divided into selecting of the proper distance and orientation. The position is adjusted when the laser lines lie in the central area of the image, and when the observed part of the body – chest – is in the central area of the image.

A custom developed measuring software was used to observe and analyze the three-dimensional chest shape in a real-time. The surface is displayed in the shaded mode and its displacements are shown numerically (waveform) and graphically (colors). In the waveform chart, the values of the selected points are plotted according to the acquisition time. The displacement at the certain point is calculated as a difference between point distances measured at the current and the reference time. It can also be calculated as a distance difference between two points at the same time.

3 RESULTS

The representative time series of images of two 3-D chest shape measurements are shown in Fig. 4. The red and blue colors clearly expose the most active regions. In the upper series the abdomen-dominant breathing was measured and the whole wall moves approximately uniformly outward.

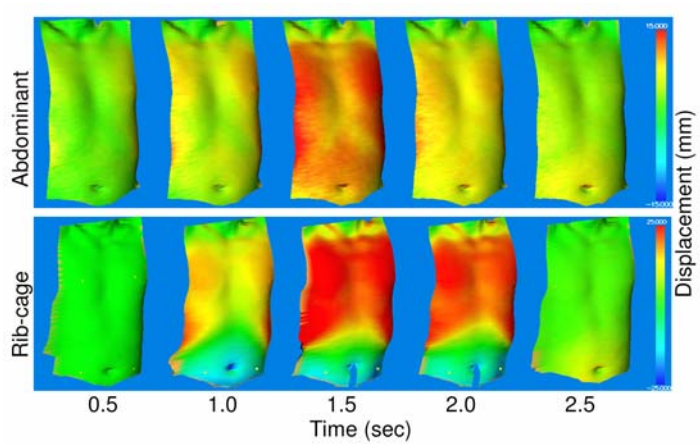

Figure 4: *3-D measurement of the chest wall during two breathing types. The displacements are presented with colors*

The rib-cage-dominant breathing is shown in the bottom series. It can be noticed that the upper chest part moves reasonably outward from the body, and that the bottom part stays in the same position or even goes a little inward.

The displacements of abdominal and rib-cage points were extracted from both measurement examples (see Fig. 5). A dissimilarity can be noticed between both types of breathing again. The tidal period is approx. 2.5 seconds in both examples. The rib-cage emphasized breathing is perhaps more interested due to significant displacements of the chest wall in both directions (Fig. 5b). The rib cage moves outward for ~30mm and the abdominal points move inward for ~15mm simultaneously. In the abdomen-dominant breathing, the maximal displacement is ~20mm for the rib-cage and the abdomen moves for half of that in the same direction.

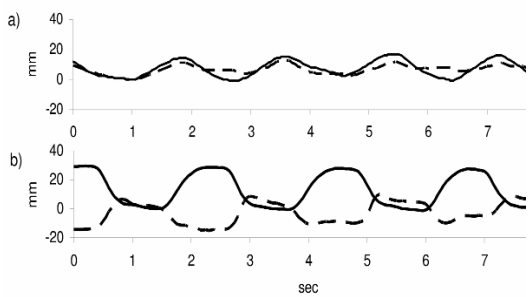

Figure 5: *The waveforms of the rib cage (—) and abdominal (---) displacement in case of: a) abdomen-dominant and b) rib-cage-dominant type of breathing*

4 CONCLUSION

The results of the presented 3-D measuring system demonstrate that it has sufficient accuracy (±0.5 mm), measuring range (400x600x500mm) and frequency (80Hz). The most important features are: the ability to measure the complete chest surface at the same time, the high measuring frequency and non-invasive measurement principle.

The presented technology shows the breathing pattern in a graphical and numerical way. In the future, it will help to train the patient how to breath by observing the image of his chest. We believe that the graphical communication with the patient is much more clear and easy to understand.

The system was developed at the University of Ljubljana, Faculty of Mechanical Engineering as a part of the applied research project L7-9391.

5 REFERENCES

[1] Gilbert, R., Auchinclus, J.H., Brodsky, J., Boden, W. *Changes in tidal volume, frequency, and ventilation induced by their measurement,* J Appl Physiol, 1972, vol.32, p.252-254.

[2] Binks, A. P., Banzett, R.B., Duvivier, C. *An inexpensive, MRI compatible device to measure tidal volume from chest-wall circumference*, Physiol. Meas. , 2007 vol. 28, p.149–159.

[3] Kondo, T., Inocchieri, S., Baldwin, D.N., Nelle, M., Frey, U. *Noninvasive monitoring of chest wall movement in infants using laser*, Pediatr Pulmonol, 2006.

[4] Drummond, G.B., Duffy, N.D., *A video-based optical system for rapid measurements of chest wall movement*, Physiol. Meas., 2001, vol.22, p.489-503.

[5] Groote, A.D., Wantier, M., Cheron, G., Estenne, M., Paiva, M. *Chest wall motion during tidal breathing*, J Appl Physiol, 1997 vol. 83, p. 1531-1537.

[6] Jezeršek, M., Gruden, V., Možina, J, *High-speed measurements of steel-plate deformations during laser surface processing*, Optics Express, 2004, vol.12, no.20, p.4905-4911.

[7] Jezeršek, M., Možina, J., *A Laser Anamorph Profilometer*, Journal of Mechanical Engineering, 2003, vol.49, no.2, p.76–89.

[8] Bračun, D., Jezeršek, M., Diaci, J. *Triangulation model taking into account light sheet curvature.* Meas. sci. technol. , 2006, vol.17, no.8, p.2191-2196.

Strojniški vestnik - Journal of Mechanical Engineering 54(2008)7-8, 507-520
UDC 678
Paper received: 03.04.2007
Paper accepted: 15.05.2008

Tailoring Functionality and Durability of Polymeric Products by Modifying Processing Conditions

Urška Florjančič [1,*] - Igor Emri [1,2]
[1] Center for Experimental Mechanics, University of Ljubljana, Slovenia
[2] Institute for Sustainable Innovative Technologies, Ljubljana, Slovenia

We investigate new possibilities for modifying functionality of polymeric products by changing their material structure during processing and consequently their time-dependent properties, which define the durability of final products. In the first part of the paper we report on significant differences in material structure as observed at atomistic scale due to differences in processing conditions. A short overview of recent studies on multi-scale phenomena in material structure formation is included. Several experimental approaches are proposed for studying the effect of processing conditions on material structure formation and hence, the macroscopic properties of the final polymeric product.

The second part of the paper deals with two questions to be answered, (i) does current industrial polymer processing equipment (in our case extruder) allows processing under such conditions that initiate nonlinearities in the material structure formation processes, and (ii) to what extent can material structure be modified, and consequently the mechanical and other properties of the final polymeric product, by changing the thermo-mechanical boundary conditions (i.e., processing conditions).

We demonstrate that it is possible to modify the functionality of the final polymeric products by modifying the inherent material structure with properly selected processing conditions. We observed that the processing conditions within the range of temperatures and pressures that are typical for industrial extrusion of polymers can be changed so that we can significantly influence the structure formation and consequently the time-dependent mechanical properties of the material in solid state and, as a result, the functionality of the final product. Durability of polymeric products made from such material can be improved by several orders of magnitude! Utilizing this approach opens new possibilities for modifying the functionality of polymeric products and hence better competitiveness in the world market.

Keywords: polymers, structural formation, functionality, durability

0 INTRODUCTION

The quality of polymeric products is defined by their functionality and durability (i.e., long-term stability), which in turn depend on the structure of material in the product. The material structure, which is formed during melt solidification in the polymer processing stage and defines the time-dependent properties of the final product in solid state (i.e., its mechanical and other physical properties), is determined by the initial kinetics (i.e., the molecular structure of material, molecular distribution and molecular topology), and also by thermo-mechanical boundary conditions to which a polymeric material is exposed during a technological process. Optimal selection of the processing conditions ensures appropriate functional properties of the material and its durability.

At this point, a question arises whether it is possible, by changing technological parameters of polymer processing in the industrial environment, to modify the structure of the material and consequently its time-dependent mechanical properties to such an extent that the functionality and durability of final products made of these materials could be improved. Knowing and understanding the effect of the technological parameters (temperature, pressure, humidity, mechanical loading) on the material structure formation which defines the behavior of the final product in solid state (i.e., its mechanical and other physical properties) offers new possibilities for the development of polymer products with improved functionality and durability.

We first discuss significant differences in material structure as observed at atomistic scale due to differences in processing conditions. A short overview of recent studies on multi-scale phenomena in material structure formation is included. Several experimental approaches are

*Corr. Author's Address: Center for Experimental Mechanics, University of Ljubljana, Aškerčeva 6, Slovenia, urska.florjancic@fs.uni-lj.si

proposed for studying the effect of processing conditions on material structure formation and hence, the macroscopic properties of the final polymeric product.

0.1 Multiscale Phenomena in Material Structure Formation

Macroscopic properties of polymeric materials in solid state depend on their inherent structures. Thus, by modifying the structure of materials one may alter their macroscopic properties. The structure formation of polymers evolves over several steps, each beginning with different size and complexity of their building blocks as schematically shown in Fig. 1. This is a highly non-linear process, during which the non-linear multi-scale interactions between the boundary conditions and the inherent molecular rearrangements take place at different time-space scales, forming higher order structures at atomistic scale up to macroscopic dimensions. When materials with appropriately modified initial kinetics [1] and [2] are exposed to certain thermo-mechanical boundary conditions, they can exhibit exceptionally nonlinear (chaotic) behavior [3]. This means that even small changes in boundary conditions may lead to a completely different material structure in the solid state. It becomes evident that changes in boundary conditions at macro-scale can cause changes in material structure at atomistic scale [4] and [5].

As presented in recent study [4] of the proton motion in 'bulk' and in highly drawn 'fiber' polyamide 6 (PA-6) by proton nuclear magnetic resonance (NMR), products manufactured at two different processing conditions exhibit significantly different structure at atomistic level. A striking difference in the molecular dynamics between the slowly cooled 'bulk' sample and the rapidly cooled 'fiber' sample, prepared by spinning and exposed to extreme mechanical straining, was observed as seen in Figs. 2 and 3. These two samples exhibit significantly different thermal properties as well (see Fig. 4).

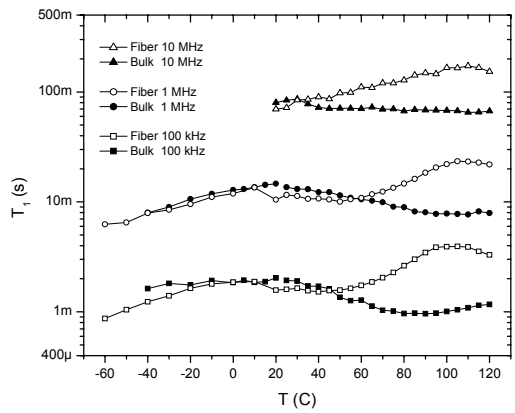

Fig. 2. *Temperature dependence of the spin-lattice relaxation time, T_1, of 'bulk' and 'fiber' PA-6 [4]*

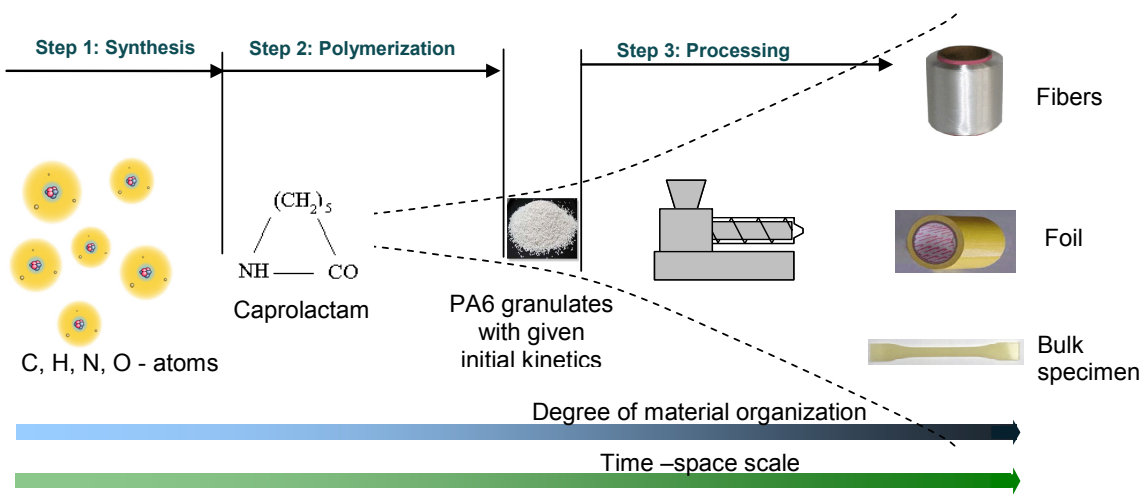

Fig. 1. *Different phases of polymer structure formation [1]*

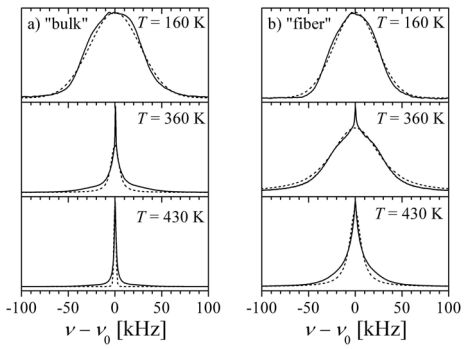

Fig. 3. *Measured (solid line) and calculated (dashed line) proton NMR spectra of (a) 'bulk' and (b) 'fiber' PA-6 [4]*

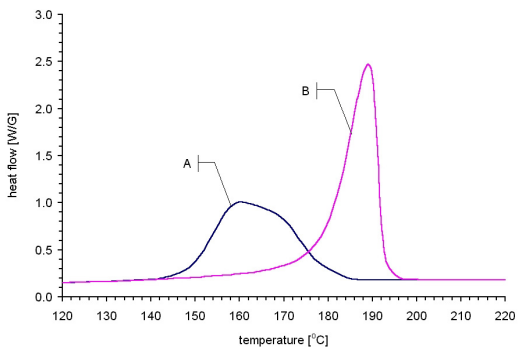

Fig. 4. *DSC measurements of (A) 'bulk' and (B) 'fiber' PA-6. The glass transition and the pre-melting phenomena are shifted to higher temperatures. The onset of melting of 'fiber' samples is shifted for about 50 °C to higher temperatures [4]*

Another example of complex multi-scale processes in the transition from the molten to the solid state is the spinning of polyamide fibers, where the variation of thermo-mechanical boundary conditions take place at about the same time-scale as the structural rearrangements of the molecules. As observed in a recent study [5] of PA-6 fiber structure by electron paramagnetic resonance (EPR), the differences in fiber production process enhance significantly different structures at atomistic level as shown in Figs. 5 and 6. Similarly the modifications in fiber production process enhance significant changes in the shrinking behavior of polyamide 66 (PA-66) fibers [6] (see Fig. 7).

Above presented experimental results correspond to the numerical simulations performed [7] to [10] and the analysis of polyamide structure formation during

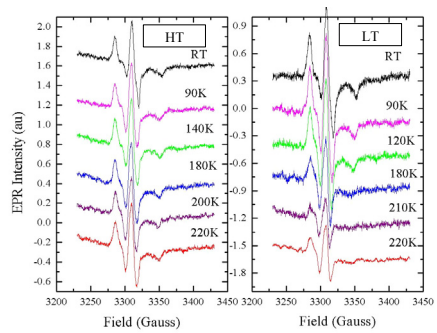

Fig. 5. *Temperature dependences of the electron paramagnetic resonance (EPR) spectra of the 'high tension (HT)' and 'low tension (LT)' nylon 6 fibers [5]*

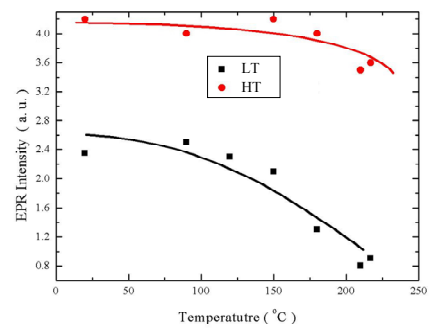

Fig. 6. *Temperature dependences of the intensity of the EPR spectra of the 'high tension (HT)' and 'low tension (LT)' nylon 6 fibers [5]*

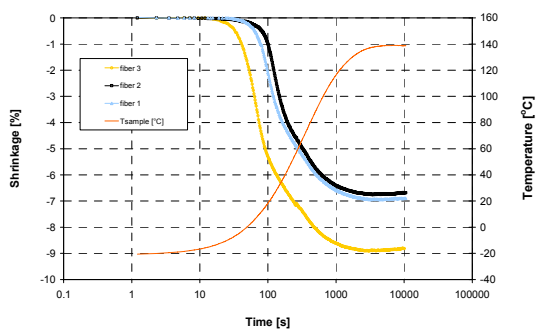

Fig. 7. *Shrinkage of PA-66 fibers subjected to three different manufacturing conditions [6]*

solidification with the aid of positron annihilation [11] and [12]. By applying proper thermo-mechanical boundary conditions (technology) we can therefore modify the material structure, which is the result of nonlinear interactions of the polymer chain reorganization processes at different time-space scales from nano- to macro-scale, thus modifying physical properties of the

material by several orders of magnitude. Similar results are reported by some other research groups in the world [3], [13] to [21].

The recent studies on multi-scale phenomena in material structure formation as presented above show that by changing the material structure we may significantly influence the physical properties and durability (i.e., long-term stability) of final products, which opens new potential for tailoring the functionality of products. Changes in the material structure can be caused by modifying the initial kinetics of the material (i.e., by changing its molecular weight distribution, by adding nanoparticles into polymeric matrix, etc.), and more important, by changing the thermo-mechanical boundary conditions (i.e., technology) to which material has been exposed during processing.

The investigation of the latter, i.e., the effect of processing conditions on the material structure formation, and hence the durability and the functionality of the final product, is discussed in the second part of this paper.

1 THE PRESENT RESEARCH

We investigate whether it is possible, by changing technological parameters of polymer processing in the industrial environment, to modify the structure of the material and consequently its time-dependent mechanical properties to such an extent that the functionality and durability of the final products made of these materials could be improved.

Let us first consider the following questions: (i) which thermo-mechanical boundary conditions cause changes in material structure at which scale, and (ii) which changes in material structure cause which changes of physical properties of the material.

In order to answer these questions, first, a good understanding of the effect of temperature and pressure on the material structure formation is required, and second, we need sophisticated experimental devices for polymer processing and material characterization.

At the *processing level*, such an equipment is a laboratory extruder PolyLab OS (Thermo HAAKE Electron Corporation), see Figure 8, which enables an accurate control of the processing conditions (pressure, temperature, screw speed, torque) along the extruder cylinder during polymer processing, but at the same time this equipment simulates (mimics) the real industrial processing conditions, appropriate for up-scaling. By using this device, the processing conditions within the range of temperatures and pressures that are typical for industrial extrusion of polymers, can be changed so that we can significantly influence the structure formation and consequently the time-dependent mechanical properties of the material and, as a result, the functionality of the final product, as discussed in the present paper. This opens new possibilities for modifying the functionality of polymer products, thus increasing their competitiveness in the global markets.

At the *material characterization level*, the analysis of changes in the material structure and the resulting physical properties of the final product, caused by variations in thermo-mechanical boundary conditions, requires at least three groups of measuring systems, i.e.:

(a) equipment for analyzing the material structure at different observation levels, from atomistic to macro scale; for this purpose several experimental techniques are widely used, i.e., PALS, NMR, EPR, WAXS, SAXS, AFM, TEM, SEM, optical microscopy, thermal methods, etc.;
(b) equipment for analyzing the time-dependent behavior of the material in solid state [22]; such an instrument, i.e., CEM apparatus for relaxation measurement [23] and [24], was recently ranked among ASTM recommendations (guidelines) for polymer testing. Proposed guidelines will be published in »Springer Handbook of Experimental Solid Mechanics« [25];
(c) experimental approach for monitoring the solidification process; several research groups actively work on this subject [16] to [21] and [26] to [30].

This research deals with two questions to be answered, (i) does current industrial polymer processing equipment (in our case extruder) allows processing under such conditions that initiate nonlinearities in the material structure formation processes, and (ii) to what extent can material structure be modified, and consequently the mechanical and other properties of the final polymeric product, by changing the thermo-mechanical boundary conditions (i.e., processing conditions).

2 EXPERIMENTAL APPROACH

For the purpose of the present research we extruded low density polyethylene (LDPE) specimens under different (extreme) processing conditions using a laboratory extruder PolyLab OS (Thermo HAAKE Electron Corporation), see Figure 8, which simulates the real industrial processing conditions, but at the same time this equipment provides a better control of the conditions (pressure, temperature, screw speed, torque) along the extruder cylinder during polymer processing. The changes in the structure of extruded LDPE samples were analysed with different experimental methods with respect to the time-space scale of the structure observation. Optical microscopy was used to analyse the morphological properties, the thermal properties were determined by DSC measurements, and the shear creep measurements were performed to study the time-dependent mechanical behavior of LDPE samples. The proposed approach enabled us to examine the type and the magnitude of the structural changes in polymer product and consequently its mechanical and other properties, which can be achieved by changing processing conditions) in the industrial environment.

The results of this research show that it is possible to change the technological conditions in the range of temperatures and pressures, typical for polymer extrusion in industrial environment, in such extent that we significantly influence the structural formation and consequently the time-dependent mechanical properties of the material, and hence the functionality of the final product. We observe that by changing the processing conditions in the industrial environment the durability of polymer products improves for several orders of magnitude! That opens new possibilities in the field of modifying the functionality of polymer products and hence better competitiveness in the world market.

3 POLYMER PROCESSING

3.1. Material

Low Density Polyethylene (LDPE) OKITEN® 245 S by Dioki was chosen for three reasons: it is the most widespread material in polymer processing technology, it is easy to handle, and does not easily form structures. Should the proposed analysis show that the processing conditions have a significant effect on the structural formation and consequently on the time-dependent mechanical behavior of the final LDPE product, this would mean that the processing technology will influence also other types of polymeric materials which form more complex structures.

3.2. Laboratory extruder

PolyLab OS laboratory extruder by Thermo HAAKE Electron Corporation (see Fig. 8) was used for the production of the LDPE specimens. It is a twin-screw co-rotational extruder with the extrusion part length to screw diameter ratio 40:1. The device allows adaptation of the length of extrusion part barrel to a ratio of 25:1. The machine, consisting of the *driving part* RheoDrive 4 and the *extrusion part* Rheomex PTW 16, operates with a through put rate of 5 kg/h in rpm range of 0–1100 min^{-1}. The maximum operating pressure is 100 bar, the maximum temperature 400°C (the lowest temperature is determined by room conditions), and the maximum torque 129.6 Nm.

Fig. 8. *The PolyLab OS laboratory twin-screw co-rotational extruder (Thermo HAAKE Electron Corporation), consisting of A – RheoDrive 4 and B – Rheomex PTW 16*

3.3 Thermo-mechanical Conditions for LDPE Extrusion

The range of processing parameters that can be changed during polymer extrusion process depends on the extruder capacity and polymer properties. The lower and the upper limit of the temperature tolerance range for LDPE, i.e., 130–270°C, was determined by DSC measurements. During the LDPE material extrusion process, we varied the number of the screw revolutions and the temperature along the extruder barrel. At a certain temperature which was the same on all ten heaters along the extruder barrel, we set the number of screw revolutions, and recorded the pressure value in the melt at the extruder outlet and the torque on both screws during the extrusion process. The tolerance range of the pressure and torque values was ±10%. The next step was to change the number of revolutions and repeat the procedure at the same temperature. At each temperature, the operating range of revolutions was 10–250 min^{-1}.

The operational range of thermo-mechanical boundary conditions under which LDPE can be extruded on the PolyLab OS laboratory extruder is shown in Figs. 9 and 10. During the extrusion, the screw torque reached a critical operating level, and therefore it was taken into account as a key parameter for determining the extreme thermo-mechanical conditions of the LDPE specimen extrusion.

3.4. Specimen Preparation Conditions

Based on the analysis of the thermo-mechanical boundary conditions of LDPE extrusion (see Figs. 9 and 10), we selected four different combinations of processing conditions, illustrating extreme conditions of extrusion, i.e., lowest pressure – lowest temperature, highest pressure – lowest temperature, lowest pressure – highest temperature, highest pressure – highest temperature. The processing parameters defining these conditions are shown in Table 1. Under these conditions, we produced the specimens of extruded LDPE intended for subsequent analysis of their structure formation as the result of these modified processing conditions.

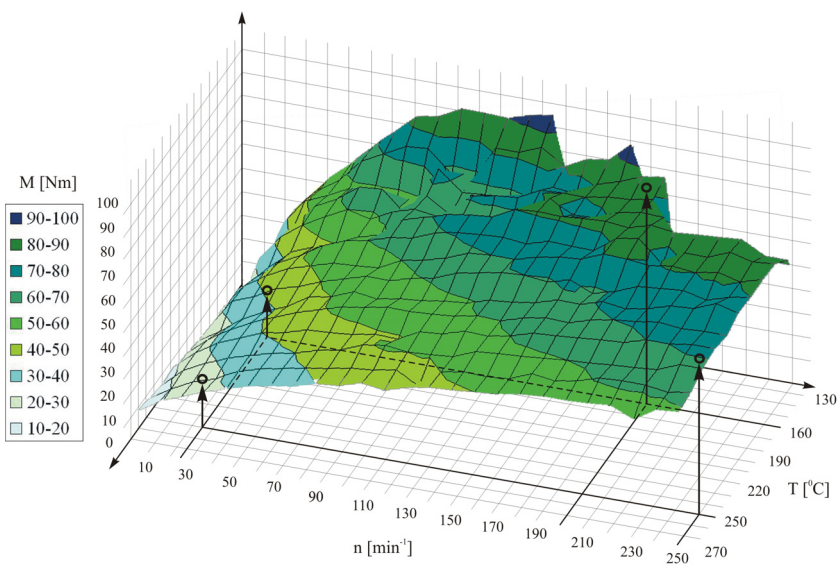

Fig. 9. *The torque, M, measured on the screws during the extrusion process, depending on the set temperature, T, along the extruder barrel and the set number of screw revolutions, n, during LDPE extrusion. It was observed that the higher the temperature in the extruder barrel the more slowly the torque on screws increases with the increasing number of screw revolutions. The extreme torque values were reached at the lowest temperatures (close to 130°C) and the number of revolutions of about 150–200 min^{-1}. Arrows indicate 4 extreme conditions at which LDPE specimens were extruded*

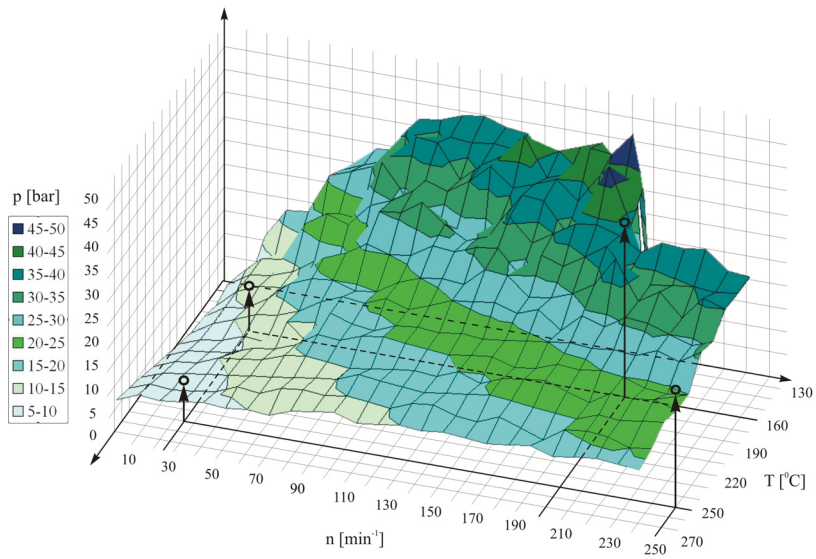

Fig. 10. *The pressure, p, measured in the melt at the extruder outlet, depending on the set temperature, T, along the extruder barrel and the set number of screw revolutions, n, during LDPE extrusion. Similarly to the torque measurement, the maximum pressure appears at low temperatures in the cylinder, but this happens at a higher number of revolutions (over 200 min-1). As opposed to torque, the increase of the pressure resulting from the increasing number of screw revolutions is less distinct at high temperatures, while at low temperatures the pressure increases more markedly than torque. Arrows indicate 4 extreme conditions at which LDPE specimens were extruded*

The geometry (i.e., shape and dimensions) of LDPE specimens, i.e., cylinders of 6 mm in diameter, was defined by the requirements of the creep measuring device [31] to [36]. For this purpose, a unique extruder die fitting was made to which a tool in the form of a glass tube with an internal diameter 6 mm and a length of 200 mm was fastened (see Fig. 11). The extrusion process of the polymer melt which exited from the extruder through the die fitting and entered into the glass tube in the selected conditions lasted until the melt was evenly mixed and constant conditions were established in the extruder barrel. Then the glass tube with melt was removed and inserted into the insulation system (see Fig. 12), where the specimen slowly cooled down. This specimen extrusion procedure was performed under four different processing conditions (see Table 1).

The specimen production process consists of three consecutive segments, i.e., heating and melting of the granulate in the extruder barrel, melt extrusion into the glass tube where the process of cooling is already going on, followed by slow cooling in the insulation system. Fig. 13 schematically illustrates the temperature profiles of specimen production at two temperatures of melt, i.e., 168ºC or 263ºC, measured at the outlet from the extruder. The melt temperature was higher than the set temperature (i.e., 160ºC or 250ºC, respectively) at all ten heaters along the extruder barrel as the consequence of the conversion of the mechanical energy generated by the rotation of screws to heat and consequently producing the rise of temperature in the barrel. The granulate in the extruder was first heated from the room temperature (approx. 25ºC) to the temperature of 168ºC or 263ºC (depending on the set temperature), which was measured at the outlet of the melt from the extruder. During this time, the melt pressure generated by the rotation of screws and measured at the outlet from extruder, increased to 23 or 77 bar (at the number of screw revolutions of 25 and 200 min^{-1}, respectively) at the lower temperature, and to 20 or 37 bar (at the number of screw revolutions of 25 and 250 min^{-1} respectively) at the higher temperature (see Table 1).

Table 1. *The set and the measured processing parameters of LDPE specimen extrusion. We selected the lowest and the highest temperature for extrusion, i.e., 160ºC and 250°C, respectively. At these two set temperatures we influenced the pressure in the melt measured at the exit from the extruder by changing the number of screw revolutions. At the lowest temperature and the number of screw revolutions of 25 and 200 min-[1], we achieved the pressures of 23 and 77 bar, respectively. In the case of the highest temperature and the number of screw revolutions of 25 and 250 min-[1], we achieved pressures of 20 and 37 bar, respectively.*

Specimen name	*Processing parameters*				
	Set quantities		*Measured quantities*		
	$T_{cylinder}$ [1] (°C)	n [2] (min^{-1})	T_{melt} [3] (°C)	p_{melt} [4] (bar)	M [5] (Nm)
LDPE_168_23	160	25	168	23	30
LDPE_168_77	160	200	168	77	105
LDPE_263_20	250	25	263	20	28
LDPE_263_37	250	250	263	37	75

[1] The temperature set on the ten heaters along the extruder barrel
[2] The number of screw revolutions
[3] The temperature of the melt measured at the outlet from the extruder barrel
[4] Pressure measured at the outlet from the extruder barrel
[5] Torque measured on the screws

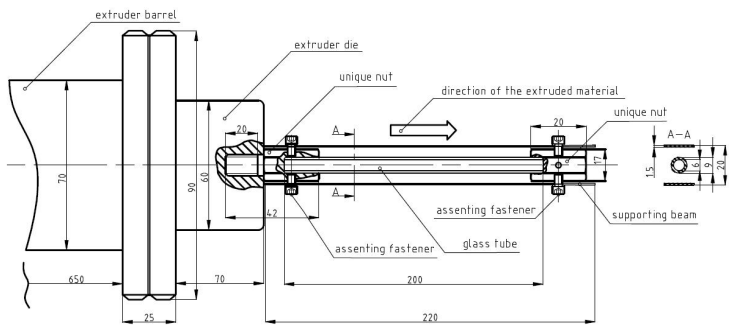

Fig. 11. *Unique die fitting with the glass tube tool*

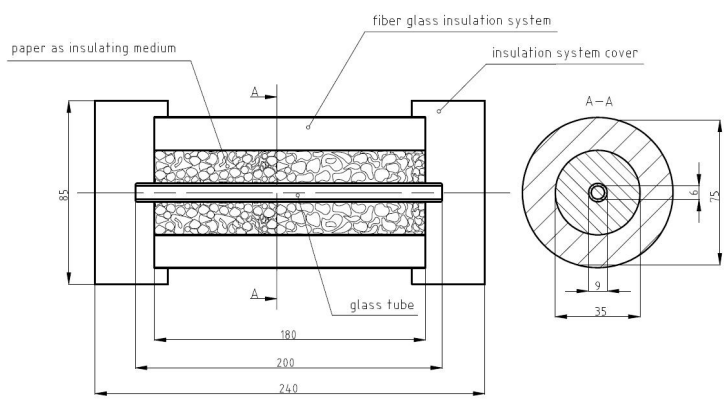

Fig. 12. *Insulation system for slow cooling of glass tubes with extruded polymer*

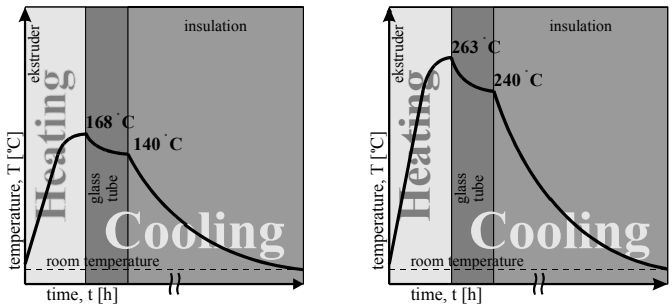

Fig. 13. *Schematic diagram of the temperature profiles for producing extruded LDPE specimens at two different temperatures of melt, i.e., the lowest temperature, 168°C (left), and the highest temperature, 263°C (right)*

The extrusion process pushed the melt at the outlet from extruder into the glass tube, which was open at the end (i.e., exposed to normal air pressure of 1 bar), whereby the pressure dropped to 1 bar, and the temperature fell to 140°C or 240°C, respectively (depending on the set temperature, see Fig. 13). After a period of approximately 10 minutes, required for the equilibrium state to be established in melt along the entire extruder barrel under the set processing conditions (i.e., temperature and the rotational speed of the screws), the extrusion process was stopped, the glass tube with the extruded LDPE removed and then inserted into the insulation system where the extrudate was cooling down to room temperature for approximately 90 minutes. The extruded LDPE specimen was then removed from the glass tube and prepared for the analysis of morphology, thermal properties and time-dependent mechanical behavior.

4 MATERIAL CHARACTERIZATION

4.1. Morphological Analysis – Optical Microscopy

The analysis of the *morphological properties* of the extruded LDPE specimens (see Fig. 14) showed that specimens extruded at a lower temperature (168°C) exhibit oriented structure in the form of concentric rings, while no orientation was observed in specimens extruded at a higher temperature (263°C). This indicates that a random structure forms at higher temperatures when the response times are short, while at lower temperatures when the material response times are long, molecules keep the configuration, which has been forced on them by the mechanical shear loading through the screw rotation and is reflected in the structural orientation of the solid product.

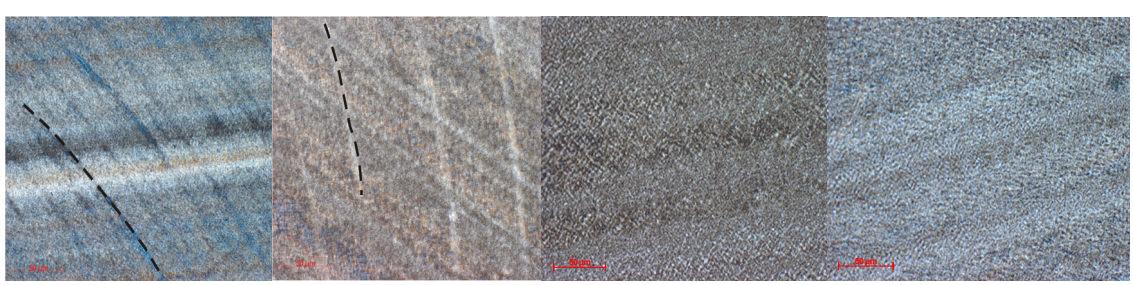

(a) LDPE_168_23 (b) LDPE_168_77 (c) LDPE_263_20 (d) LDPE_263_37

Fig. 14. *Optical microscopy images of extruded LDPE specimens, produced at different processing conditions, (a) LDPE_168_23: T = 168°C, p = 23 bar, M = 30 Nm, n = 25 min^{-1}, (b) LDPE_168_77: T = 168°C, p = 77 bar, M = 105 Nm, n = 200 min^{-1}, (c) LDPE_263_20: T = 263°C, p = 20 bar, M = 28 Nm, n = 25 min^{-1}, (d) LDPE_263_37: T = 263°C, p = 37 bar, M = 75 Nm, n = 250 min^{-1}. The optical microscope Axioskop 2 MAT (Carl Zeiss) was used to analyze the morphological structure of 40 μm thick LDPE extrudates at 500x magnification using polarized light*

The results are in conformity with the theory of the nonlinear processes in the material during structure formation as a consequence of three effects: temperature, pressure and shear. For detailed explanation see [31].

4.2. Thermal Analysis – Differential Scanning Calorimetry

The *thermal analysis* of the extruded LDPE specimens showed no difference in thermal properties (i.e., crystallization and melting temperatures) due to different processing conditions (see Table 2). It is highly probable that because of the nature of this experiment the method is not sufficiently sensitive to detect changes in the structure by measuring the thermal characteristics of the material.

4.3. Analysis of time-dependent mechanical properties – Shear creep testing

The *analysis of the time-dependent mechanical properties* of the extruded LDPE specimens was done based on the shear creep experiments, performed by using the shear creep torsiometer, which was developed in CEM [31] to [36]. The results of shear creep compliance analysis determine (i) the temperature stability of products, (ii) their time stability which determines durability, and (iii) the frequency stability of products during dynamic loading.

4.3.1 Temperature stability

The temperature stability analysis tells us how much the shear creep compliance changes with a change in temperature. It becomes evident that the effect of temperature on shear creep compliance is least distinctive in the material with the most complex (oriented) structure (i.e., the specimen extruded at 168°C and 23 bar) as seen in Fig. 15. A change in temperature from 30 to 80°C initiates a noticeably smaller change in this material than in other materials. This shows that the material with the most oriented structure is also most temperature-stable.

4.3.2 Time stability

The comparison of the shear creep curves at the reference temperature of 39°C (see Fig. 16)

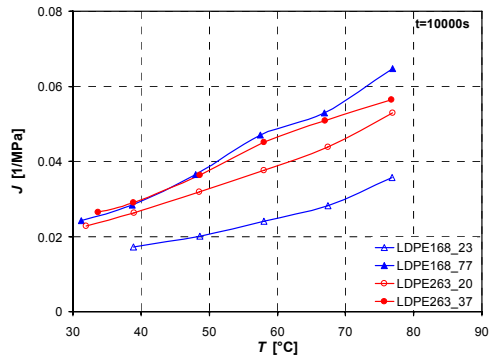

Fig. 15. *Temperature dependence of shear creep isochrones at the longest time of 10.000 s, determining the experimental window of the measurement, obtained from the segments of shear creep measurement for four extruded LDPE specimens produced under different processing conditions*

shows that by changing the processing parameters within the operating range of the laboratory extruder we can improve the time dependence by as much as ten to more than one million times.

The comparison of the time and temperature stability of the extruded specimens shows that the effect of the same polymer processing conditions on the temperature stability differs from the effect on the time stability of these products, which indicates an extremely nonlinear effect of the thermo-mechanical boundary conditions.

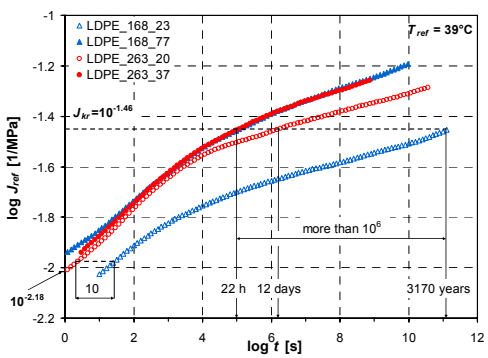

Fig. 16. *The shear creep master curves at the reference temperature of 39°C, showing logarithmic time-dependence of the shear creep compliance for four extruded LDPE specimens produced under different processing conditions*

If we are able to maintain the processing conditions (in our case extrusion) very accurately,

operation in the range of nonlinear processes within the material can be used to our advantage in order to improve the mechanical properties by several orders of magnitude.

4.3.3 Frequency stability

In line with the theory of linear viscoelasticity, we calculated the dynamic properties of the LDPE extrudates from experimentally determined shear creep curves by using software based on the Emri-Tschoegl algorithm [37] to [42] for the calculation of dynamic material functions from static ones across the mechanical spectrum. By comparing the dynamic material functions of the extruded LDPE specimens (see Figs. 17 and 18), we analyzed the behavior of materials under dynamic loading.

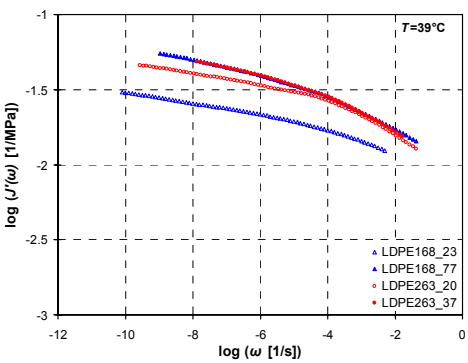

Fig. 17. *Frequency dependence of the real part of dynamic shear creep compliance, J', calculated from the master curves of shear creep at the reference temperature of 39°C for four extruded LDPE specimens produced under different processing conditions*

The material with the highest degree of orientation, which was produced at the lowest temperature and the lowest pressure (168°C, 23 bar), has better frequency stability than others regarding the ability of the material to return to the initial state after the cessation of loading. On the other hand, this material has the least ability to dissipate energy (damping) compared to the materials produced at a higher temperature and a higher pressure, which is reflected in the smallest value of the imaginary part of dynamic shear creep compliance, *J''*. At the same time, it is evident that with respect to the amount of energy

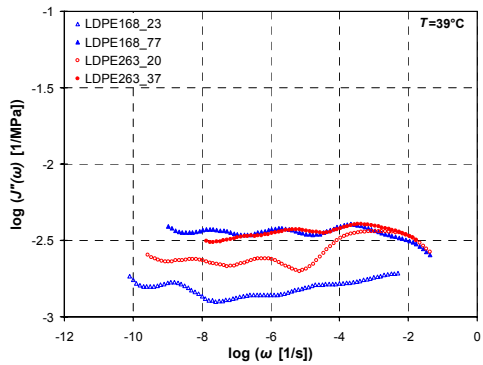

Fig. 18. *Frequency dependence of the imaginary part of dynamic shear creep compliance, J'', calculated from the master curves of shear creep at the reference temperature of 39°C for four extruded LDPE specimens produced under different processing conditions*

lost, which is not returned by the material after unloading, the frequency stability, $J'(\omega)$, is similar for all materials. We arrive to a similar conclusion by comparing the frequency dependence of the damping indicator, tan δ (see Fig. 19), which expresses the damping characteristics of the material. We find that all four specimens of extruded LDPE are frequency-stable at lower frequencies, while at higher frequencies they become very sensitive to any changes in the excitation frequency.

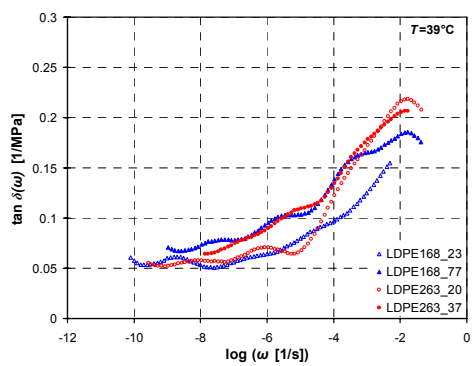

Fig. 19. *Frequency dependence of the damping indicator, tan δ, calculated from the master curves of shear creep at the reference temperature of 39°C for four extruded LDPE specimens produced under different processing conditions*

There is a critical frequency below which the material damping is practically independent of the

excitation frequency and above it the frequency dependent material damping changes by a factor of more than 2 (100%).

The relevant findings indicate that modification of the processing conditions within the range of temperatures and pressures typical for industrial polymer extrusion processes can improve the temperature stability of LDPE consumer products exposed primarily to static loads during their use by a factor of 2, the time-stability can be improved from 10 to more than 1,000,000 times (see Fig. 16), and the frequency stability above the critical frequency can differ for a factor of more than 2 (100%).

Improving the mechanical properties generally decreases production capacity which means that an optimum balance between the product quality and quantity produced should be found for each product within a price bracket. When producing simple products, technology optimization is of no special relevance since the quantity of product (and not the quality level) is a decisive factor in production. However, when manufacturing products whose durability and temperature stability are important requirements, the optimization of the technological process is of the key relevance.

5 CONCLUSIONS

The recent studies on multi-scale phenomena in material structure formation show that by changing the material structure we may significantly influence the physical properties and durability (i.e., long-term stability) of final products, which opens new potential for tailoring the functionality of products. Changes in the material structure can be caused by modifying the initial kinetics of the material (i.e., by changing its molecular weight distribution, by adding nanoparticles into polymeric matrix, etc.), and more important, by changing the thermo-mechanical boundary conditions (i.e., technology) to which material has been exposed during processing.

The investigation of the latter, i.e., the effect of processing conditions on the material structure formation, and hence the durability and the functionality of the final product, has found that by changing the processing conditions within the scope of the temperatures and pressures typical for polymer extrusion in industrial conditions it is possible to significantly affect the material structure formation and consequently its time-dependent mechanical properties, which determine the functionality and durability of the final product. These findings open new possibilities in modifying the functionality of polymer products, and consequently contribute to their better competitiveness in the global market.

6 ACKNOWLEDGEMENT

Authors thank to coorporation Thermo HAAKE Electron Corporation for supporting the research activities.

7 REFERENCES

[1] Emri, I., von Bernstorff, B.S. The Effect of Molecular Mass Distribution on Time-Dependent Behavior of Polymers, *Journal of Applied Mechanics-Transactions of the ASME,* 2006, vol.73, no.5, p.752-757.

[2] Sedlarik, V., Saha, N., Kuritka, I., Emri, I., Saha, P. Modification of poly(vinyl alcohol) with lactose and calcium lactate: potential filter from dairy industry, *Plastics rubber and composites*, 2006, vol.35, no.9, p.355-359.

[3] Greer, A.L. Too hot to melt, *Nature* 404, 2000, p.134-137.

[4] Blinc, R., Apih, T., Jeglič, P., Emri, I., Prodan, T. (2005) Proton NMR study of molecular motion in bulk and in highly drawn fiber polyamide-6, *Appl. Magn. Reson.* 29, p.577-588.

[5] Cevc, P., Arčon, D., Blinc, R., Emri, I. (2005) Electron paramagnetic resonance of stressed fibre nylon 6: annealing effects, *J. phys. D: Appl. phys.* 38, p.2299-2301.

[6] Emri, I., von Bernstorff, B., Voloshin, A. (2006) A Simple Technique for Studying Shrinkage Dynamics of Fibers, *Experimental Mechanics* vol.46, no.6, p.683-690.

[7] Balabaev, N.K., Darinskii, A.A., Neelov, I.M., Lukasheva, N.V., Emri, I. (2002) Molecular dynamics simulation of a two dimensional polymer melt, *Polymer Science Series* A vol.44, no.7, p.781-790.

[8] Darinskii, A.A., Tupytsina, A.I., Birhstein, T.M., Safyannikova, M.G., Amoskov, V.M., Emri, I. (2003) Microphase

separation in brushes capable of liquid crystal ordering, *Polymer Science Series* A vol.45, no.7, p.665-675.

[9] Tupitsyna, A.I., Darinskii, A.A., Birhstein, T.M., Amoskov, V.M., Emri, I. (2004) Self-consistent Brownian dynamics simulation of an anisotropic brush under shear flow, *Macromol. theory simul.* vol.13, no.9, p.771-782.

[10] Lyulin, S.V., Lyulin, A.V., Darinskii, A.A., Emri, I. The effect of dendrimer charge inversion in complexes with linear polyelectrolytes, *Polymer Science Series* A47(11), 2005 p.1217-1227.

[11] Dlubek, G., Supej, M., Bondarenko, V., Pionteck, J., Pompe, G., Krause-Rehberg, R., Emri, I. Ortho-positronium lifetime distribution analyzed with MELT and LT and free volume in poly(e-caprolactone) during glass transition, melting, and crystallization, *J. polym. sci. Part B-Polym. phys.,* 2003, vol.41, no.23, p.3077-3088.

[12] Supej, M. *The relation between the free volume and the mechanical properties of viscoelastic materials*, MSc. Thesis. University of Ljubljana, Ljubljana, 2002.

[13] Fréchet, J.M.J. Functional Polymers and Dendrimers: Reactivity, Molecular Architecture, and Interfacial Energy, *Science*, 1994, 263, p.1710-1715.

[14] Aharoni, S.M. *n-Nylons: Their Synthesis, Structure and Properties*. J. Wiley & Sons, Inc., New York, 1997.

[15] Doi, M., Edwards, S.F. *The Theory of Polymer Dynamics*. Oxford University Press, Oxford, UK, 1986.

[16] Salem, D.R. *Structure Formation in Polymer Fibers*. Carl Hanser Verlag, 2001, p.521-552.

[17] Swartjes, F.H.M., Peters, G.W.M., Rastogi, S., Meijer, H.E.H. Stress Induced Crystallization in Elongational Flow, *International Polymer Processing,* 2003, 13, p.53-66.

[18] Swartjes, F.H.M. *Flow induced crystallization in elongation flow*, Ph.D. thesis. Eindhoven University of Technology, 2001, http://www.mate.tue.nl.

[19] Kornfield, J.A., Kumaraswamy, G., Verma, R.K. Novel flow apparatus for investigating shear-enhanced crystallization and structure development in semicrystalline polymers, *Rev. Sci. Instrum.* , 1999, 70, p.2097.

[20] Eder, G., Janeschitz-Kriegl, H. Structure Development during Processing: Crystallization, in Meijer, H.E.H. (ed.) *Materials Science and Technology* 18. VCH, Weinheim, 1997, p.269-342.

[21] Eder, G., Janeschitz-Kriegl, H., Liedauer, S. Crystallization Processes in Quiescent and Moving Polymer Melts under Heat Transfer Conditions, *Progr. Polym. Sci.*, 1990, 15, p.629-714.

[22] Emri, I. Rheology of Solid Polymers, in Binding, D.M., Walters, K. (eds.) *Rheology Reviews 2005*. TA Instruments, New Castle, 2005, p.49-100.

[23] Emri, I., Prodan, T. A Measuring System for Bulk and Shear Characterization of Polymers, *Experimental Mechanics*, 2006, vol.46, no.4, p.429-439.

[24] Kralj, A., Prodan, T., Emri, I. An apparatus for measuring the effect of pressure on the time-dependent properties of polymers, *J. Rheol.*, 2001, vol.45, no.4, p.929-943.

[25] Sharpe, W.N., Jr. (ed.), *Springer Handbook of Experimental Solid Mechanics*, to be published (http://refworks.springer.com/)

[26] Filipe, S., Cidade, M.T., Wilhelm, M., Maia, J.M. Evolution of morphological and rheological properties along the extruder length for blends of a commercial liquid crystalline polymer and polypropylene, *Polymer,* 2004, vol.45, no.7, p.2367-2380.

[27] Filipe, S., Cidade, M.T., Wilhelm, M., Maia, J.M. Evolution of the morphological and rheological properties along the extruder length for compatibilized blends of a commercial liquid-crystalline polymer and polypropylene, *Journal of applied polymer science,* 2006, vol.99, no.1, p.347-359.

[28] Covas, J.A., Carneiro, O.S., Costa, P., Machado, A.V., Maia, J.M. Online monitoring techniques for studying evolution of physical, rheological and chemical effects along the extruder, *Plastics rubber and composites,* 2004, vol.33, no.1, p. 55-61.

[29] Covas, J.A., Carneiro, O.S., Maia, J.M., Filipe, S.A., Machado, A.V. Evolution of chemistry, morphology and rheology of

various polymer systems along a twin-screw extruder, *Canadian journal of chemical engineering,* 2002, vol.80, no.6, p.1065-1074.

[30] Potente, H., Bastian, M., Gehring, A., Stephan, M., Potschke, P. Experimental investigation of the morphology development of polyblends in corotating twin-screw extruders, *Journal of applied polymer science,* 2000, vol.76, no.5, p.708-721.

[31] Mohar, U., Ferfolja, J. *The Analysis of the Effect of Structure (Morphology) on Time-Dependent Behavior of Polymers – The Effect of Processing Conditions on Time-Dependent Mechanical Properties of Extruded LDPE*, Research work, rewarded with Prešeren Award for students. University of Ljubljana, Ljubljana, 2006.

[32] Metlikovič, P., Emri, I. Analiza procesa lezenja viskoelastičnih materialov pod vplivom strižne obremenitve, *Kovine, zlitine, tehnologije* , 1994, vol.28, no.1-2, p.407-409.

[33] Metlikovič, P. Analiza procesa lezenja viskoelastičnih materialov pod vplivom strižne obremenitve (Magistrska naloga). *Fakulteta za strojništvo*, Ljubljana, 1989.

[34] Metlikovič, P., Emri, I. Naprava za merjenje lezenja torzijsko obremenjenih polimernih preizkušancev, *Stroj. vestn.*, 1989, vol.35, p.56-58.

[35] Metlikovič, P., Emri, I. Naprava za merjenje lezenja torzijsko obremenjenih polimernih preizkušancev, *Stroj. vestn.,* 1990, 36, p.101-104.

[36] Cvelbar, R., Emri, I. Analiza prehodnega pojava pri merjenju lezenja viskoelastičnih materialov, *Kovine, zlitine, tehnologije,* 1994, vol.28, no.1-2, p.359-362.

[37] Emri, I., Tschoegl, N.W. Generating Line Spectra from Experimental Responses. 1. Relaxation Modulus and Creep Compliance, *Rheologica Acta,* 1993, vol.32, no.3, p.311-321.

[38] Tschoegl, N.W., Emri, I. Generating Line Spectra from Experimental Responses. 2. Storage and Loss Functions, *Rheologica Acta,* 1993, vol.32, no.3, p.322-327.

[39] Tschoegl, N.W., Emri, I. Generating Line Spectra from Experimental Responses. 3. Interconversion between Relaxation and Retardation Behavior, *International Journal of Polymeric Materials,* 1992, vol.18, no.1-2, p.117-127.

[40] Emri, I., Tschoegl, N.W. Generating Line Spectra from Experimental Responses 4. Application to Experimental-Data, *Rheologica Acta,* 1994, vol.33, no.1, p.60-70.

[41] Emri, I., Tschoegl, N.W. Generating Line Spectra from Experimental Responses. 5. Time-Dependent Viscosity, *Rheologica Acta,* 1997, vol.36, no.3, p.303-306.

[42] Emri, I., Tschoegl, N.W. Determination of Mechanical Spectra from Experimental Responses, *International Journal of Solids and Structures,* 1995, vol.32, no.6-7, p.817-826.

Strojniški vestnik - Journal of Mechanical Engineering 54(2008)7-8, 521-530
UDC 621.91
Paper received: 06.11.2007
Paper accepted: 19.12.2007

The Effects of Cutting Speed and Feed Rate on Bue-Bul Formation, Cutting Forces and Surface Roughness When Machining Aa6351 (T6) Alloy

Hasan Gokkaya[1] - Ahmet Taskesen[2,*]
[1] Zonguldak Karaelmas Universitesi Safranbolu Meslek Yuksekokulu, Turkey
[2] Makine Egt. Bolumu, Teknik Egt. Fakultesi, Gazi Universitesi, Turkey

In this paper, the effects of machining parameters such as cutting speed and feed rate on BUE, BUL, main cutting force and surface roughness were experimentally investigated. Optimal and critical cutting parameters were determined. It was found that the cutting speed must be selected above 400-500 m/min in order to prevent BUE and BUL formation when machining of AA6351 (T6) alloy with uncoated carbide inserts. The results of this study show that the most important parameter affecting main cutting force and surface roughness is feed rate. As a result of this study, optimum cutting force and optimum feed rate were found in order to minimize surface roughness of the work piece.

Keywords: machining, built-up edge (BUE), built-up layer (BUL), cutting forces, surface roughness

0 INTRODUCTION

Turning operations constitute major portion of machining processes. Although most of the cutting processes are oblique cutting, two different cutting processes such as orthogonal and oblique cutting exist in metal cutting operations. However, since cutting mechanic behavior is two dimensional, generally orthogonal cutting method is used for the determination of the effects of machining parameters [1] to [3]. In addition to mechanical properties of work piece; other parameters such as tool rigidity, cutting speed, feed rate, depth of cut and tool geometry are also important factors for the determination of ideal machinability behaviors [4] to [6].

Aluminum alloys have been used for many years in the aviation industry. AA6351 alloy whose main alloy elements are Mg and Si, is one of the most important alloy among 6xxx series and has a natural aging capability. Strength and hardness of AA6351 alloy can be increased by heat treatment [4],[7] and [8].

Generally AA6351 (T6) alloy is machined by metal removing processes. When aluminum alloys are machined at low cutting speeds, BUE formation occurs on the rake face of the cutting tool, causing surface roughness (*Ra*) to increase [4],[9] and [10]. Due to low frictional forces on the tool rake face at high cutting speeds, increasing the cutting speed causes the cutting forces to decrease. This case results in a general elimination of BUE formation causing to improve surface roughness of the work piece [11]. Sometimes, BUE formation positively affects the surface roughness of the work piece, since BUE formation increases tool nose radius [12].

In this paper, the effects of machining parameters namely cutting speed (V_C) and feed rate (f) on BUE, BUL, main cutting force (F_C) and surface roughness (Ra) were investigated. Analysis of Variance (ANOVA) of these machining parameters was carried out; and optimal and critical cutting parameters were determined. AA6351 aluminium alloy having T6 heat treatment was machined with uncoated carbide tools using CNC turning machine under dry cutting conditions. Four different cutting speeds (200 m/min, 300 m/min, 400 m/min, 500 m/min), five different feed rates (0.10 mm/rev, 0.15 mm/rev, 0.20 mm/rev, 0.25 mm/rev, 0.30 mm/rev) and a constant depth of cut were selected.

1 MATERIALS AND METHOD

1.1. Material

In this experimental study, the effects of machining parameters on BUE-BUL formation, main cutting force and average surface roughness were investigated and a correlation between these parameters was determined. Cutting speed and feed rate were used as machining parameters.

*Corr. Author's Address: Makine Egt. Bolumu, Teknik Egt. Fakultesi, Gazi Universitesi, Ankara, Turkey, taskesen@gazi.edu.tr

Test specimens used for the experiments were heat treated (T6) AA6351 aluminum alloy having 80 mm diameter and 500 mm length. Chemical composition and mechanical properties of the test specimens are shown in Table 1.

Brinell hardness number (BHN) of the work piece material used in the experiments was 102 BHN. The hardness values of the specimens were measured by means of a "Reicherter Brinell" hardness measuring device. Fine machined test specimens having 10 mm depth were prepared for the measurements. The test specimens were measured from outside through the center for 10 times and average measured value was used.

1.2. Machining Parameters, Cutting Tool and Tool Holder

Turning experiments were carried out at 20±1ºC ambient temperature using changeable carbide inserts having CCGT 120404FN-ALU geometry and K10 quality degree. Rake angle and clearance angles of the cutting tools were 7^o and 5^o, respectively. The tool holder used for the tests was CSRNR 2525 M12 having 90^o approaching angle and agreeable to ISO 5608. Cutting parameters used for the experiments are shown in Table 2. Four different cutting speeds (200 m/min, 300 m/min, 400 m/min, 500 m/min), five different feed rates suggested by ISO 3685 (0.10 mm/rev, 0.15 mm/rev, 0.20 mm/rev, 0.25 mm/rev, 0.30 mm/rev) and 1.5 mm constant depth of cut were selected. A total of 20 experiments according to cutting parameters and machining levels shown in Table 2 were conducted. All turning tests were carried out under continuous dry cutting conditions.

1.3. Machine Tool and Measuring Equipment

All the tests were done with a "JOHNFORD T35" industrial type CNC turning machine having 10 KW power and revolving capability of 50-3500 rev/min. Kistler 9257B dynamometer was used to measure all cutting forces (F_C, F_f, F_p), where F_C, was the main cutting force, F_f, was the feed force and F_p, was the ploughing force.

MAHR-Perthometer M1 measuring equipment was used to measure surface roughness of the work piece material. All of the tests achieved were repeated three times in order to guarantee its precision. In order to measure surface roughness, cut-off length and sampling length were assumed to be 0.8 mm and 5.6 mm, respectively. Finally, after each turning test, the tools were further observed in a JEOL-JSM 6060 scanning electron microscope (SEM).

Table 1. *Chemical and mechanical properties of AA6351 alloy*

a) Chemical composition (% weight)

Si	Fe	Cu	Mn	Mg	Zn	Al
1,03	0,237	0,0723	0,584	0,665	0,003	Balance

b) Mechanical properties

Density (x1000 kg/m^3)	Elastic modulus GPa	Tensile Strength MPa	Elongation %	Hardness BHN
2.7	75	250	20	102

Table 2. *Cutting parameters used for the tests*

Level	Cutting speed V_C (m/min)	Feed rate f (mm/rev)	Depth of cut ap (mm)	Cutting Tool	Tool Holder
1	200	0.10	0.15	Uncoated Carbide CCGT 120404FN-ALU	CSRNR 2525 M125
2	300	0.15			
3	400	0.20			
4	500	0.25			
5		0.30			

The experimental results were analyzed with analysis of variance (ANOVA), which was used for identifying the factors significantly affecting the performance measures namely main cutting force and surface roughness.

2 RESULTS AND DISCUSSION

2.1 BUE and BUL Formation

Generally, tool life is determined by tool wear in machining processes. It can be observed from past studies that the wear mechanism which operates in the widest range of cutting temperatures is the adhesion mechanism [2]. Usually, adhesion wear occurs by the direct transfer of tool particles to the metallic chips. These particles adhered to the cutting tool face during machining process are mechanically unstable and, thus, they can be removed from the tool surface by the action of the high strength cutting forces that are produced. The work piece material adheres to the rake face of the tool in two different forms. The first and most known one involves the formation of a Built-up Edge (BUE) which is the adhesion of the work piece material to the cutting edge of the tool. In the second one, the material transferred is poured to wider areas on the rake face of the tool, giving rise to the so-called Built-up Layer (BUL) [2]. Generally, this BUL formation is seen during the machining of ductile materials. BUE and BUL regions can be clearly seen in Fig. 1.

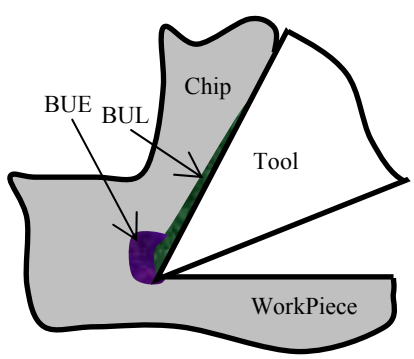

Fig. 1. *Schematic image of cutting tool with BUE and BUL*

The cutting tool is gradually worn since BUE formation is repeated periodically during metal cutting. It is known that a strong adhesion exists during machining of aluminum alloys [12]. Therefore, BUE and BUL formations must be taken into consideration when machining these aluminum alloys.

In this part of the study, four different cutting speeds were used in order to obtain the effects of cutting speed on BUE and BUL formation, then, SEM images of BUE-BUL formations were evaluated. Since the highest BUE and BUL formation was observed to SEM Image of BUE and BUL formed on uncoated insert surface at 200 m/min and 0.30 mm/rev is shown in Fig. 2. occur at the feed rate of 0.3 mm/rev, this rate was assumed to be the constant feed rate.

It is observed from this figure that, a metal accumulation on the tool surface is associated with the BUL formation and on tool edge with the BUE. It can also be seen from Fig.2 that the major part of BUE formation occurs at the tool main cutting edge and at the region that chip contacts with the air from tool nose through tool holder. This case is connected with the temperature at the second deformation region which is called tool-chip interface. Temperature of tool-chip interface decreases as moving away from tool nose through tool holder [13]. Test results showed that lesser amount of BUE was formed close to tool nose. This case can be attributed to less temperature at this region then that of max BUE region. Past studies claimed that BUE formation caused tool rake angle to increase [14] to [16]. The experimental results of this study also agree with the results of past studies.

BUE and BUL formation regions on tool surface at various cutting speeds (300 m/min, 400 m/min and 500 m/min) are depicted in Figs. 3 to 5, respectively.

From the Figs. 2 to 3, BUE formation can bee seen at tool nose region and main cutting edge. Moreover, comparison of Fig. 2. with Fig. 3. shows that larger cutting speeds have a favorable effect on reduction of BUE-BUL formation. Increasing the cutting speed from 300 to 400 m/min, BUE-BUL reduction can be seen more clearly.

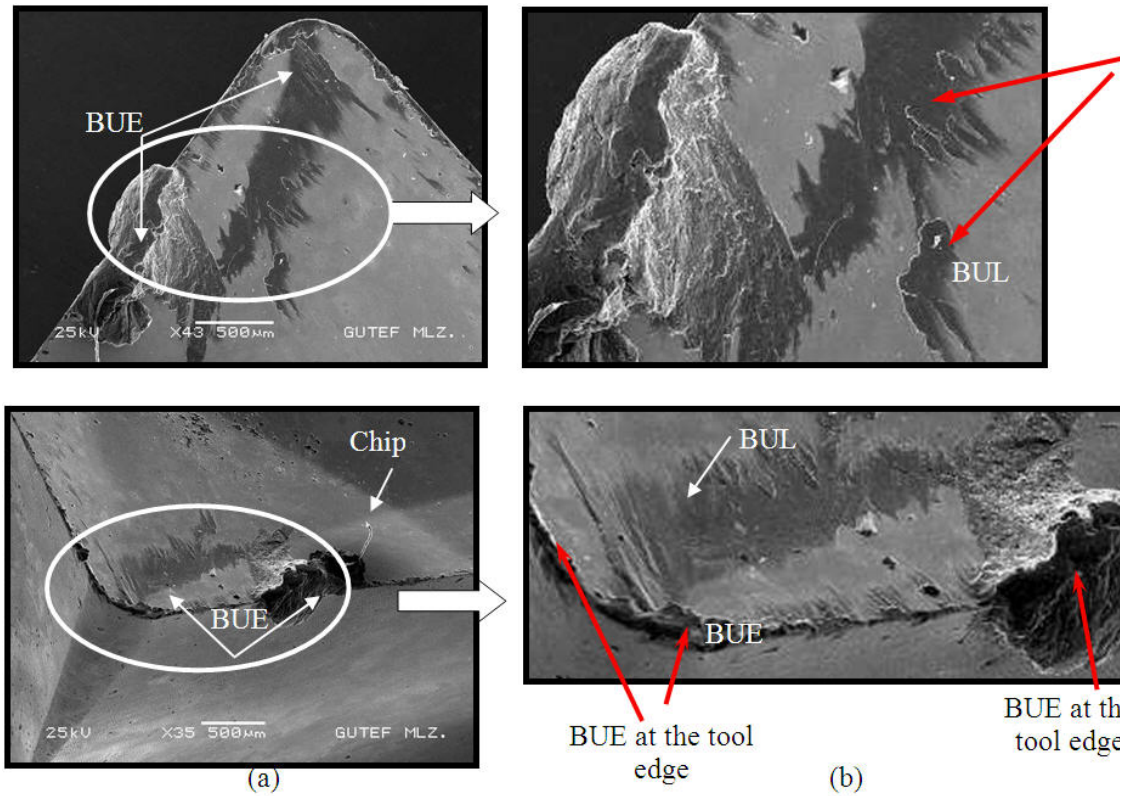

Fig. 2. *SEM Image of BUE and BUL formed on uncoated insert surface at 200 m/min and 0.30 mm/rev. a) SEM image of tool rake face b) 3D SEM image*

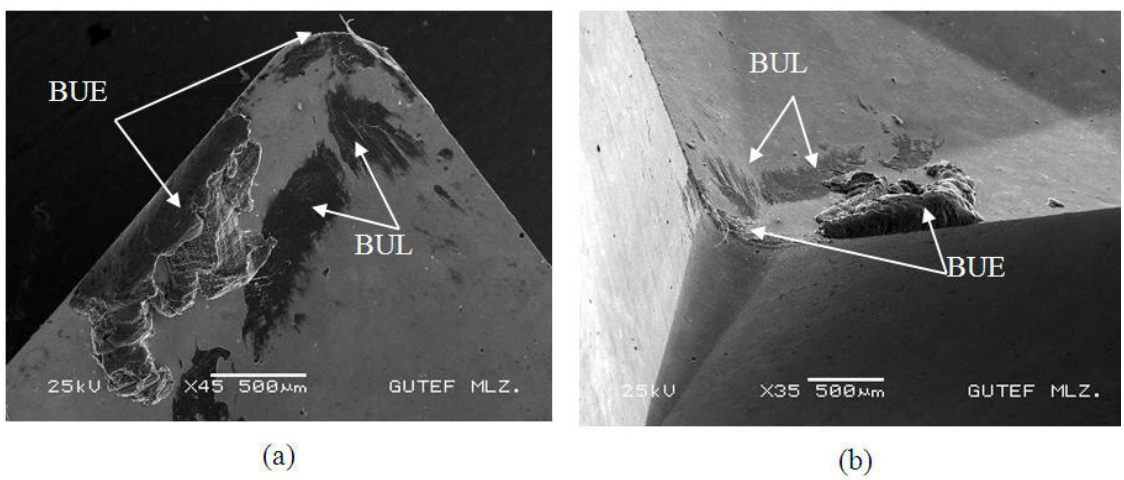

Fig. 3. *SEM Image of BUE and BUL formed on uncoated insert surface at 300 m/min and 0.30 mm/rev. a) Tool rake face x45 magnification b) 3D SEM image*

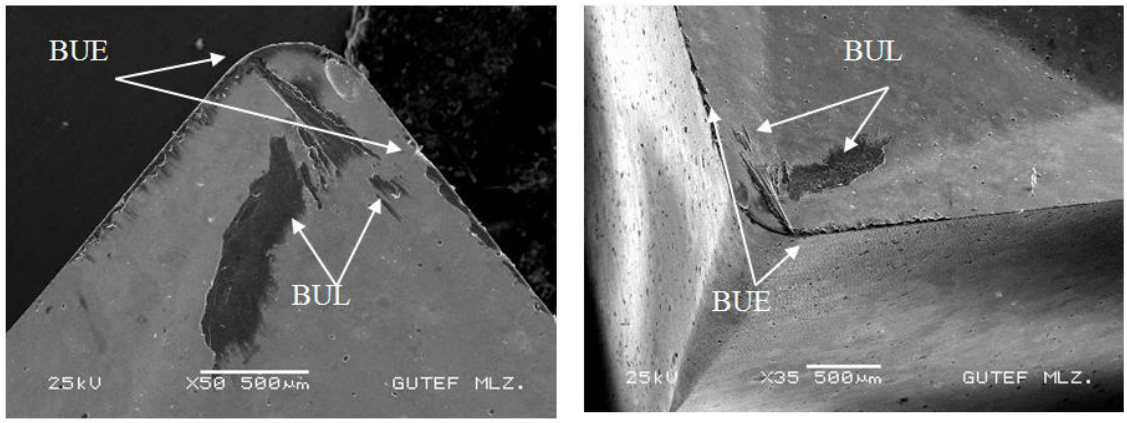

Fig. 4. *SEM Image of BUE and BUL formed on uncoated insert surface at 400 m/min and 0.30 mm/rev. a) Tool rake face x50 magnification b) 3D SEM image*

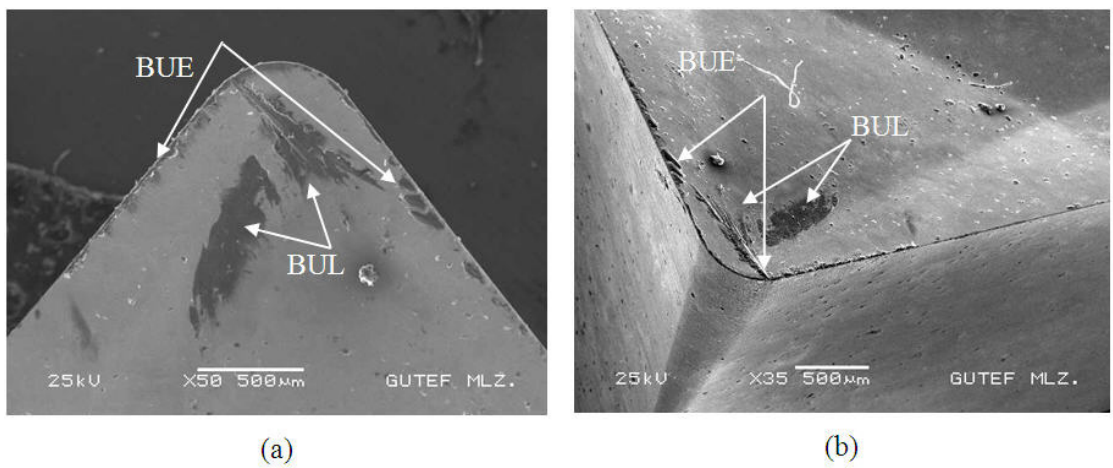

Fig. 5. *SEM Image of BUE and BUL formed on uncoated insert surface at 500 m/min and 0.30 mm/rev. a) Tool rake face x50 magnification b) 3D SEM image*

This is caused by temperature increase at second deformation zone since temperature at the second deformation zone increases with cutting speed [8]. Fig. 5 shows the BUE-BUL formation at 500 m/min. Comparison of this figure with Fig. 4 shows a weak increase in BUE-BUL. Test results show that lower cutting speeds (200m/min and 300 m/min) cause greater BUE-BUL formation on tool surface when machining AA6351 alloys. It can be concluded from these results that 400 -500 m/min or higher cutting speeds must be selected in order to prevent BUE-BUL formation.

2.2 Cutting Forces and Surface Roughness

2.2.1 Cutting Forces

The effects of cutting parameters on main cutting force were evaluated in this part of the study. Main cutting force and surface roughness values determined from the experiments depending on cutting parameters namely cutting speed (V_C) and surface roughness (Ra) are shown in Table 3.

The experimental results were analyzed with analysis of variance (ANOVA), which is used for identifying the factors significantly affecting the performance measures.

Table 3. *Main cutting force (F_C) and average surface roughness (Ra) values depending on cutting speed (V_C) and surface roughness (Ra)*

Test No	Factors		Performance measures	
	V_C m/min	f mm/rev	F_c N	Ra μm
1	200	0.10	113	0.80
2	200	0.15	163	1.19
3	200	0.20	203	1.45
4	200	0.25	303	2.13
5	200	0.30	326	4.97
6	300	0.10	132	1.19
7	300	0.15	182	1.85
8	300	0.20	264	3.25
9	300	0.25	290	4.42
10	300	0.30	343	5.47
11	400	0.10	130	1.54
12	400	0.15	177	2.43
13	400	0.20	226	3.43
14	400	0.25	276	4.71
15	400	0.30	326	5.98
16	500	0.10	118	0.70
17	500	0.15	165	1.08
18	500	0.20	214	2.07
19	500	0.25	265	3.42
20	500	0.30	316	5.32

The results of the ANOVA with the cutting force are shown in Table 4. This statistical analysis was performed for a confidence level of 95%. *P*-values shown in Table 4 are the realized significance levels, associated with the *F*-tests for each source of variation. The sources with a *P*-value less than 0.10 are considered to have a statistically significant contribution to the performance measures [17]. Moreover, the last columns of the Table 4 shows the percent contribution of each source to the total variation indicating the degree of influence on the result. Table 4 shows that the only significant factor for the cutting force F_C is feed rate *f*, which explains 96.6% of the total variation. It can be concluded from Table 4 that cutting speed V_C having 1.73% significance level does not have a significant contribution to total variation. According to test results, minimum cutting force considering feed rate and cutting speed was determined at 0.10 mm/rev and 500 m/min, respectively.

Main cutting forces depending on cutting speed and feed rate determined from experiments are depicted in Fig. 6. Earlier studies have shown that as cutting speed is made larger, the cutting forces become smaller [1], [5] and [13]. However, the results of this figure indicate that lower cutting speeds (200 m/min) give lower cutting forces up to a certain cutting speed (300 m/min). It is considered that high temperature at the flow zone and decreasing surface area are the reasons of this case. Reduction amount in cutting forces depends on work piece material, working conditions and cutting speed ranges. Fig. 6 indicates that the relationship between cutting forces and cutting speed is inversely proportional after 300 m/min. BUE and BUL formations cause the tool rake angle to increase and thus, the results of past studies indicate that increasing the tool rake angle improve the cutting stability and decreases cutting forces [4], [5] and [15]. Experimental results agree with these results. Therefore, BUE and BUL formations are considered to be responsible for this inverse relationship between cutting speed and cutting force, Figs. 2. to 4. Increasing cutting speed for 66.6% caused cutting force to decrease for 11.15% according to the test results. Maximum cutting force value (343 N) was determined at 300 m/min cutting speed and 0.30 mm/rev when machining AA6351 alloy while minimum cutting force was determined at 200 m/min and 0.10 mm/rev. According to feed rate, minimum and maximum main cutting forces were observed at 0.30 mm/rev and 0.10 mm/rev, respectively.

The results of the experiments conducted with five different feed rates indicated that higher feed rates caused higher cutting forces. For example, according to the test results, increasing the feed rate for 200% resulted in a 165.8% increase in cutting forces. It is suggested that the feed rate must be decreased in order to decrease cutting forces [13].

Table 4. *Analysis of variance (ANOVA) for main cutting force*

Source of Variance	SS	df	Variance	F- Value	P- Value	C (%)
A (VC, m/min)	1947.6	3	649.2	4.16	0.031	1.73
B (f, m/min)	108634.8	4	27158.7	173.87	0	96.60
A·B	1874.4	12	156.2			1.67
Error	0	0	0			
Total	112456.0	19				100

SS: sum of squeres , df: degree of freedom , C: percent contribution

2.2.2. Surface roughness

The surface roughness values determined from experiments when machining AA6351 alloy are shown in Table 3. The effects of cutting speed and feed rate on surface roughness were investigated in this part. The experimental results were analyzed with ANOVA and these results with the surface roughness are shown in Tables 5.

Table 5 shows that the only significant factor for surface roughness Ra is feed rate f, which explains 84.4% of the total variation. It can be concluded from Table 5 that cutting speed V_C having 12.2% significance level has less contribution to total variation then that of feed rate. According to test results, minimum surface roughness considering cutting speed and feed rate was determined at 200 m/min and 0.10 mm/rev, respectively. The test results show that maximum surface roughness (5.98 µm) was obtained at 400 m/min cutting speed and 0.30 mm/rev feed rate while minimum surface roughness (0.70 µm) was obtained at 500 m/min cutting speed and 0.10 mm/rev feed rate, Table 2. Detailed average surface roughness values versus cutting speed and feed rate are depicted in Fig. 7.

Producing a better surface finish at higher cutting speed is not something unusual in metal cutting, but the conventional explanations are usually related to BUE [17]. That is, the formation of a built-up-edge is favored in a certain range of cutting speed. By increasing cutting speed beyond this region, BUE will be eliminated and as a result the surface finish will improve [17]. The experimental results show that this cutting speed is above 500 m/min.

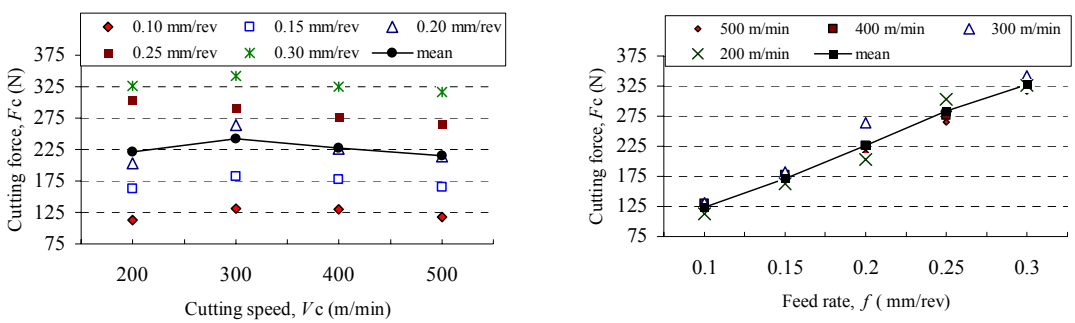

Fig. 6. *Cutting forces using uncoated carbide tools*
a) Cutting forces vs cutting speed
b) Cutting forces vs feed rate.

Table 5. *Analysis of variance (ANOVA) for surface roughness (Ra)*

Source of Variance	SS	df	Variance	F- Value	P- Value	C (%)
A (VC, m/min)	6.990	3	2.330	14.34	0.0003	12.2
B (f, m/min)	48.503	4	12.126	74.64	0	84.4
A·B	1.949	12	0.162			3.4
Error	0	0	0			0
Total	57.443	19				100

SS: sum of squeres , df: degree of freedom , C: percent contribution.

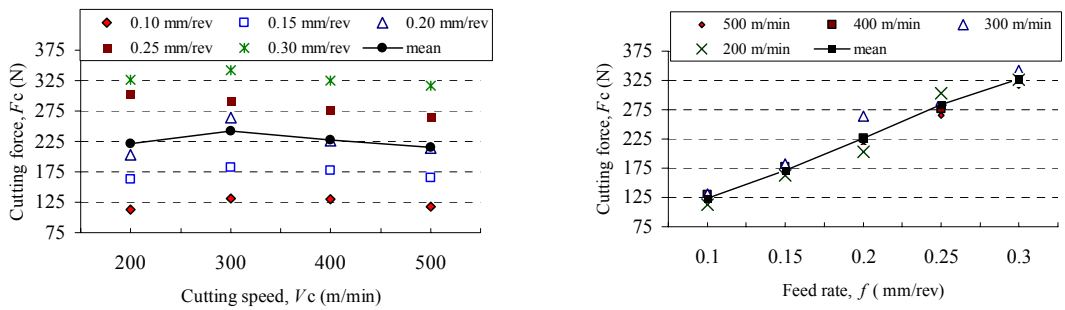

(a) (b)

Fig. 7. *Surface roughness values using uncoated carbide tools*
a) Surface roughness vs cutting speed
b) Surface roughness vs feed rate

It can be concluded from Fig. 7 that depending on the cutting speed, minimum surface roughness was obtained at 200 m/min. Interestingly, when the cutting speed was increased to 300 m/min, surface roughness also increased. It is considered that larger BUE formations existing on the cutting tool at lower cutting speeds (200 m/min) caused the tool geometry to change as seen in Fig. 2. Therefore, cutting tool geometry was effected by cutting speed depending on BUE and BUL formation. It was observed from experiment results that BUE formations increased the tool nose radius causing to improve surface roughness. These results agree with some earlier studies [12]. Since less BUE formation exists at the cutting speed of 400 m/min, maximum surface roughness was determined at this cutting speed. This case can be attributed to a small mount of BUE formation on tool surface (Fig. 3, initial BUE formation). Previous studies claimed that surface roughness shows a decrease at higher cutting speeds [5], [10] and [18] to [20]. In agreement with the earlier studies [5], [10], [13] and [18], in the present study, surface roughness gradually decreases after 400 m/min as the cutting speed increases as shown in Fig. 7. The possible reasons of this case can be explained as high temperature, BUE elimination and high deformation velocity [4] and [16].

Test results show that the surface roughness increases as feed rate increases (Fig. 7). Depending on the feed rate, minimum surface roughness (1.06 μm) was obtained at 0.10 mm/rev while maximum roughness (5.43 μm) was obtained at 0.30 mm/rev. Surface roughness showed 412.2% increase when increasing feed rate about 200%. It can be concluded that feed rate must be reduced in order to improve surface quality. Although roughness is affected by feed rate, the trend is less significant for the tools with large nose radius. A recommendation can

therefore be made to the tool users that if the inserts of 1 mm nose radii are used, feed rates as large as 0.3 mm/rev may be used in order to promote productivity when finishing without significant deterioration in surface roughness [18].

3 CONCLUSIONS

The effects of machining parameters namely cutting speed and feed rate on BUE, BUL, main cutting force and surface roughness were both experimentally and statistically investigated.

BUE and BUL formations caused the tool nose radius and effective rake angle of cutting tool to increase. BUE was formed at especially low and middle cutting speeds. BUE-BUL formations positively affected the cutting forces and surface roughness at lower cutting speeds. Higher cutting speeds caused BUE formation to reduce improving machined surface quality.

It was observed from test results that the most important parameter affecting main cutting force FC and surface roughness was the feed rate. Significance level of these effects was 96.6% for main cutting force and 84.4% for surface roughness. Contribution of cutting speed V_C to total variation was found be more important for surface roughness.

BUE-BUL formations on tool surface at the cutting speeds of 200 and 300 m/min were found to be larger than those of 400 and 500 m/min. Maximum BUE-BUL formation was observed at 200 m/min cutting speed. It was concluded that cutting speed must be selected above 400 - 500 m/min cutting speed in order to prevent BUE and BUL formation.

According to feed rate and cutting speed, maximum cutting force value (343 N) was determined at 300 m/min cutting speed and 0.30 mm/rev when machining AA6351 alloy while minimum cutting force was determined at 200 m/min and 0.10 mm/rev.

In order to minimize surface roughness, optimum cutting speed and feed rate were found to be 500 m/min and 0.10 mm/rev, respectively. The test results showed that maximum surface roughness (5.98 μm) was obtained at 400 m/min cutting speed and 0.30 mm/rev feed rate while minimum surface roughness (0.70 μm) was obtained at 500 m/min cutting speed and 0.10 mm/rev feed rate.

4 REFERENCES

[1] Modern Metal Cutting, Practical Handbook, Sandvik Coroman, Sweden, 1994.

[2] Sanchez-Carrilero, M., Sanchez-Sola, J.M., Gonzalez, J.M., Contreras, J.M., Marcos, M. Cutting Forces Compatibility Based On A Plasticity Model. Application to The Oblique Cutting Of The AA2024 Alloy, *Int. J. of Machi Tools & Manuf*, 2002, no.42, p.559-565.

[3] Y. Sahin, Y., Talas Kaldirma Prensipleri 1, Gazi Kitabevi, Ankara, 2003, (In Turkish).

[4] Aydin, B., Ozcatalbas, Y. AA2014 (T6) Alasiminin Islenebilirlik Ozelliklerine Kesici Takim Geometrisinin Etkisi, *Makine Tasarimi ve Imalati Dergisi*, 2003, no.5, p.89-95, (in Turkish).

[5] Ozcatalbas, Y. Dusuk Alasimli Celikte Yiginti Talas Olusumunun Isleme Ozelliklerine Etkisi, *8. Uluslar arası Makine Tasarimi ve Imalat Kongresi*, ODTU, 1998, p.25-33 (in Turkish).

[6] Trent, E.M. Metal Cutting, Taner Ltd. London, 1988.

[7] Etibank Aluminyum Isletmesi Muessesi Mudurlugu Urun Katalogu, (In Turkish), 1995

[8] Hong, S.Y., Ding, Y., Jeong, W., Friction and cutting forces in cryogenic machining of Ti–6Al–4V, *Int. J. Machi Tools & Manuf.*, 2001, no.41, p.2271-2285.

[9] Dae, E.K., Dong, H.H. Experimental Investigation of the Contact Sliding Behaviour of Metals, *J Manufac Sci and Eng*, 1998, no.120, p.395-400.

[10] Jeelani, S., Musail, M. Dependence of Fatigue Life on the Surface Integrity in the Machining of 224-T 351 Aluminum Alloy Unlubricated Conditions, *J Mater Sci*, 1986, no.21, p.155-160.

[11] Oishi, K. Mirror Cutting of Aluminium with Sapphire Tool, *J Mater Proc Tech*, 1996, no.62, p.331-334.

[12] Rubio, E.M., Camacho, A.M., S´anchez-Sola, J.M., Marcos, M. Surface Roughness of AA7050 Alloy Turned Bars, Analysis of the Influence of the Length of Machining, *J Mater Proc Tech*, 2005, p.162–163, p.682–689.

[13] Altın, A., Gökkaya, H., Nalbant, M. Isleme Parametrelerinden Kesme Hizinin Inconel 718 Super Alasimin Islenebilirligine Etkisi, *Gazi Universitesi Muhendislik Fakultesi, Muhendislik-Mimarlık Fakultesi Dergisi,* 2005, (in Turkish).

[14] Seker, U. Talasli Imalatta Takim Tasarimi Ders Notlari, *Gazi Universitesi Fen Bilimleri Enstitusu Yuksek Lisans Ders Notlari,* Ankara, 2000, (in Turkish).

[15] Liew, W.Y.H., Hutchingsand, I.M., Williams, J.A. The Interaction Between Tool Material Environment and Process Conditions in the Machining of Aluminum Alloys, *Mach Tech*, (2), 1999, p.286-373.

[16] Gokkaya, H., Sur, G., Dilipak, H. PVD ve CVD Kaplamalı Sementit Karbür Kesici Takımların İşleme Parametrelerine Bağlı Olarak Yüzey Pürüzlülüğüne Etkisinin Deneysel Olarak İncelenmesi, *Z.K.U. Karabuk Teknik Egitim Fakultesi Teknoloji Dergisi*, 2004, no.7, (in Turkish).

[17] Aslan, E., Camuscu, N., Birgoren, B. Design optimization of cutting parameters when turning hardened AISI 4140 steel (63 HRC) with Al2O3 + TiCN mixed ceramic tool, *Mat Des*, 2006, in Press.

[18] Chen, W. Cutting forces and surface finish when machining medium hardness steel using CBN tools, *Int J Mach Tools & Manuf*, 2000, no.40, p.455–466.

[19] Altin A, Nalbant M, Taskesen A. The effects of cutting speed on tool wear and tool life when machining Inconel 718 with ceramic tools, *Mat Des*, 2007, no.28, p.2518–2522.

[20] Taskesen, A., Altin, A., Nalbant, M. The Effects of Cutting Speed on Tool Wear and Tool Life When Turning Inconel 718 with Ceramic and Coated Carbide Inserts, *Trans. Indian Inst. Met*, 2007, vol.60, no.4, p.1-8.

Strojniški vestnik - Journal of Mechanical Engineering 54(2008)7-8, 531-538
UDC 621.9:669.14
Paper received: 12.09.2007
Paper accepted: 19.12.2007

Experimental Examination of Main Cutting Force and Surface Roughness Depending on Cutting Parameters

Ihsan Korkut[1,*] - Mehmet Boy[2]
[1] Gazi University, Turkey
[2] Karabük University,Turkey

Main cutting forces acting on cutting tool depending on cutting parameters when machining AISI 1117 steel were examined experimentally. Experimental results obtained were compared with the empirical results. For the experimental studies, a Kistler 9257A three component (Fc, Ff and Fp) piezoelectric dynamometer was used to measure cutting forces. This dynamometer was associated with a 5019 B130 charge amplifier connected to a PC running Kistler Dynoware force measurement software. The empirical results were obtained through Kienzle approach. Five different cutting speeds, five different feed rates and two different depth of cuts were used in the experiments. It was observed that cutting forces decreased as the cutting speed increased and increased by the feed rate. Experimental results also showed similar trends with the empirical results. At the end of experiments, it was observed that surface quality increased by with increasing cutting speed and decreased with increasing feed rate.

Keywords: machining, steel, cutting forces, surface roughness, cutting parameters

0 INTRODUCTION

Cutting forces developed during machining influence cutting performance and unit part cost directly. Although cutting edges of tools used in machining metals and their alloys are sharp enough, they hardly bear high stresses developed during machining. So, many researches have been performed to determine ideal tool geometry and optimum cutting tool cross section which facilitates machining metals. Making use of the contemporary computer technology in machining, many problems encountered in conventional machining have been eliminated. Significant improvements in mechanics of machining have been achieved by using computers software to estimate cutting forces and stress values before machining [1] and [2].

It can be seen from various studies that cutting forces have a direct influence on various cutting parameters such as; cutting speed, feed rate, depth of cut, rake angle and cutting tool life. Therefore various force measurement methods have been developed to this relationship. It is known that piezoelectric, thermo-electric, photoelectric, load-cell etc. transducer type dynamometers developed for cutting force measurements are known to convert the mechanic energy to electric signals by measuring the strain [2] and [3].

There are also various experimental studies for direct cutting force measurements along with estimating cutting forces depending on the cutting parameters. Simple analytic models are also used to show effects of cutting parameters such as cutting speed and feed rate [4] and [5].

In this work, the cutting parameters which effect main cutting forces acting on the cutting tool when orthogonal machining was examined.

1 MATERIALS AND METHOD

The machining tests were performed by single point continuous turning of AISI 1117 steel specimens in cylindrical form on a Johnford TC35 CNC turning centre, with a variable spindle speed of up to 4000 rpm and a power rating of 10 kW. The workpiece specimens were 400 mm long and 60 mm in diameter. Prior to the tests, the surfaces of the specimens were turned at 1 mm depth of cut to remove any possible hardened layers, scale, defects or other impurities. The chemical composition of the workpiece materials is given in Table 1. Coolant was not used during the tests. The cutting tools used were commercial grade cemented carbide inserts produced by Stellram with the geometry of SCMW 12 M508-S2F in accordance with ISO 1832. These inserts did not have chip breaker and are recommended

[*]Corr. Author's Address: Gazi University,Technical Education Faculty, 06500, Besevler, Ankara, Turkey
ikorkut@gazi.edu.tr

for machining steels at high cutting speeds due to their high wear resistance. The grades of these inserts were between P10 and P20.

These inserts were clamped mechanically on a rigid tool holder with an ISO designation of SBCR 25 25 M12. The cutting parameters are given in Table 2. The cutting parameters were chosen by taking into consideration the recommendations in ISO 3685 [6].

Surface roughness measurements were carried out on the machined surfaces using a Mitutoyo Surftest 211 instrument. Three measurements were made on the each surface. Cutting force was measured with a Kistler 9257A three component piezoelectric dynamometer and an associated 5019 B130 charge amplifier connected to a PC employing Kistler Dynoware force measurement software. Fig. 1 shows the dynamometer and the tool holder.

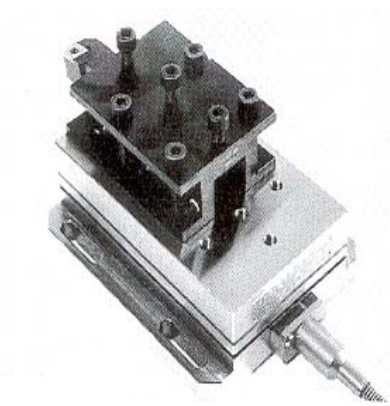

Fig. 1. *Kistler 9257A dynamometer and the tool holder*

According to Kienzle, main cutting force (FC); is equal to product of cross-section of chip and specific cutting resistance of workpiece material.

$$F_C = A_0 \,.\, k_s \tag{1}$$

where, A_0: is cross-section area of chip (mm^2) and k_s specific cutting resistance (N/mm^2). To calculate the cutting force for many machining operations, F_C is determined by this approach. In this calculation, chip geometry is important. The most important factor which determines the chip cross-section is cutting edge angle (Fig. 2).

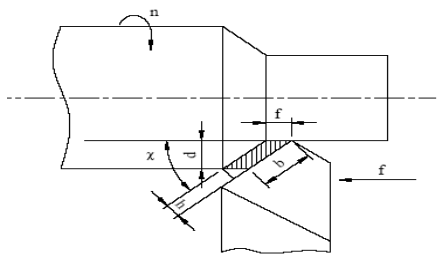

Fig. 2. *Relationship between chip cross-section and cutting edge*

In figure 2, (χ) stands for cutting edge angle, and can be written as as $A_0 = a.f$ or $A_0 = b.h$ chip cross-sectional area. Cutting edge angle can be found as

$$\sin\ (\chi)\ = \frac{h}{f} \tag{2}$$

so, we can write following equations for chip width and chip thickness, respectively:

$$b\ = \frac{a}{\sin(\chi)} \tag{3}$$

$$h = f \times \sin(\chi) \tag{4}$$

Specific cutting resistance used in calculation of main cutting force (FC) is found by following equation:

$$k_s\ =\ \frac{k_{11}}{h^m} \tag{5}$$

where: k_{11} specific cutting force of a section where h = 1 mm and b = 1 mm; m: a constant value depending on the type of material which is the characteristic slope of the curve showing logarithmic relation between k_s value and h value. Specific cutting resistance decreases by increasing chip thickness (h). m value is always different for each material.

As reported by many experimental researches, there are different factors effecting main cutting force during machining.

Cutting speed factor (k_v), rake angle factor (k_γ), tool wear factor (k_α) and cutting tool material factor (k_t) are the most significant factors. Similarly, use of the following equation to calculate k_γ is a common application.

$$k_\gamma\ = \frac{C - 1.5\gamma}{100} \tag{6}$$

Table 1. *Chemical composition of the workpiece material*

C	Si	S	P	Mn	Ni	Cr	Mo	Cu	Al	Nb	Ti	W	Pb	Sn
.114	.004	.382	.076	1.48	.345	.098	.027	.065	.011	.002	.001	.037	.002	.034

Table 2. *The cutting parameters used for the tests*

Group No.	Experiment no.	Cutting speed V m/min	Feed rate f mm/rev	Depth of cut a mm
1	1-5	50, 75, 100, 125, 150	0,10	1
2	1-5	50, 75, 100, 125, 150	0,15	1
3	1-5	50, 75, 100, 125, 150	0,20	1
4	1-5	50, 75, 100, 125, 150	0,25	1
5	1-5	50, 75, 100, 125, 150	0,30	1
6	1-5	50, 75, 100, 125, 150	0,10	2
7	1-5	50, 75, 100, 125, 150	0,15	2
8	1-5	50, 75, 100, 125, 150	0,20	2
9	1-5	50, 75, 100, 125, 150	0,25	2
10	1-5	50, 75, 100, 125, 150	0,30	2

where C is a constant and is determined depending on the type of material (for steel materials C = 109, for casting materials C = 103).

When these factors are taken into consideration, equation giving main cutting force can be derived as ;

$$F_C = A_0\, k_s\, k_v\, k_\gamma\, k_\alpha\, k_t \qquad (7)$$

Many empirical models are used in calculation of main cutting force. Since k_s value is difference for each material, empirical results are obtained by using Equation 7 in this study and compared with experimental data [1] and [7].

2 RESULTS AND DISCUSSIONS

2.1. Evaluation of the Effect of Cutting Speed, Feed Rate and Depth of Cut on Cutting Forces

Table 3 shows average values of cutting forces developed for the uncoated cutting tool. By taking experimental results as reference, average of five different cutting speeds, and change of main cutting forces (F_c) depending on feed rate is shown in Fig. 3. It can be seen from Fig. 3 that for the five feed rates, cutting forces decrease by 14% to 27% as the cutting speed increases from 50 m/min to 150 m/min. This situation can be attributed to reaching enough level of energy needed for plastic deformation of material, a decrease in friction between cutting tool rake face and chips, and moving chips from flow zone fast [4] and [8] to [9].

When the cutting speed is increased from 50 to 100 m/min, cutting forces decrease by 16% to 24% (Fig. 3). It can be seen from Fig. 4 that for the five cutting speeds, cutting forces increased by 70% to 92% as the feed rate increased from 0.1 to 0.3 mm/rev.

Experimental results show that in contrast to cutting speed, increasing feed rate improves cutting force. Equation 1 defines this relationship between cutting force and feed rate. It can be seen from Table 3 that cutting force increase by 108% to 228% as the depth of cut is increased from 1 to 2 mm. It was observed that the cutting forces peak at 2 mm depth of cut and 50 m/min cutting speed. This situation can be attributed to excessive friction between cutting tool rake face and chip at low cutting speed.

Regular decrease is seen in main cutting force values (between 25% to 56%) when cutting speed is increased from 50 to 150 m/min with 2 mm depth (Fig.5). This situation can be attributed to reaching enough level of energy needed for plastic deformation of material, decreasing shear angle and decreasing friction between tool-chip interface. When theoretical approach is taken into consideration, cutting speed factor (k_v) decreases when cutting speed decreases, so main cutting force decreases in calculation of main cutting force.

Table 3. *Main cutting forces obtained for different cutting speeds, feed rates and depth of cuts*

Cutting Speed *V* m/min	Feed rate *f* m/rev	Depth of cut *a* mm	Exp. no.	Main cutting forces (*N*)			Depth of cut *a* mm	Exp. no.	Cutting Forces (*N*)		
				F_C Exp.	F_C Emp.	Deviation %			F_C Exp.	F_C Emp.	Deviation %
50	0.10	1	1	283	271	4.24	2	26	745	656	-13.56
	0.15		2	364	335	7.96		27	993	886	-12.07
	0.20		3	379	347	8.44		28	1260	1128	-11.7
	0.25		4	433	401	7.39		29	1373	1236	-11.08
	0.30		5	483	483	0		30	1586	1412	-12.32
75	0.10	1	6	267	251	5.99	2	31	691	638	-8.3
	0.15		7	339	311	8.25		32	832	822	-1.21
	0.20		8	363	322	11.29		33	983	1000	1.7
	0.25		9	409	373	8.8		34	1163	1185	1.85
	0.30		10	458	448	2.18		35	1348	1378	2.17
100	0.10	1	11	229	244	-6.55	2	36	574	591	2.87
	0.15		12	285	302	-5.96		37	772	794	2.77
	0.20		13	295	313	-6.1		38	937	971	3.5
	0.25		14	342	362	-5.84		39	1137	1154	1.47
	0.30		15	441	435	-3.4		40	1248	1251	0.23
125	0.10	1	16	238	239	-0.42	2	41	540	580	6.89
	0.15		17	290	296	-2.06		42	752	781	3.71
	0.20		18	290	307	-5.86		43	905	952	4.93
	0.25		19	339	354	-4.42		44	996	1075	7.34
	0.30		20	422	426	-0.94		45	1141	1226	6.93
150	0.10	1	21	228	236	-3.5	2	46	476	554	10.46
	0.15		22	267	293	-9.7		47	740	763	3.01
	0.20		23	274	304	-10.94		48	880	942	6.58
	0.25		24	326	351	-7.66		49	940	1064	11.65
	0.30		25	414	422	-1.89		50	1076	1213	11.29

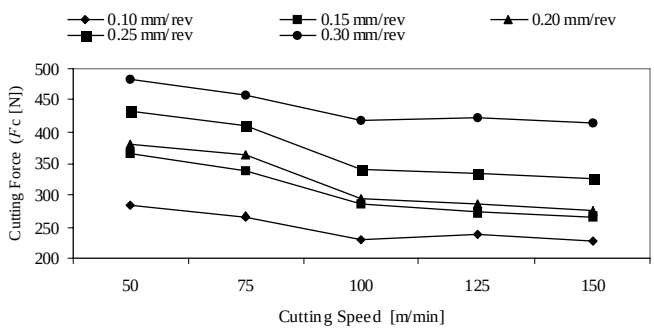

Fig. 3. *Main cutting force variations depending on the cutting speed at 1 mm depth of cut when machining with uncoated cutting tool*

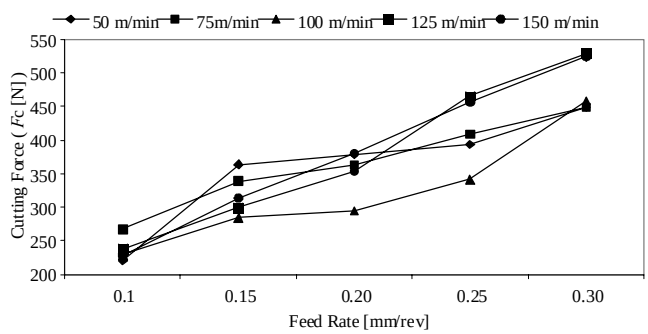

Fig. 4. *Cutting force variations depending on feed rate at 1 mm depth of cut when machining with uncoated cutting tool*

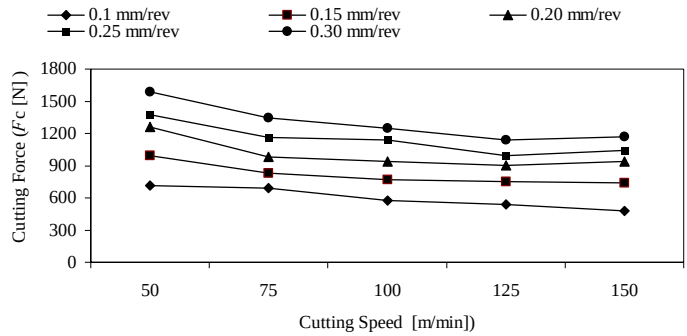

Fig. 5. *Cutting force variations depending on the cutting speed at 2 mm depth of cut when machining with uncoated cutting tool*

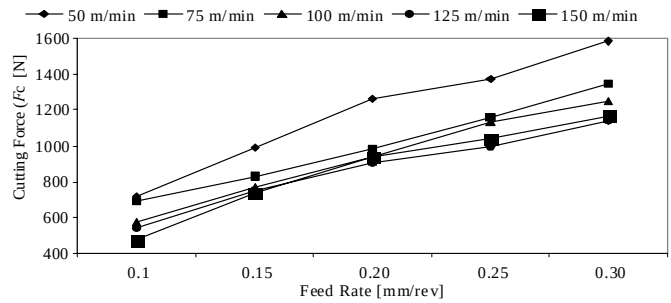

Fig. 6. *Cutting force variations depending on feed rate at 2 mm depth of cut when machining with uncoated cutting tool*

At 2 mm depth of cut, it can be seen from Fig. 6 that for the five cutting speeds, cutting forces increased by 95% to 126% as the feed rate increased from 0.1 to 0.3 mm/rev.

There is not enough and certain information in the literature for k_s value of AISI 1117. For determination of k_s value, various experimental studies were performed and main cutting force obtained through these experiments was used. Using Equation 7, k_s values were found from the results obtained from the experiments and arithmetical average of them was taken. Empirical results were taken by using ks values obtained from this.

Cutting speed factor (k_v) in the equation was taken as 1.11 for 50 m/min, 1.03 for 75m/min, 1 for 100 m/min, 0.98 for 125 m/min and 0.97 for 150 m/min. Main cutting forces obtained by experimental and empirical results at 1 mm depth of cut show similar trends at all the cutting speeds (Fig 7). It was observed that there were some deviations between experimental and empirical results. Chip cross-sectional area increases with increasing feed rate, so it causes increase in the amount of deviation. Maximum deviation was observed at cutting speeds of 50 and 75 m/min. Main cutting forces obtained from experimental results are higher than empirical ones. This can be due to low feed rate in ductile materials at 1 mm depth of cut and the built-up edge (BUE) problem created by cutting speed. This situation showed that experimental work is more reliable.

Main cutting forces obtained by experimental and empirical results at 2 mm depth of cut show similar trends at all the cutting speeds (Fig. 8). Maximum deviation occurred at cutting speed of 50 m/min. These deviations originate from parameters in Equation 7. Here, the most effective factors are depth of cut (a) and feed rate (f). Other causes are k_s and cutting speed factor. Values used in empirical model are data obtained at the end. There are different values related to these parameters of AISI 1117 steel.

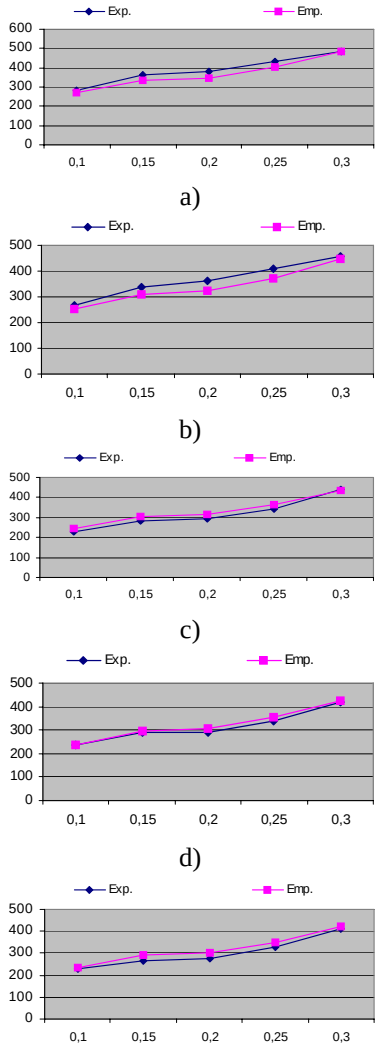

Fig. 7. *Main cutting forces obtained from empirical and experimental results at 1 mm depth of cut a) 50 m/min, b) 75 m/min, c) 100 m/min, d) 125 m/min and e) 150 m/min.*

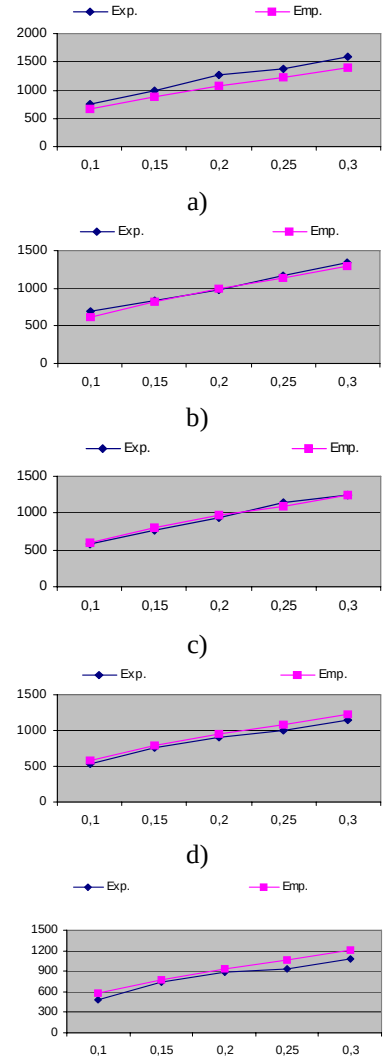

Fig. 8. *Main cutting forces obtained from empirical and experimental results at 2 mm depth of cut a) 50 m/min, b) 75 m/min, c) 100 m/min, d) 125 m/min and e) 150m/min*

2.2. Evaluation of the Effect of Cutting Speed, Feed Rate and Depth of Cut on Surface Roughness

Average surface roughness values (*Ra*) obtained for five different cutting speeds and feed rate and two different depth of cuts are listed in Table 4.

Fig. 9 shows the variation of surface roughness by cutting speed for 1 mm depth of cut and five different feed rates.

It is known that surface roughness has a decreasing trend with increasing cutting speed. The findings obtained also support the same trend. Especially, when speed increases from 50 m/min to 75 m/min, a serious improvement in surface roughness and an increased improvement in surface quality for feed rates with cutting speed are observed. When the results given in Table 4 are evaluated according to feed rate, a reverse trend of one stated for cutting speed appears (Fig. 10).

For all cutting speeds, surface quality decreases and *Ra* values increase by increasing feed rate. In theoretical approach, it is known that surface roughness increases in direct proportion of square feed rate.

According to results obtained from the experiments performed at 2 mm dept of cut, variation of surface roughness depending on cutting speed and feed rate are given in Figs. 11 and 12.

The most important result of increasing depth of cut to 2 mm is better surface quality than surface quality obtained from 1 mm depth. In normal conditions, the worsening in surface quality is expected by increase in cut depth, however a reverse trend was observed in experiment. This situation can be evaluated as negative reaction of 0.8 mm tool nose radius chosen for intermediate machining conditions. Normally, while 2.5 mm depth of cut is given as reference in ISO 3685 for 0.8 mm tool nose radius, 2 mm depth of cut also exist between boundaries given for tool nose radius of 0.8 mm (Figs. 11-12). By taking depth of cut as 1 mm, the boundaries given for tool nose radius of 0.8 mm are exceeded. Furthermore, 1 mm is a low depth of cut, so it can be said that there is a worsening in surface quality as negative effect of machine tool and tool vibrations.

3 CONCLUSIONS

The most suitable cutting speeds for 1 mm and 2 mm depth of cuts were found as 100 m/min 75 m/min respectively in terms of cutting forces. It was observed that the highest cutting forces were obtained at lower cutting speeds. Cutting forces decreased when cutting speed was increased. It was also observed that cutting forces increased with increasing feed rate.

Considering *Ra* and cutting parameters it was observed that increasing cutting speed improves the surface quality but increasing feed rate worsens it. These findings are in agreement with the literature. By increasing depth of cut from 1 to 2 mm, a trend of improvement in surface quality was observed. This situation shows that 1mm depth of cut is not suitable for 0.8 mm tip radius which is suitable for intermediate cutting conditions.

Table 4. *Average surface roughness obtained from different cutting parameters*

Cutting Speed *V* m/min	**Feed rate *f* mm/rev**	**Exp. no.**	**Depth of cut *a* mm**	**Average surface roughness µm**	**Exp. no.**	**Depth of cut *a* mm**	**Average surface roughness µm**
50	0.1	1	1	4.6	26	2	2.52
	0.15	2		5.23	27		3.3
	0.20	3		5.12	28		3.55
	0.25	4		5.35	29		4.31
	0.3	5		5.75	30		5.14
75	0.1	6	1	2.97	31	2	1.95
	0.15	7		3.72	32		2.39
	0.20	8		3.58	33		3.18
	0.25	9		3.59	34		3.52
	0.3	10		4.74	35		4.64
100	0.1	11	1	2.42	36	2	1.63
	0.15	12		2.92	37		1.82
	0.20	13		2.76	38		2.49
	0.25	14		3.11	39		3.18
	0.3	15		4.41	40		4.39
125	0.1	16	1	1.88	41	2	1.29
	0.15	17		1.98	42		1.56
	0.20	18		2.43	43		2.14
	0.25	19		2.8	44		2.75
	0.3	20		4.35	45		4.23
150	0.1	21	1	1.51	46	2	1.1
	0.15	22		1.73	47		1.52
	0.20	23		1.96	48		1.9
	0.25	24		2.69	49		2.37
	0.3	25		4.25	50		4.37

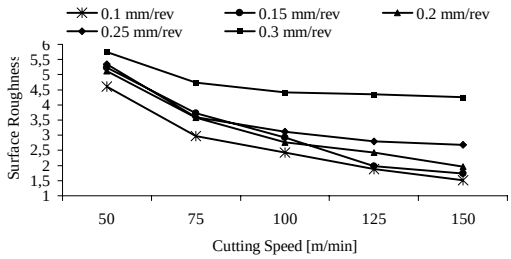

Fig. 9. *Average surface roughness variations depending on cutting speed at 1 mm depth of cut*

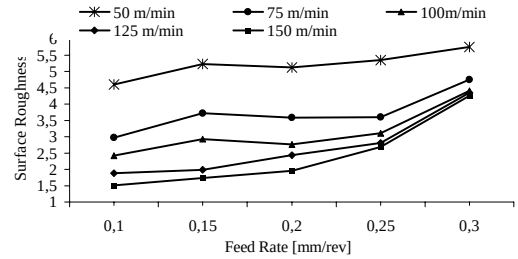

Fig. 10. *Average surface roughness variations depending on feed rate at 1 mm depth of cut*

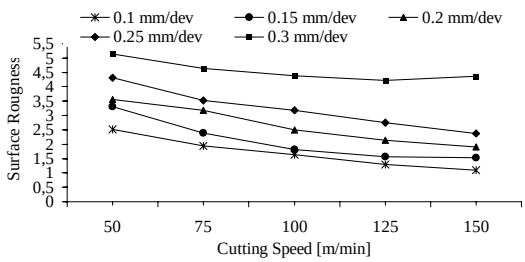

Fig. 11. *Average surface roughness variations depending on cutting speed at 2 mm depth of cut*

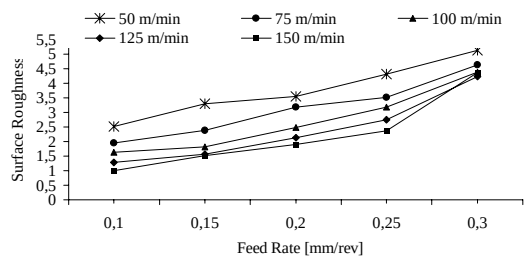

Fig. 12. *Average surface roughness variations depending on feed rates at 2 mm depth of cut*

3 ACKNOWLEDGEMENT

The authors would like to acknowledge Gazi University Scientific Research Projects (07/2004-29) for the financial support throughout this study.

4 REFERENCES

[1] Seker, U. Lecture Notes, Tool Design in Machining Production, Gazi University Institute of Science and Technology, Ankara, 2000.

[2] Shaw, M.C. Metal Cutting Principles, Oxford University Press, London, 1984. Sikdar, S. K., Chen, M., Relationship between tool flank wear area and component forces in single point turning, *Journal of Material Processing Technology,* 2002, no.128, p.210-215.

[3] Wang J., The effect of the multi-layer surface coating of carbide insers on the cutting forces in turning operations, *Journal of Material Processing Technology*, 2000, no.97, p.114-119.

[4] Strafford, K.N., Audy, J. Indirect monitoring of machinability in carbon steels by measurement of cutting forces, J. Mater. Process. Technol, 1997, no.67, p. 1–3, p. 150–156.

[5] ISO 3685, Tool Life Testing, International Standard Organisation, 1992.

[6] Gunay, M., Korkut, I, Aslan, E., Seker,U. Investigation of the effect of rake angle on main cutting force, International Journal of Machine Tools & Manufacture, 2004, no.43, p.953-959.

[7] Benardos, P.G., ve Vosniakos, G.C., Predicting surface roughness in machining: a review International Journal of Machine Tools and Manufacture, 2002, 43, p.833-844.

[8] Huang, L.H., Chen, J.C. ve Chang, T., Effect of Tool/Chip Contact Length on Orthogonal Turning Performance, *Journal of Industrial Technology*, 1999, p.15-2.

Strojniški vestnik - Journal of Mechanical Engineering 54(2008)7-8, 539-546
UDC 681.586, UDC 621.38
Paper received: 20.07.2007
Paper accepted: 19.12.2007

Modelling and Analysis of a Combined Electronic and Micro-mechanical System

Maja Atanasijević-Kunc[1,*] - Vinko Kunc[2] - Janez Diaci[3] - Rihard Karba[1]
[1] University of Ljubljana, Faculty of Electrical Engineering, Ljubljana, Slovenia
[2] IDS d.o.o. Integrated circuits, Ljubljana, Slovenia
[3] University of Ljubljana, Faculty of Mechanical Engineering, Ljubljana, Slovenia

The modelling of micro-mechanical systems in combination with integrated electronic circuits is a complex task demanding a knowledge of mechanical and microelectronic design in combination with system-modelling expertise, especially in cases where new possibilities regarding system construction and its properties are taken into account. Such modelling is becoming increasingly important because of the rapid growth of so-called "smart sensor" applications based on micro-mechanical devices. Our task was to create a reliable model of a micro-mechanical acceleration sensor that uses an extremely small and easy-to-produce mechanical system. The suspended mass and the output signal of this sensor are one order of magnitude smaller than existing systems. The described model was used for the further development of the mechanical and electrical parts of the system. The modelling inputs were the measurement data of the prototype devices, comprising the static characteristics of the device and the system responses to step-function excitation. Together with known physical properties and basic theoretical equations these data enabled us to create the described model, which showed good agreement with the measurement results.

Keywords: micro-mechanical system, modelling, acceleration sensor, control design

0 INTRODUCTION

Micro-mechanical devices are mechanical systems where the sizes of the features are in the micron or even sub-micron range. These devices are produced using techniques that are similar to those used in micro-electronic production; this makes the two technologies very compatible. The micro-mechanical system can be a stand-alone element or it can be realized as an integral part of the micro-electronic system. The result is a system comprising an electrical part that is capable of the complexity offered by the existing capabilities of micro-electronic technology and a mechanical part that can be produced with extremely precise dimensions.

If the mechanical part is a stand-alone element it is normally produced using a bulk micro-machining technology. This technology enables three-dimensional mechanical design, where the dimensions of the suspended element are in μm and the mass is measured in mg [9], [12], [15] and [16]. More recent systems use a surface micro-machining technology, where the mechanical part is produced on top of the electronics in the post-processing steps following the usual production of micro-electronic devices [2], [3] and [5]. There are, however, severe limitations imposed on the surface of the micromachined mechanical part due to currently available production techniques. The choice of material for the mechanical part is mainly limited to silicon and silicon oxide, and the geometry of the mechanical design is predominantly two dimensional as the thickness of the element is limited to a few μm. Of course the suspended mass in such systems is much smaller than that of bulk micro-machined devices and is typically in the range of μg.

The system described in the paper goes one step further. To ensure minimum production costs, which is a very important aspect of the design, the mechanical part is reduced to a single cantilever with extremely small dimensions (490 x 211 x 0.9 μm). The resulting suspended mass is only 0.23 μg, which is 3-4 orders of magnitude lower than bulk micro-machined devices and an order of magnitude lower than typical surface micro-machined devices.

Also the capacitive position sensing is much more demanding in the described system

*Corr. Author's Address: University of Ljubljana, Faculty of Electrical Engineering, Tržaška 25, SI-1000 Ljubljana, Slovenia, maja.atanasijevic@fe.uni-lj.si

due to the extremely small dimensions. The capacitance of the sensing capacitor in the case of bulk micro-machined devices is typically 10-20pF, and in the case of surface micro-machined devices it is typically 1-2pF. In the described system the sensing capacitor's capacitance is only 0.1pF.

In our case the situation was made worse because the described system only uses a one-sided sensing capacitor, while typical solutions make use of differential capacitive sensing [2], [3], [5], [9], [12], [14] and [16]. To cope with the problem of an extremely small mechanical device we had to construct a system model that would be reliable and accurate enough for engineering purposes, while still suitable for a complete system simulation that involves both open and closed-loop operation with pulse-width-modulated electrostatic force feedback.

1 MATHEMATICAL SYSTEM MODELLING

The development of the model can be divided into two main phases. In the first phase a theoretical model based on the proposed geometry of the mechanical part and the physical properties of the material used was constructed. To make this model usable in practise for the simulation and animation it had to be simplified and transformed into a discrete-element system with the minimum degradation of model performance. This model provided the basic data on the predicted performance of the mechanical part, which was then translated to the required specifications for the electronic part of the system. The electronic design team was able to meet the demands made by the extremely small signal of the sensor (approximately 50 electrons resolution in a 200Hz signal bandwidth) so the production of prototype samples was started.

The second modelling phase applied the measurements of the prototype samples for model improvement. The improved model showed good matching with the measurement results, which gave us the confidence to belive it could be used for further development of the measurement system. This model was later successfully used for closed-loop system development comprising pulse-width electrostatic feedback and variations of the system with different measurement ranges.

1.1. The Theoretical Model

The geometry of the mechanical part was governed mainly by the desire for simple and cheap production of the sensor system. This limited the mechanical system to a single cantilever of 490 μm in length, 211 μm wide and 0.9 μm thick. At one end it was attached to the bulk silicon, and at the other end it was free to move. The cantilever beam was placed above the measurement electronics, comprising three capacitor plates forming capacitance to the beam. The beam was electrically connected to the ground node of the measurement electronics. The basic physical situation is presented in Fig. 1, which shows a cross-section of the micro-mechanical measurement system.

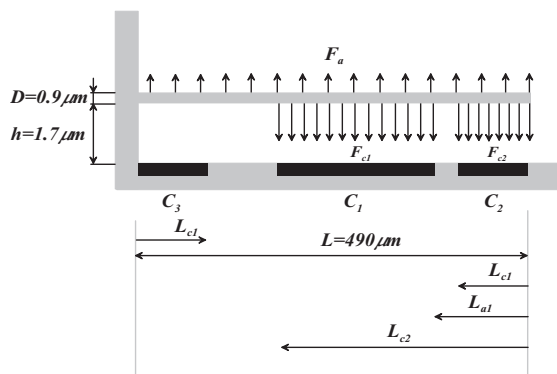

Fig. 1. *The cross-section of the micro-mechanical system*

Two capacitor plates form variable capacitors, with the beam acting as a grounded electrode. One capacitor (C_2 in Fig. 1) was used as a distance-measurement capacitor. In combination with capacitor 1 (C_1 in Fig.1) it was also used to apply an actuation force. Capacitor 3 (C_3 in Fig.1) was used only to verify the distance of the beam from the silicon surface.

The dynamics of the cantilever motion can generally be described by the following partial differential equation [13] (see Fig. 2):

$$\rho DB\ddot{y}(x,t) + q_{\mathrm{d}}(y,y,x,t) + EI\frac{\partial^4 y(x,t)}{\partial x^4} = q_{\mathrm{c1}}(y,x,t) + q_{\mathrm{c2}}(y,x,t) - \rho DB\alpha(t) \quad (1)$$

with the boundary conditions:

$$y(L,t)=0; \qquad \frac{\partial y(L,t)}{\partial x}=0$$

$$\frac{\partial^2 y(o,t)}{\partial x^2}=0; \qquad \frac{\partial^3 y(0,t)}{\partial x^3}=0$$

where:

$y(x, t)$ is the deflection of the beam at distance x from the tip;

ρ, D, B, L are the beam density, thickness, width and length;

E is the Young's modulus for silicon;

I is the area moment of inertia;

q_d, q_{c1}, q_{c2} are distributed loads (force per unit length);

$a(t)$ is the acceleration of the system.

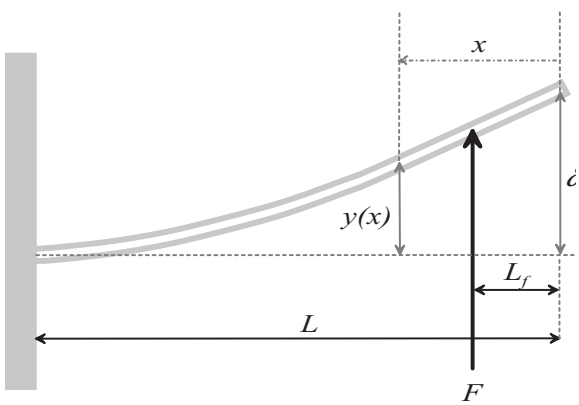

Fig. 2. *Cantilever deflection*

The distributed electrostatic forces q_{c1} and q_{c2} are of the form:

$$q_{ci}(y,x,t)=\frac{1}{2}\varepsilon B U_{ci}^{\,2}\frac{\Pi(x,L_{ci},L_{a1})}{\left(h+y(x,t)\right)^2}$$

with

$$\Pi\left(x,L_{ci},L_{a1}\right)=\begin{cases}1 & for \quad 0\le x\le L_{c1}\\ 1 & for \quad L_{a1}\le x\le L_{c2}\\ 0 & elsewhere\end{cases}$$

where index i=1 designates the first, i=2 the second capacitor, and h is the distance of the unloaded beam above the bottom surface.

The distributed damping load, q_d, can be determined from another partial differential equation [4,8,18] describing the motion of the gas (air) below the beam, which is induced by the motion of the beam.

In order to obtain the beam deflection $y(x,t)$, which is the basis for determining the output voltage, it would be necessary to numerically solve a highly non-linear system of partial differential equations, which is not suitable for dynamic simulation purposes [10].

To overcome this problem we have discretized the beam into twenty equidistant segments (L_s=L/20), and approximated the equation (1) with the corresponding boundary conditions, using the following assumptions:

$$y(x,t)\approx y\left(x_j,t\right)=y_j(t)$$

$$\frac{\partial y\left(x_j,t\right)}{\partial x}\approx\frac{1}{2L_s}\left[y_{j+1}(t)-y_{j-1}(t)\right]$$

$$\frac{\partial^2 y\left(x_j,t\right)}{\partial x^2}\approx\frac{1}{L_s^{\,2}}\left[y_{j+1}(t)-y_j(t)+y_{j-1}(t)\right]$$

$$\frac{\partial^3 y\left(x_j,t\right)}{\partial x^3}\approx\frac{1}{2L_s^{\,3}}\left[y_{j+2}(t)-2y_{j+1}(t)+2y_{j-1}(t)-y_{j-2}(t)\right]$$

$$\frac{\partial^4 y\left(x_j,t\right)}{\partial x^4}\approx\frac{1}{L_s^{\,4}}\left[y_{j+2}(t)-4y_{j+1}(t)+6y_j(t)-4y_{j-1}(t)+y_{j-2}(t)\right].$$

The result was a set of ordinary differential equations of the form:

$$m_s\ddot{y}_j(t)+b_j\left(y_j\right)\dot{y}_j(t)+k_s\left[y_{j+2}(t)-4y_{j+1}(t)+6y_j(t)-4y_{j-1}(t)+y_{j-2}(t)\right]=F_{cj}-F_{aj}(t)$$

$$j=1,2,3,\cdots,20 \qquad (2)$$

where the meaning of the notation in (2) is the following:

F_{cj} (t) is the electrostatic (point) force acting upon the j-th beam segment,

$F_{aj}(t) = m_s\, a$ is the acceleration force,

$m_s = \rho DBL_s$ is a segment mass,

$k_j = E\, I / L_s^{\,3}$ is the characteristic spring stiffness,

$b_j(y_j)$ is a damping coefficient; the damping element was omitted only at the tip segment to meet the boundary conditions.

The air-gap width between the cantilever and the silicon surface is extremely small (1.7 μm) compared to the cantilever width (211 μm). This implies that the air cannot move freely. In order to determine the damping coefficients b_j we employed the squeeze-film-damping model [18]. The basic equation of damping by an air-film squeezed between two rectangular plates is:

$$b_j\left(y_j\right)=\frac{\mu B^3 L\alpha\left(B/L\right)}{h^3\left(1+\frac{y_i}{h}\right)^3} \tag{3}$$

where μ is the dynamic (absolute) viscosity, and α is a geometry-dependent constant [18]. This formula is strictly valid only for the parallel motion of the two plates. We estimated however that this relation contains the relevant parameters and is dimensionally correct also for the spatially variable gap geometry. We also expected that we could, if necessary, modify the equation on the basis of experimental data.

The nonlinear model of the mechanical part is therefore of the 40th-order and represents in our view a suitable compromise between the requirement for accurate modelling of the relevant physical phenomena (distributed nonlinear loads, distributed detection) and the computational resources at our disposal.

1.2 The Electronic Part of the System

The design of the electronic part was mainly driven by the demand for a precise and low-noise position-measurement system. To enable simple production of the mechanical system the beam is electrically connected to the sensor-chip substrate and thus to the ground potential. The noise analysis of the system indicated that the most effective input structure would, in our case, be a simple capacitive divider, because we are using only one electrode to measure the capacitance. The capacitive divider consists of the capacitance between the sensing electrode and the grounded beam (C_x) and the excitation signal supplying the capacitor (C_r) connected between the sensing electrode and a source of the AC signal (excitation signal), as shown in Fig. 3 where the meaning of the marks is the following:

1 – grounded cantilever
2 – voltage follower system
3 – phase selective sampling
4 – subtraction and DC adjust
5 – gain
6 – DC adjust control
7 – gain control
8 – position output

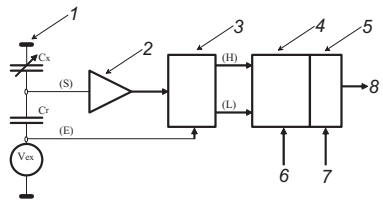

Fig. 3. *Electronical part of the system*

The beam-tip position displacement changes the capacitance of the sensing electrode to the beam (C_x - capacitor 2) and thus influences the amplitude of the signal on the node S. It can be described with the following:

$$U_{\mathrm{S}}=\frac{U_{\mathrm{E}}C_{\mathrm{r}}}{\left(C_{\mathrm{r}}+C_{\mathrm{x}}\right)} \tag{4}$$

where U_E is the peak-to-peak value of the excitation signal. Node S is a node with an extremely high impedance, so the voltage of this node cannot be directly accessed. To observe the voltage of this node a special patented voltage-follower system was designed, having only a 1fF (10^{-15}F) effective input capacitance. This was a key parameter, as the capacitance of both capacitors in the divider system does not exceed 90fF and a higher follower input capacitance would drastically reduce the available signal.

The output of the voltage follower is further processed in a system where the upper and lower peak values of the signal are sampled (signals (H) and (L)). The voltage difference of both signal peaks is calculated in next signal-processing step and the DC offset is removed using zero-position adjustment. The electronic position-measurement system thus basically transforms the displacement of the beam tip to a change in the peak-to-peak voltage of the divided excitation signal, which is further converted to a direct voltage output by means of peak-to-peak sampling. The high-level model of the electronic system must reflect three main parameters of the real electronic system.

- The first is the nonlinearity of the transformation from beam-position change

to output voltage. The change in the beam position is reflected in the change of the peak-to-peak voltage swing on node (*S*), as described in (4). This parameter is inherent in the system we are using and we can only influence it by changing the mechanical properties of the system, i.e., the distance of the beam from the measurement electrode and the stiffness of the beam. Of course the improvements in open-loop linearity (bigger distance and stiffer beam) cause a reduction of the sensitivity, and so the optimum had to be found. The linearity is not a problem in a closed-loop system as it can be greatly improved by the feedback control.

- The second is the delay of the electronic processing of the signal. This is mainly dependent on the frequency of the AC excitation signal, as the peak-to-peak measurement system requires at least one clock cycle of the AC signal to display the correct output value. Of course we want the delay to be as short as possible, especially in the case of closed-loop realization, due to potential stability problems. For this we have to increase the frequency of the AC excitation signal, where the limitation is the settling time of the voltage-follower amplifier.
- The third is the gain (*K*). For an open-loop measurement system it must be chosen so that the output-voltage swing covers the desired measurement range. In the closed-loop configuration it influences the level of system linearity and signal bandwidth. The obvious limitations are the system stability and the increase of the noise level in the loop.

For a complete system description and simulation the model of the electrical part has to be merged with the model of the mechanical part, as the properties of the electrical part can significantly influence the overall system behavior. For this reason we have decided to include in the model description all three mentioned parameters. The non-linearity of the system is incorporated through (4). The measurement-system delay, which is equal to one period of the excitation signal, was taken to be 50 μs, as this is an optimal value coming from transistor-level simulations of the measurement electronics [6] and [7]. The gain (*K*) is a parameter that we can choose to suit the system requirements. So the function of the beam deflection to the output voltage of the measurement system can be defined as:

$$U_{\text{out}} = K \frac{U_{\text{E}} C_{\text{r}}}{\left(C_{\text{r}} + \dfrac{\varepsilon A_2}{h + y(z)} \right)} \tag{5}$$

and the output is sampled every 50 μs. In (5) ε is the dielectric constant and A_2 is the area of the capacitor 2 (see Fig.2).

We should mention that the functionality and the desired properties of the electrical part itself were optimized with a simulation in SPICE [6] and [7].

1.3 Comparison of the Model to the Measurement Results

The experiments with the prototype samples were divided into observations of the static and dynamic properties. First, the electrostatic actuator system was used to apply a force to the cantilever. This system uses both capacitors in the middle and at the tip to apply the attraction force to the beam. Since the capacitor beneath the beam tip is also used for the distance measurement, the actuation and measurement function are multiplexed on the same capacitor. This results in a 50% duty ratio of actuation, which was also included into the model for force calculations. The measurements of the beam-tip deflection as a result of the electrostatic force are presented in Table 1.

Table 1. *Static characteristics of the combined system*

Actuation voltage [V]	Output voltage [V]	Tip capacitance value	Calculated applied force on the tip	Cantilever tip distance to surface	Relative position [nm]
0.0	0.00	84.86	0+11	2204	0
0.3	-0.10	85.04	1+11	2199	5
0.6	-0.28	85.37	4+11	2190	14
0.9	-0.99	86.71	9+11	2157	47
1.2	-1.74	88.15	17+12	2121	83
1.5	-2.67	90.01	28+12	2078	126
1.8	-3.91	92.58	42+13	2019	185
2.1	-5.58	96.25	62+14	1943	261
2.4	-8.13	102.2	90+16	1829	375

The actuation voltage in the first column is the voltage applied to the actuation capacitors. The output voltage is the output of the tip-capacitor measuring system. The third column represents the calculated capacitance value of capacitor number 2. The fourth column shows the calculated applied force on the cantilever tip from the actuation capacitors and from the measurement system (the excitation voltage used for the capacitance measurement also exhibits electrostatic force). Knowing the characteristics of the capacitance-measurement electronics the cantilever-tip distance to the silicon surface was then calculated as presented in the fifth column.

The described data were used to improve the static properties of the mechanical part of the model. Comparing these results to the model the obvious difference was the starting position of the cantilever. In the real system the beam was bent back so that the beam tip was 0.5 μm further from the surface than the core of the beam. This is the result of residual stress caused by the production procedure of the cantilever. To implement this in the model we applied a pull-up force along the whole cantilever length, which resulted in the beam bending observed in the measurements. We also made minor changes to the beam stiffness to fit the model to the measurements. These differences could result from the fact that the beam material was polycrystalline silicon, and from the uncertainty of the beam thickness.

The dynamic response of the system was also measured using the actuation voltage as the input stimulus. The actuation voltage was changed step-wise by 350 mV at different DC starting points of the actuation voltage. The DC starting actuation voltage created an attraction force so the beam position at the start of each step function (350 mV amplitude) was different for each measurement. The capacitance change at the beam tip, as measured by the position-sensing electronic system, was observed using a digital oscilloscope. The step change in the actuation voltage resulted in an increase of the attraction force as the capacitor voltage was increased. This additional force required a change in the beam-tip position to compensate the new value of the electrostatic force with the spring force of the cantilever. The beam movement was, of course, damped by the air-damping mechanisms. The oscilloscope shots (as shown in Figs. 4 and 6) present the time-dependent movement of the beam tip.

These results were compared to the theoretical model. Here, the differences between the model and the measurement results were bigger compared to the static measurements of the system. The measurement results showed that the damping factor was increased by more than a factor of two if the cantilever position was moved from 2204 to 1829 nm. This is an even higher ratio than the theoretically calculated factor of 1.73. This led us to the conclusion to use (in Eq. (3) in denominator) the dimensionless-gap width to the power of four in our damping calculations.

The improved model showed very good agreement with the measurement results over the whole operating range of the system, which is illustrated with two pairs of figures. In the first pair (Figs. 4 and 5) the system responses are presented for an input voltage change from 359 to 13mV. In Fig. 4 the oscilloscope plots are illustrated.

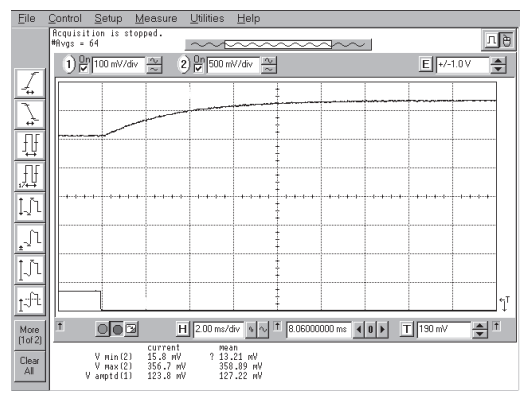

Fig. 4. *Oscilloscope plots of the transient response caused by the actuation-voltage change from 359 to 13 mV*

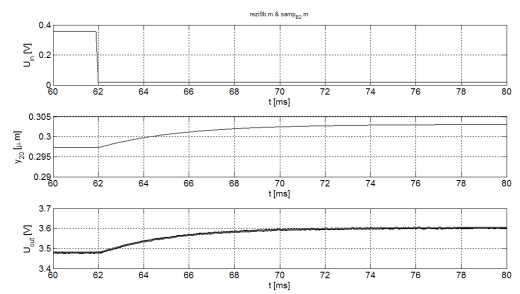

Fig. 5. *Transient responses of the model in comparison with the measurement data for the actuation-voltage change from 359 to 13 mV*

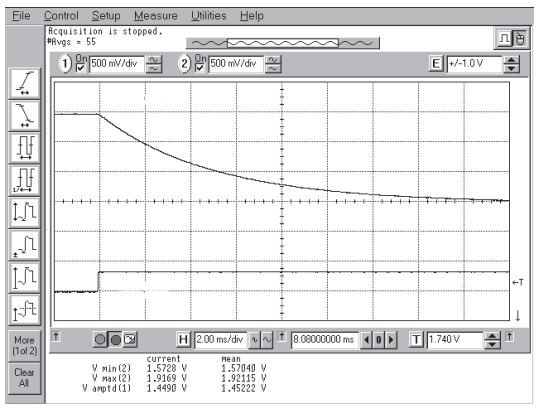

Fig. 6. *Oscilloscope plots of the transient response caused by the actuation-voltage change from 1.57 to 1.921V*

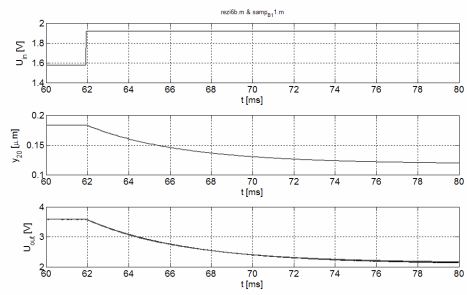

Fig. 7. *Transient responses of the model, in comparison with the measurement data, caused by the actuation-voltage change from 1.57 to 1.921V*

The oscilloscope plots present the response of the cantilever-tip position-measurement electronics as the upper trace (trace 1), and the actuation voltage as the lower trace (trace 2). The measurements below show the lower voltage level of the actuation voltage (Vmin(2)), the higher level of the actuation voltage (Vmax(2)) and the resulting difference of the position-measurement signal (Vamptd(1)). The input stimuli is a step-voltage change in the actuation voltage and the levels are Vmin(2) and Vmax(2). The time scale in all the plots is 2 ms per division.

Fig. 5 is divided into three subplots, where it is possible to observe the applied input voltage (upper part), the movement of the cantilever tip (middle part) and the corresponding output-voltage signal (lower part) of the model. In this lower part of the plot the measurement data from Fig. 4 are also presented in black color, while model responce is gray. A similar comparison of the model and the system responses are presented in Fig. 6 and 7 for an input voltage-change from 1.57 V to 1.921 V.

We should mention that the simulation of the described measurement system and the animation of the mechanical part were realized in Matlab with Simulink [11] and [17].

2 SUMMARY

The model of the presented micro-mechanical system was a team effort by specialists in the field of microelectronic design, mechanical design and control. It was developed in a cyclic procedure, where the introduced simplifications made it possible to include the whole system in the same simulation environment. Several iterations were needed because all of the system properties and parameters were not known in advance.

The starting model was based on theoretical equations and was further improved using measurement data taken from prototype devices. The development of the model involved two major steps.

The first step covered the static characteristics of the system resulting from the equilibrium of the electrical actuation force and the cantilever spring force.

The second step was the introduction of the dynamic properties governed mainly by air-damping mechanisms. The final result has a high degree of compliance with the actual measurements and has been used for the further development of the measurement system.

This model was used in the development of a closed-loop measurement system, where the beam-tip position is kept at a constant distance by the electrostatic actuator using pulse-width modulation to adjust the force. The acceleration force is measured by the amount of electrostatic force needed to keep the equilibrium position of the beam tip. The model is also being used to develop an acceleration sensor for low acceleration values where the cantilever stiffness and gas pressure are optimized for the best performance.

3 REFERENCES

[1] Atanasijević-Kunc, M., Kunc, V., Diaci, J., Karba, R., Modelling and Analysis of Combined Electronic and Micro - Mechanical System, *Proceedings of the 4th IMACS Symposium on Mathematical Modelling*, Troch, I., Breitenecker, F. (ed.), Vienna, Austria, 2003.

[2] Baschirto, A. Gola, A., Chiesa, E., Lasalandra, E., Pasolini, F., Tronconi, M., Ungaretti, T., A ±-g dual-axis linear accelerometer in a standard 0.5-µm CMOS technology for high-sensitivity applications, *IEEE Journal of Solid-State Circuits*, July 2003, vol.38, p.1292-1297.

[3] Boser, B. E., Howe, R. T., Surface micromachined accelerometers, *IEEE Journal of Solid-State Circuits*, March 1996, vol.31, p.366-375.

[4] Daugherty, R. L., Franzini, J. B., Finnemore, E. J., Fluid Mechanics with Engineering Applications, *McGraw - Hill*, 8th ed., Singapore, 1985.

[5] Gola, A., Chiesa, E., Lasalandra, E., Pasolini, F., Tronconi, M., Ungaretti, T., Baschirotto, A., Interface for MEMS-based rotational accelerometer for HDD Applications with 2.5 rad/s^2 resolution and digital output, *IEEE Sensors Journal*, August 2003, vol.3, no.4.

[6] HSPICE, Version H92, Elements and Models, User's Manual, *Meta-Software*, 1992.

[7] HSPICE, Version H92, Analysis and Methods, User's Manual, *Meta-Software*, 1992.

[8] IJntema, D. J., Tilmans, H. A. C., Static and dynamic aspects of an air-gap capacitor, *Sensors and Actuators*, 1992, A, 35, p.121-128.

[9] Marco, S., Samitier, J., Herms, A., Morante, J. R., Analysis of electrostatic - damped piezoresistive silicon accelerometers, *Sensors and Actuators*, 1993, A37 - 38, p.317-322.

[10] Matko, D., Karba, R., Zupančič, B., Simulation and modeling of continuous systems, A case study approach, *Prentice Hall*, 1992.

[11] MATLAB, The Language of Technical Computing, Version 5, *The MathWorks Inc*., 1999.

[12] Matsumoto, Y., Esashi, M., Integrated capacitive accelerometer with novel electrostatic force balancing, *Technical Digest of the 11th Sensor Simposium*, 1992, p.47-50.

[13] Popov, E. P., Engineering Mechanics of Solids, *Prentice Hall*, , 1990, New Jersey.

[14] Rudolf, F., Jornod, A., Bencze, P., Silicon microaccelerometer, Transducers'87, 1987, p.395-398.

[15] Rudolf, F., Jornod, A., Bergqvist, J., Leuthold, H., Precision accelerometers with µg resolution, *Sensors and Actuators*, , 1990, A21-A23, p.297-302.

[16] Siedel, H., Riedel, H., Kolbeck, R., Mück, G., Kupke, W., Königer, M., Capacitive silicon accelerometer with highly symetrical design, *Sensors and Actuators*, , 1990, A21-A23, p.312-315.

[17] Simulink, User's Guide, *The MathWorks Inc*. 1999.

[18] Starr, J. B., Squeeze-film Damping in Solid-State Accelerometers, *IEEE Solid-State Sensor and Actuator Workshop*, , June 1990, Hilton Head Island, p.44-47.

Strojniški vestnik - Journal of Mechanical Engineering 54(2008)7-8, 547-556
UDC 696.135, UDC 628.3
Paper received: 06.12.2007
Paper accepted: 12.03.2008

Experimental Investigations of Porosity and Permeability of Flocs in the Suspensions of Biological Water Treatment Plants

Boštjana Žajdela[1,*], Matjaž Hriberšek[2], Aleš Hribernik[2]
[1] Regionalna razvojna agencija Mura, Slovenia
[2] Univerza v Mariboru, Fakulteta za strojništvo, Slovenia

This paper deals with the movement of flocs in suspension, as they appear in biological wastewater treatment (BWT) plants. Basic equations for solving the problem and analysis of wastewater composition of BWT plant Lendava are presented. Greater attention is given to the geometrical and sedimentation characteristics of solid flocs, key parameters for developing a fast numerical procedure for simulating flocs' movements. An extensive analysis regarding floc size distribution and settling velocity is presented. Based on the results of experimental investigations, the main physical parameters of the flocs are defined and calculated by considering floc porosity.

Keywords: wastewater treatment, biological treatment plants, sedimentation, permeability

1 DESCRIPTION OF PROBLEM

Monitoring and predicting processes within multiphase compounds, when acting as working material in biological wastewater treatment plants, is closely linked to understanding the phenomena relating to transfer, such as the transfer of momentum, heat and mass. In regard to those processes running within biological wastewater treatment plants, the most common forms of multiphase systems are solid-liquid and solid-liquid-gas. The impact of solid particles on transfer processes in such systems is, therefore, one of the key factors needing to be considered in order to provide an accurate description of processes within biological wastewater treatment plants. Solid impurities of either organic (algae, bacteria, remains of dead organisms) or inorganic (clay, silt, soil, mud, sand) origins are normally heavier than water. Sedimentation in the sedimentation pool is intended for clearing the wastewaters of suspended mass with density higher than those of the surrounding water. Particle movement accelerates for as long as form resistance and liquid friction forces at the particle's surface do not equal the gravity and buoyancy. Form resistance is normally considerably higher than friction resistance, thus allowing for the latter to be ignored.

Considerable influence on sedimentation duration is exercised by the sludge flocs' shapes (influencing the drag coefficient), the sizes of primary particles and sludge flocs, the permeability of sludge flocs and their densities. These parameters are also important when modelling the flocs' sedimentation.

In earlier work [1] we payed greater attention to determining the size distributions and main geometrical parameters of the sludge flocs, by means of image analysis. Additionally, free-settling tests were used in connection with empirical models for determining drag coefficient (C_d), in order to evaluate the flocs' densities.

Image analysis is often used for size analysis. Li and Ganczarczyk [2] and [3] used image analysis to examine the size distributions and internal structures of activated sludge flocs. Their work focused on automated image analysis for characterizing sludge settling properties and to obtain sludge concentration data.

The internal structure of an activated sludge floc is porous. Flocs are composed of several primary particles. Lee et. al. [4] estimate that the diameter of primary particles is between 1 and 20 μm. Li and Ganczarczyk [2] arbitrarily took d_p as between 1 and 10 μm and they used the 2 μm diameter of a primary particle for permeability porosity correlations. Also Huang [5] determined that the size of a primary particle's

*Corr. Author's Address: Boštjana Žajdela, Regionalna razvojna agencija Mura, Slovenia
bostjana.zajdela@rra-mura.si

diameter is smaller that 10 μm. Jorand et al. [6] analysed floc structure, which was obtained by breaking-down activated sludge flocs using ultrasound. They estabished that in activated sludge flocs the predominating macrofloc size was 125 μm. These are formed from 13 μm microfloc aggregates, which are made up of smaller particles of size 2.5 μm.

Floc porosity does not only influence their density; it also enables internal permeation of liquid through particles. In practice this fact is often neglected [7] and [8], although research into this theme does exist. Floc porosity according to Huang [5] increases (density decreases) as floc size increases. Lee et al. [4] came to the same conclusions when investigating settling activated by drilling sludge floc from a sea's bottom. They state that permeability might change from 10^{-17} to 10^{-8} m^2. Mutsumoto and Suganuma [9] experimentally researched the effect of permeability on the settling velocity of a porous sphere by using a permeable model floc made of steel wool and ascertained that the effect of permeability on a model floc's settling velocity can be neglected at lower values. Li and Yuan [10] presented data on the permeability of microbial aggregates for an activated sludge treatment plant and ascertain that flocs (1.0 – 2.5 mm) are porous and fractal. Here settling velocities were only slightly higher as those predicted by Stoke's law for identical but impermeable particles. Microbial aggregates could have largely reduced permeability, as the pores between the microorganisms in the aggregates may be clogged.

In most studies, ρ_p density of primary particle, is assumed to be equal to the dry density of aggregate ρ_{SS} [7] and [11], which is true if the primary particle does not contain liquid. Li and Yuan [10] observed the settling of activated sludge in liquid of different densities, and ascertained that the density of an individual cell (primary particle) is 1.059 g/cm^3. Lee et al. [4] used a free-settling test for estimating activated sludge floc density. Their estimation was obtained on the basis of a single floc's terminal velocity and its diameter.

This paper describes a procedure for defining those floc characteristics that influence the course of interaction with the liquid phase and are necessary for numerical modelling of floc sedimentation. By processing images, taken through a microscope, and recording floc projections at three basic levels, we calculated the volumes of the flocs and evaluated their morphological characteristics. Then the flocs were recorded during free sedimentation and the images processed using software which defined the sizes of flocs and their locations on the images. By considering the time-interval between two successive shots (0.75 s), it was possible to calculate the flocs sedimentation velocities. The experimentally defined results were used to develop empirical models for porosities and densities of flocs.

2 FLOC SEDIMENTATION MODELLING

2.1 Basic Equations

Floc sedimentation can be simulated using a simplified model of force balance for a floc:

$$m_k \frac{d\vec{v}_k}{dt} = -\frac{1}{8}\pi\rho_t d_k^2 \Omega C_d \left|\vec{v}_k - \vec{v}_t\right|(\vec{v}_k - \vec{v}_t) + \frac{1}{6}\pi d_k^3(\rho_k - \rho_t)g \quad (1)$$

this model considers inertial force and dynamic buoyancy, the other forces being ignored as previous research has shown [1] that Reynolds number values are (Re) < 3. This ensures that the importance of drag coefficient (C_d), comprising the flow characteristics of floc and the resistance forces ratio between permeable and impermeable floc (Ω), will be calculated with an appropriate empirical model. Namely a model will be selected which will predict sedimentation velocity based on particle permeability closest to the measured sedimentation velocity.

A generalized Stoke's model for terminal sedimentation velocity calculation (2) considers the force balance of the resistance force, the buoyancy and gravity:

$$v_s = \left[\frac{4g(\rho_k - \rho_t)d_k}{3\rho_t C_d}\right]^{\frac{1}{2}} \quad (2).$$

Several correlations have been developed for calculating C_d for Re > 1 and flocs of non-spherical shape, which thus induced us to carry-out comparative study [1]. Based on the results of this study, the Chien [12] model was selected for impermeable flocs within the range $0.2 \leq \psi \leq 1$ and $Re < \sim 5000$:

$$C_d = (30/\mathrm{Re}) + 67.289 \cdot \exp^{(-5.03\psi)} \quad (3)$$

where the *Re* is calculated using the following expression:

$$Re = \frac{v_k \rho_t d_k}{\eta_t} \quad (4).$$

A floc consists of a large number of primary particles, having densities within the range $\rho_k < \rho_p < \rho_{ss}$ [10]. When the particles contain no liquid, then ρ_p equals ρ_{ss} [7] and [11], which does not hold in the case of activated sludge flocs. Therefore, in our case, we used the primary particle density (ρ_p =1059 g/l), as defined by Li and Yuan [10].

The force balance for floc being porous ($\varepsilon > 0$) and permeable ($\Omega < 1$), and moving steadily, can be written as follows [5] and [13]:

$$\frac{\rho_k - \rho_t}{\rho_p - \rho_t} = 1 - \varepsilon = \frac{3\rho_t \Omega C_d}{4g(\rho_p - \rho_t)d_k} v_s^2 \quad (5).$$

Although the impact of permeability is often ignored [7] and [8], and (Ω) is set to 1, we decided to consider the permeability. Therefore, expression (5) was used to derive at an expression for calculating sedimentation velocity based on porosity and permeability, which is as follows:

$$v_s = \sqrt{\frac{4g(\rho_p - \rho_t)(1-\varepsilon)d_k}{3\rho_t \Omega C_D}} \quad (6).$$

For highly-porous spheres moving steadily through an infinite medium, the (Ω) factor can be calculated using the Brinkman model, as updated by Debye [4] and [13]:

$$\Omega = \frac{2\beta^2\left[1 - (\tanh(\beta))/\beta\right]}{2\beta^2 + 3\left[1 - (\tanh(\beta))/\beta\right]} \quad (7).$$

This is done using the permeability factor (β), which is a function of a floc's diameter and its permeability:

$$\beta = \frac{d_k}{2\sqrt{k}} \quad (8).$$

Permeability (k) has been calculated by various authors according to various models. Our investigation tested those models proposed by Brinkman, Carman-Kozeny and Davies [4]:

Brinkman $$k = \frac{d_p^2}{72} \cdot \left(3 + \frac{4}{1-\varepsilon} - 3\sqrt{\frac{8}{1-\varepsilon} - 3}\right) \quad (9)$$

Carman-Kozeny $$k = \frac{\varepsilon^3}{5\left(\frac{6}{d_p}\right)^2 (1-\varepsilon)^2} \quad (10)$$

Davies $$k = \frac{d_p^2}{4} \cdot \frac{1}{16(1-\varepsilon)^{3/2}\left(1 + (56(1-\varepsilon)^3\right)} \quad (11)$$

3 FLOCS' FEATURES

3.1. Wastewater from the Lendava Biological Treatment Plant

This paper focuses on research results regarding sedimentation pool samples from the Lendava biological wastewater treatment plant (Slovenia). Wastewater samples were kept in a beaker, protected from air-inflow, for 1-3 days until performing dilution and analysis. The samples were kept at 20°C. The wastewater used during the analysis consisted of technological and municipal wastewaters in the ratio 75 : 25, the major part of the technological wastewater originating from the pharmaceutical industry. The municipal wastewater originated from the town of Lendava, and its surrounding villages.

3.2 Flocs' Shapes and Volumes

The shapes of flocs have been defined in previous studies [1], in which we estimated a 3D-shape of floc, having the face proportions of an equivalent cuboid. Our conclusion was that a floc can be approximated to a cuboid with faces in the ratios A : B : C = 1 : 0.89 : 0.69. By taking the A : B : C ratio into consideration, measurements of floc projections in plane A should suffice for estimating the remaining projected surfaces B and C, as well as the edges of the equivalent cuboid *a*, *b* and *c*. Thus we can simply estimate floc volume ($V = a \cdot b \cdot c$) and calculate the shape factor – the floc sphericity (ψ):

$$\psi = \frac{A_{\mathrm{sphere}}}{A_k} \quad (12)$$

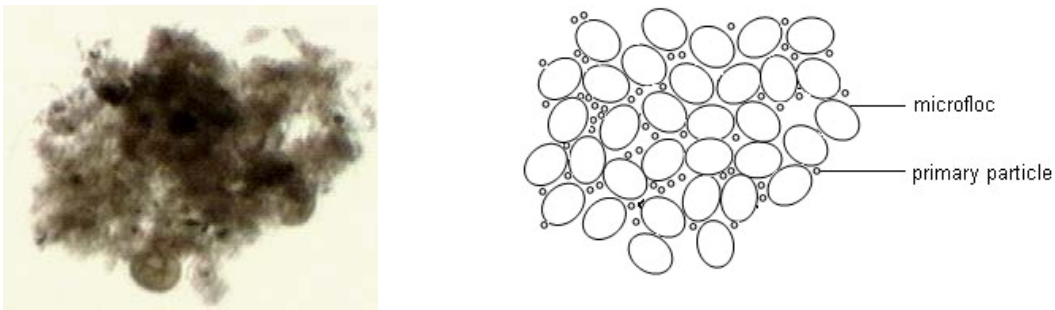

Fig 1. *Floc's image (left) and its schematic sketch (right)*

which is defined as the ratio of a sphere's surface area to the surface area of a floc with the same volume, and is used in expression (3) to calculate C_d. Sphericity, in our case, amounts to 0.796 and is very close to 0.8, the value defined by Tambo and Watanabe [7]. Figure 1 shows the grey image and schematic sketch of the floc, where its structure is evident.

It is clear from Fig. 1, that a floc consists of numerous smaller primary particles, which is emphasized in the schematic sketch of floc structure.

3.3. The Sizes of Primary Particles

The sizes of primary particles were defined using an Axiotech 25 HD (+pol) (ZEISS) stereoscopic microscope, an AxioCam MRc (D)high resolution microscopic camera with a digital interface and software (ZEISS), as well as KS 300 Rel. 3.0 image-analysis software with a supplement for true colour analysis (ZEISS). A freshly stirred (mixed for 2 hours at 600 rpm) and diluted sample (1:20) was dripped on to a microscope's slide, covered with a cover slip (transmission microscopy) and analysed at a magnification of 500x (lit with a halogen lamp). Figure 2 shows the results of microscopy. An image analysis system was used to process the images. An appropriate threshold was selected for all the images taken, in order to convert them to binary images. This then enabled automatic processing, which eventually provided morphological features of the particles (the particle surface area and diameter in relation to the equivalent circle). The results of processing Fig. 2, are shown in Fig. 3, regarding particle size distribution. Fig. 2 shows some bigger particles with characteristic fractal floc structure ($d_p > 5$ µm), which were later ignored. Also, all particles smaller than 1 µm were omitted, as the microscope is intended for processing particles up to the size of 1 µm. Thus, the resulting 70 particles rank among primary particles and have equivalent diameters between 1.077 µm and 4.746 µm, see Fig. 4.

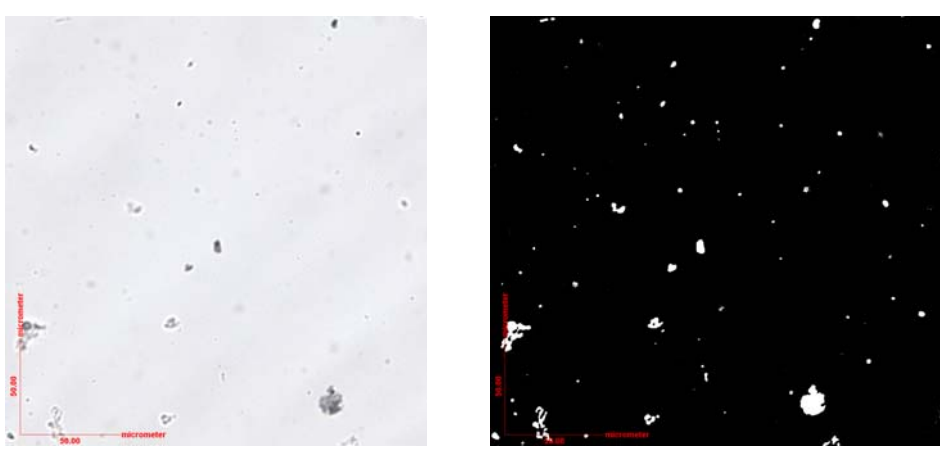

Fig. 2: *Microscopic and binary images of primary particles*

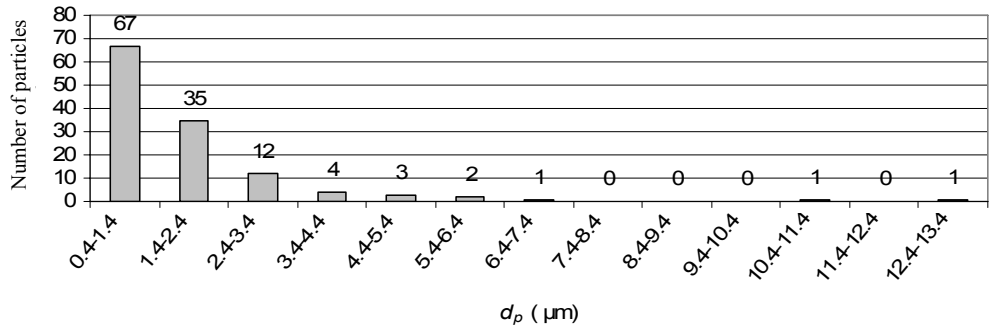

Fig.3. *Particle size distribution for particles captured in Fig. 2*

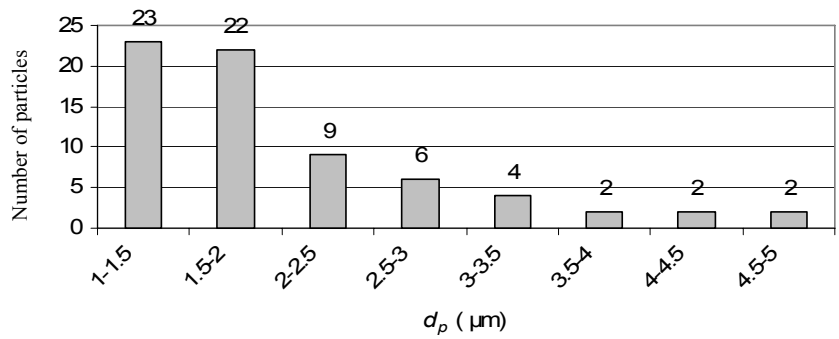

Fig. 4. *Particle size distribution*

It is evident that the majority of particles fall into the first two classes within sizes ranging from 1 µm to 2 µm, representing as much as 64.3 % of all particles.

The average diameter of all particles from Fig. 2 is 2.019 µm, which can be considered the average equivalent primary particle diameter. This value falls within the size range of primary particles (1 µm -20 µm), as stated by other authors [2], [4] to [6] and [11].

3.4 Sizes and Velocities of Floc Sedimentation

Sedimentation velocity was measured by dropping small amounts (drops) of a previously diluted sample (1:1) at 20°C into a glass tower of size 330 x 260 x 60 mm, filled with distilled water, where the floc freely sedimented. A camera was used to shoot flocs sedimentation at a depth of 230 mm.

The Nikon Hi Sence camera was used which takes shots of floc movements over set time-intervals. Images were processed using special software written in Java language, which determines position (coordinates x and y) and sizes – surfaces of each floc on the image. With a procession of successive images we can calculate the speeds of flocs and determine their route through the observed area. The time-interval between shots can be set, in our case 0.75 s. The software also computes the size – surface areas of flocs (2D projection) on the images, which is used to calculate the equivalent diameters of flocs.

The results for individual free-settling tests were merged and any change in deviation (σ) monitored by increasing the number of measurements. As evident from Fig. 5, σ decreases with the number of flocs and settles when $n > 250$. It can be assumed, with sufficient probability, that this is the lower size limit of the representative sample when defining the sizes of flocs, as well as the sedimentation velocity.

The whole sample processed by the presented method consists of 307 flocs. Their diameter ranges between 0.147 mm and 1.736 mm. Floc size distribution is presented in Fig. 6.

It is evident from Fig. 6 that the first, second and third class sizes with floc size ranging from

0.147 to 0.676 mm comprise the majority of flocs, while later on the number of flocs decreases.

Fig. 7 shows the measured velocities of the 307 flocs observed. It shows the comparison between the measured sedimentation velocities (v_k) and those velocities predicted by the general Stokes model (v_s) (Eq. 6), and by considering the drag coefficient C_d according to Chien (Eq.3) [12], the constant porosity (ε = 0.977) according to Li and Yuan [10] and the assumption of impermeable floc (the resistance forces ratio between permeable and impermeable floc (Ω =1) [4], [7]).

The measured velocity of a floc's sedimentation increases with diameter, which agrees with the results of other authors [4]. However, there is a difference between measured and calculated velocities, which is due to having applied constant floc porosities. The porous structure of flocs has a direct impact on floc density and a floc's resistance force. Further research was carried-out to observe this phenomenon and improve the empirical model for predicting the terminal velocity of floc sedimentation.

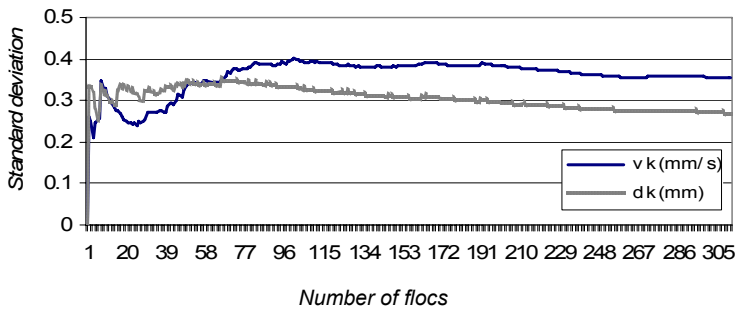

Fig. 5. *Variations in the standard deviatio diameters of flocs, as presented by the observed flocs*

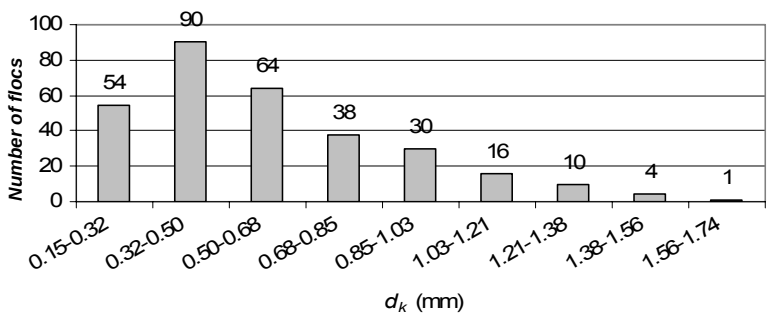

Fig. 6. *Size distribution of flocs*

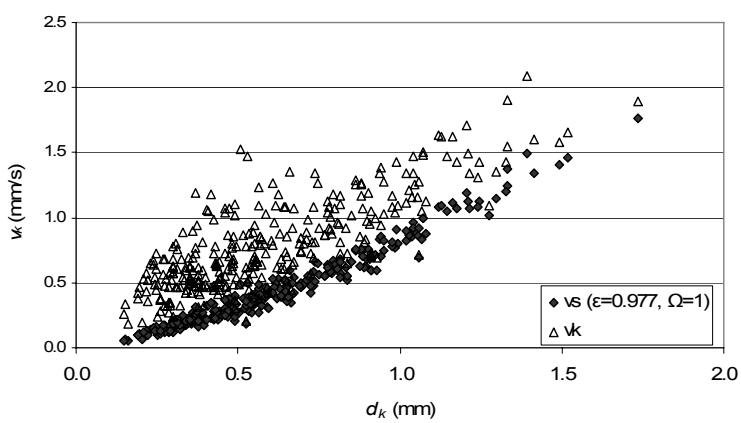

Fig. 7. *Measured velocities of flocs (v_k) in comparison with those velocities predicted using the general Stokes model (v_s) (Eq. 2)*

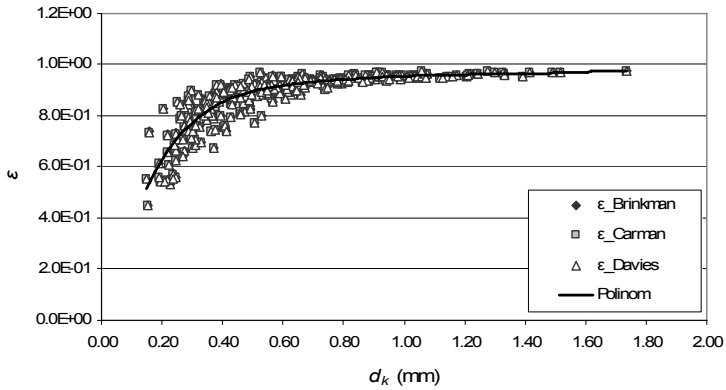

Fig. 8. *The porosities of flocs calculated using permeability models: Brinkman, Carman-Kozeny and Davies*

3.5. Permeability of porous flocs

In order to consider permeability when calculating sedimentation velocity the following models of permeability were used: (Eq. 9), (Eq. 10) and (Eq. 11). Interdependence between porosity (ε) and permeability (k) was considered when calculating the resistance forces ratio of permeable and impermeable flocs (Ω) (Eq. 7).

Combining expressions (5) and (7-11), in principle, enables the following to be stated:

$$1-\varepsilon=\frac{3\rho_t\Omega(\beta(k(d_p,\varepsilon)),d_k)C_d}{4g(\rho_p-\rho_t)d_k}v_s^{\,2} \qquad (13).$$

The expression (13) was evaluated iteratively for each of the 307 flocs previously measured considering their sedimentation velocities and equivalent diameters (Fig. 7). All the three presented models were used to calculate porosity and permeability $k(d_p,\varepsilon)$. Fig. 8 shows the calculated values for porosities.

The results show that porosity increases withthe increase in floc diameter. From 1 mm onwards, porosity does not change significantly. We also observed that the predicted trend regarding porosity, depending on floc diameter, is not influenced by the model used for calculating permeability. Any changes in porosity do not exceed 1%. For the simple calculation of porosity, we therefore derived the average regression polynomial valid within the range 0.2 to 1.8 mm, and acquired on the basis of all three sets of results:

$$\begin{aligned}\varepsilon=&-0.53d_k^6+3.61d_k^5-10.01d_k^4\\&+14.52d_k^3-11.74d_k^2\\&+5.14d_k-0.03\end{aligned} \qquad (14).$$

The expression for floc porosity, defined in such a way, has been put into expressions for permeability (9) to (11). Fig. 9 presents permeability values calculated in this manner.

In contrast to porosity, the permeability of flocs does differ when using different models, which is particularly evident for larger flocs. Yet all three models show the same trend, which is an increase in permeability with any increase in floc size, a result also observed by other authors [4].

Absolute permeability values are very small, typically about 10^{-12} m^2 which means, that the flow of liquid through a floc is very slow. In regard to the fact that the velocities of moving flocs by sedimentation are relatively large, we can conclude that the influence of permeability on the change of velocity during sedimentation is small.

Fig. 10 shows the permeability factor (β), representing the ratio between floc diameter and permeability. As it turns out, the permeability factor is the largest with small flocs (d_k < 0.5 mm) and then decreases, only to become independent of floc size for large flocs.

After calculating the permeability factor (β), Eq. (7) was used to calculate resistance forces ratio between permeable and impermeable floc (Ω), which has a direct impact on floc sedimentation velocity (Eq. (6)) and thus enables

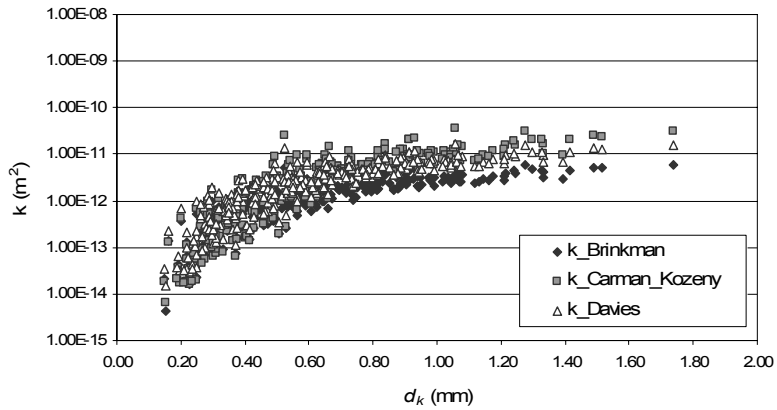

Fig. 9. *Floc permeability according to models: Brinkman, Carman-Kozeny and Davies*

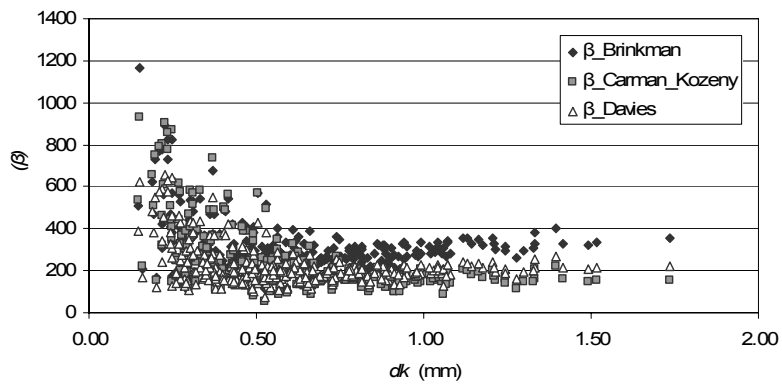

Fig. 10. *Permeability factor (β) according to permeability models: Brinkman, Carman-Kozeny and Davies*

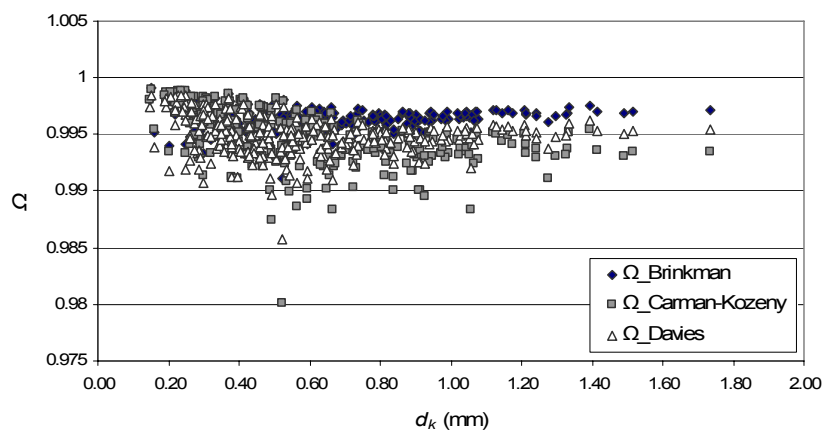

Fig. 11. *Resistance forces ratio between permeable and impermeable flocs (Ω) using permeability models: Brinkman, Carman-Kozeny and Davies*

evaluation of the importance of permeability for floc sedimentation. The dependence of factor (Ω) on the choice of a permeability model is shown in Fig. 11. The resistance force ratio between permeable and impermeable flocs (Ω) is close to the value of 1 for all three permeability models. The highest impact on (Ω) when increasing floc diameter is shown by the Carman-Kozeny permeability model, which was developed for primary particles of spherical shape. A high impact on (Ω) is also evident when observing the Davies permeability model, which was developed for fibrous primary particles. The lowest impact of floc size on (Ω) appears when using the Brinkman permeability model. Despite of a slight deviation of (Ω) values between various permeability models, low permeabilities mean that the velocity of liquid through the floc is very low in all cases, and can thus be ignored, which is also true for floc permeability, confirming the result of some authors [9], [13].

3.6. Floc density

Floc density has been derived from expression (5) and is as follows:

$$\rho_k = \rho_t + (1-\varepsilon)(\rho_p - \rho_t) \quad (15).$$

With known liquid density, the calculated floc porosity and the defined density of the primary particle 1.059 g/cm^3 [10], we used expression (15) to calculate the floc density. Fig. 12 shows the results of density differences between floc and liquid (16).

$$\Delta\rho = \rho_k - \rho_t \quad (16).$$

It is evident that smaller flocs have higher densities than larger flocs, which is in line with the findings by Lee et al. [4] who observed a decrease in value $\Delta\rho$ from 100 to 0.1 kg/m^3 with any increase in floc diameter from 0.1 mm to 10 mm. The density differences can change according to the wastewater composition and type of BTW.

For the results within the same sample from selected BTW the difference in density (Fig. 12) is a consequence of varying floc porosity. Big flocs with large porosities have smaller differences in densities than small flocs, which are more compact.

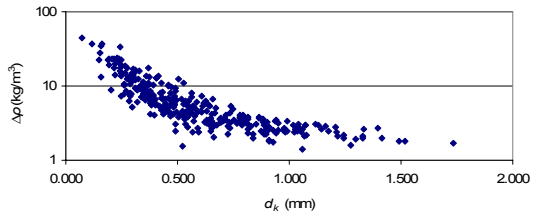

Fig. 12. *A presentation of differences between floc and liquid densities depending on floc diameter*

4 CONCLUSIONS

A detailed study of sedimentation of wastewater sludge flocs was performed. Based on the measured velocities of sedimentation for various sizes of flocs and the use of a generalized Stokes' model for sedimentation velocity, we derived values for flocs' porosities, considering that the flocs are permeable and composed of smaller primary particles.

Experimental results and obtained empirical correlations demonstrate that porosity values of flocs increase with their size (equal diameter). With increasing the size of a floc the difference between the floc's density and the liquid (water) density decreases. From the main findings, i.e. low values of permeability, we conclude, that in practice the influence of the liquid flow through the porous floc can in most cases be neglected.

On the other hand, developed correlations for the floc porosity and permeability can be used in deriving a suitable numerical model for sedimentation of sludge flocs, which is the next step in modelling of the sedimentation process.

5 NOMENCLATURE

C_d		drag coefficient
g	mm/s^2	gravitational acceleration
d_k	mm	floc diameter
d_p	mm	primary particle diameter
v_s	mm/s	settling velocity of floc predicted by Stokes' law
v_k	mm/s	settling velocity of floc (measured)
v_t	mm/s	velocity of fluid
ε		porosity
k	mm^2	permeability
Ψ		sphericity
m_k	g	floc mass
ρ_k	g/mm^3	floc density
ρ_t	g/mm^3	fluid density
ρ_p	g/mm^3	primary particle density
ρ_{ss}	g/mm^3	dry density of floc
η_t	g/mms	dynamic viscosity
$\Delta\rho$	g/mm^3	differences in floc and liquid density
Ω		the ratio of the resistance of permeable and impermeable floc
β		dimensionless permeability factor
A_k	mm^2	surface area of floc
A_{krogle}	mm^2	surface area of equivalent sphere
A,B,C	mm^2	projection areas of equivalent cuboid
a, b, c	mm	edges of equivalent cuboid

6 REFERENCES

[1] Žajdela, B., Hribernik, A., Hriberšek, M. Experimental investigations of sedimentation of flocs in suspensions of biological water treatment plants, *Computation methods in multiphase flow,* 2007, *IV*, pp. 293-302.

[2] Li, D.-H. & Ganczarczyk, J. J. Advective transport in activeted sludge flocs, *Wat. Env. Res.,* 1992, *64*, pp. 236-240.

[3] Li, D.-H. & Ganczarczyk, J. J. Stroboscopic determination of settling velocity, size and porosity of activated sludge flocs, *Wat. Re.,,* 1987, *21*, pp. 257-262.

[4] Lee, D. J., Chen, G. W. & Hsieh, C. C. On the free-settling test for estimating activated sludge floc density, *Wat. Res.,* 1996, *30*, pp. 541-550.

[5] Huang, H. Porosity – size relationship of drilling mud flocs: fractal structure, *Clay Miner,* 1993,*41*, pp. 373-379.

[6] Jorand, F., Zartarian, F., Block, J.C., Bottero J. Y., Villemin, G., Urbain, V., Manem, J. Chemical and strutural (2D) linkage between bacteria within activated sludge flocs, *Wat. Res.,* 1995, *29*, pp. 1639-1647.

[7] Tambo, N. & Watanabe, Y. Physical characteristics of flocs. 1. The floc density function and aluminum floc, *Wat. Res.,* 1979, *13*, pp. 409-419.

[8] Concha, F. & Almerdra, E. R. Settling velocities of particulate system, 1. Settling velocities of individual spherical particles, *Int. J. Min. Process.,* 1979, *5*, pp. 349-367.

[9] Matsumoto, K., Suganuma, K. Settling velocity of a permeable model floc, *Chem. Engng.,* 1977, *32*, pp. 445-447.

[10] Li, X., Yuan, Y. Settling velocities and permeabilities of microbial aggregates, *Wat. Res.,* 2002, *36*, pp. 3110-3120.

[11] Li, D.-H. & Ganczarczyk, J. J., Size distribution of activated sludge flocs, *Res. Jour. WPCF.*, 1991, *63*, pp. 806-814.

[12] Chien, S. F. Settling velocity of irregularly shaped particles, *SPE Drilling and Completion*, 1994, pp. 281-289.

[13] Neale, G., Epstein, N. & Nader, W. Creeping flow relative to permeable spheres, *Chem. Engng.,* 1973, *28*, pp. 1865-1874.

[14] Crowe, C., Sommerfeld, M., Tsuji, Y. Multiphase flow whit droplets and particles, *CRC Press*, 1998, pp. 92-93.

Strojniški vestnik - Journal of Mechanical Engineering 54(2008)7-8, 557-564
UDC 614.86:631.372
Paper received: 13.08.2007
Paper accepted: 19.12.2007

The Research of the Number of Accidents with the Agriculture and Forestry Tractors in the Europe and the Main Reasons for those Accidents

Rajko Bernik[1] - Robert Jerončič[2,*]
[1] University of Ljubljana, Biotechnical Faculty, Ljubljana, Slovenia
[2] Ministry of Transport, Transport Directorate, Ljubljana, Slovenia

The agriculture and forestry tractors represent big potential danger for traffic and working accident. Because of their construction they have very high centre of gravity and are therefore very unstable vehicle. In the Republic of Slovenia (RS) from 1981 to 2005 died 773 peoples. Fortunately the number of victims is less every year. The main reason for accidents with the agriculture and forestry tractors is overturning. This is the case in the RS as well as in other countries. The number of deaths in accidents with the agriculture and forestry tractors was acquired with the help of foreign type-approval and registration bodies.

Keywords: agricultural tractors, foresty tractors, traffic accidents

1 GENERALLY ABOUT ACCIDENTS

In the RS as in every other developed country due to the high standard of living the number of motor vehicles is growing all the time. This is the cause of several difficulties. Our surrounding is polluted with toxic gases and noise, the traffic is increasingly dense and last but not at least there are also a lot of traffic accidents. Causes of accidents are various but the majorities are due to unsuitable speed and alcohol. It is not possible to prohibit selling alcohol and it is also impossible to limit all the vehicles to an appropriate (i.e. safety) speed. Therefore we have to make changes in other fields. In addition to building better roads we can also improve the safety of motor vehicles. For these reason experts all around the world carry out investigations, perform tests on vehicles and their parts and then write the technical prescriptions and legislation for motor vehicles to make them better and safer. The legislation that regulates vehicles before their registration or before their giving into service is the legislation in the area of conformity assessment of motor vehicles. Beside this there are also the rules that regulate the equipment of the vehicles and the rules for vehicles in use (rules on technical inspections of the vehicles).

However, these rules are not valid only for road motor vehicles and their trailers but also for agriculture and forestry tractors. These kinds of vehicles are in traffic on roads and also at work on fields and in forests. Accidents with these vehicles are very often and because of various reasons.

These kinds of vehicles are nowadays present on almost every farm in the Slovenia or in the world. According to the statistical data is the Slovenia with 116 tractors on 100 farms between the states with highly developed agriculture (Portugal 51, Italy 59, Austria 132, France 158, Great Britain 205). According to the number of tractors on ha of area that is in Slovenia 0.25 tractor/ha, we are even ahead of EU Member States (France 0.08, Austria 0.10).

In accidents with agriculture and forestry tractors similar to other motor vehicles every year a lot of drivers or their attendees are killed. These kind of vehicles are in use on public roads as well as on macadamized roads and at work on fields. Therefore the accident could happen anywhere. On public roads is a lot of various traffic and tractors which are proportionally slow vehicles are therefore often in dangerous. Even worse is with their use outside public roads where the driving surface is not smooth and flat.

We divide accidents with agriculture and forestry tractors on traffic accidents and working accidents. Traffic accidents occurs when the tractor is on public roads while working accidents are those that occurs at work on farm, field, meadow, forest, …

*Corr. Author's Address: Ministry of Transport, Transport Directorate, Langusova 4, Ljubljana, Slovenia, robert.jeroncic@gov.si

2 GENERALLY ABOUT REASONS FOR ACCIDENTS

There are a lot of reasons for the accidents. We could divide them on those that are related to:

- the driver (inexperience, alcohol, incorrect reaction of the driver …),
- the tractor (technical condition of the vehicle, maintenance …),
- the driving conditions (slippery driving surface, bad weather conditions …).

The most frequent reason for accidents in agriculture and forestry is unprofessional use (driving of the tractor with inappropriate technique and speed on inclined driving surface, overturning …) or unprofessional maintenance (various repairing or interventions, replacement of the pneumatic tyres, filling the fuel …). The correct maintenance of the tractor stability is in the literature mentioned as a factor of eliminating various accidents and risks that could happened in the case of instability of the tractor and overturning around longitudinal or transversal axis.

Accidents that happened because of overturning of tractors represent about 40% of all accidents with tractors. On uneven surfaces is tractor very unstable vehicle that because of its construction overturn fast. That is because the tractor has relatively high centre of gravity, short distance between axles and short wheelbase. The stability of the tractor (static and dynamic) is changing due to acting of various reasons: slope and characteristic of the driving surface, inappropriate speed according to the conditions, skidding of the driving wheels, the size of the force on pulling rode and fast changes of movement of the tractor like standstill – driving, driving – inappropriate stopping.

Although the producers build more and more safer tractors, they cannot build a tractor that could recognise the dangerous situation. With safety arcs or cabins and safety belts the number of victims is reducing but with the development of new tractors also their capabilities are higher and higher. Overturning could happen because of too fast driving according to the driving conditions, sudden obstacles on the road (rocks, holes, ...), driving over canals, pushes by towing and also inappropriate use of front loading devices.

The research about the reasons for accidents was done in [1] and [2]. It was found that the main reasons for traffic accidents with agriculture and forestry tractors were:

- Unsuitable speed (19%); According to the research unsuitable speed is the most important reason for appearance of accidents. Driving conditions (day, night, dry, wet, ice ...) are changing all the time so the driver has to take this into consideration to avoid accidents.
- Consideration (or non-consideration) of having precedence when driving through crossroads (14.9%). This reason for accidents is very connected with the psychophysical condition of the driver and the amount of driving experience.
- Driving on wrong the side of the road or in the opposite direction (13.5%). According to this reason it appears that drivers of tractors are very often wilfully exposed to potential risks.
- Psychophysical condition of the driver (15%). Among these reasons for more than one tenth of all accidents is driving under the influence of alcohol. Other reasons are tiredness, falling asleep and carelessness.
- Technical conditions of the vehicles (4.9%). This reason is the responsibility of the driver himself as a user.

Other research shows that more than 70% of all accidents with forestry and agriculture tractors happened on local roads and more than 21% on regional roads. This fact shows us the specific use of this kind of vehicles (mostly in the countryside).

Most of victims in such accidents are between 35 and 54 years age. FIt was found that main reasons for these accidents are [2]:

- bad estimating of the field, when the tractor slipped, overturned and crushed the driver. That reason was especially fatal for tractors without a safety arch or a cabin.
- unsuitable speed,
- wrong selection of the gear,
- too much load on the trailer,
- driving on the edge of the road or field,
- incaution of the driver,
- bad technical conditions of the vehicles.

The main faults were on light signalling devices, steering, tyres and on braking systems.

In the study [12] was found that in Ontario 244 people died as a result of tractor-related accidents between 1980 and 1994.

Table 1: *Data about deaths in traffic accidents with agriculture and forestry tractors*

	1990	1991	1992	1993	1994	1995	1996	1997	1998	1999	2000	2001	2002	2003	2004	2005
Slovenia	18	8	11	12	13	8	6	9	7	6	5	10	4	4	9	2
Finland	-	2	7	3	1	5	5	4	1	3	4	2	2	3	1	0
Austria	-	24	13	18	20	20	15	7	13	12	19	15	12	10	7	8
Netherlands	-	7	1	5	3	1	2	2	2	4	3	1	2	5	5	5
Sweden	-	5	4	2	1	5	0	3	3	6	4	0	3	2	5	1
Germany	-	-	115	112	94	107	134	112	101	106	95	96	104	110	87	-
Luxemburg	-	0	0	0	0	0	0	1	1	0	2	0	0	0	0	0
Great Britain	-	2	2	2	0	0	1	1	1	2	7	3	1	11	7	0
Portugal	-	57	58	55	36	38	36	35	33	30	38	32	31	26	35	33
Estonia	32	23	12	14	17	9	4	4	9	1	2	7	4	2	-	2
Latvia	-	-	-	-	-	14	7	12	15	10	7	10	9	11	10	-
Poland	175	123	115	111	93	98	68	84	82	72	72	62	47	61	57	67
Switzerland	-	-	-	-	-	-	27	26	26	24	28	23	20	25	18	13
Serbia	107	94	80	69	74	66	72	106	81	55	58	-	-	-	-	-
Belgium	0	4	2	1	2	4	3	2	3	4	5	0	1	2	3	1
Danmark	-	3	3	3	4	2	0	0	3	2	3	1	0	0	0	3
France	-	43	37	28	32	32	36	35	22	20	26	12	20	25	13	12
Greece	-	114	93	79	99	81	44	80	61	71	54	72	43	46	37	26
Italy	-	51	40	42	47	30	38	31	23	38	28	24	23	24	23	23
Spain	-	43	40	23	26	30	36	33	30	32	35	28	16	23	40	26
Croatia	-	-	-	-	-	-	20	14	8	3	10	13	14	8	10	13

For more than half of them the cause was overturning the tractor to the side or the rear. Among other causes they quote also touches with rotating power takeoff (PTO) shafts, running of the tractor into objects, slipping and falling by driving up or down …

3 OBTAINING THE DATA

Most of the data about the responsible bodies for agriculture and forestry tractors and the number of deaths was gathered with the inquiry. Questions were sent to type-approval and registration authorities or statistical institutions to the other EU Member States. A lot of data for the most of EU Member States was gathered with this approach. Some statistical data was acquired also from the EU data base CARE (Community database on accidents on the roads in Europe) that is on web.

4 THE OVERVIEW OF CAUSES

4.1 Causes in Slovenia

In Slovenia 758 people died as a result of tractor traffic and working accidents between 1981 and 2002, mainly tractor drivers and their passengers on tractor or its trailer or attachments. Most accidents (over 75%) happened because of the overturning of the tractor that then buries the driver or the passenger. For many years were the consequences of traffic accidents much badly than those at work. But in the recent years is number of deaths at work significant greater than those on traffic.

Serious concern is the fact that the circumstances which causes the most badly accidents with tractors is equal every year. After the implementation of the Road traffic safety act (from 1982) that prescribed that all tractors, placed on the market from 1st January 1984 have to be equipped with the safety arc or the cabin, and all tractors in use have to be equipped with the safety arc or the cabin until 1st January 1986, the number of deaths in traffic accidents with the tractor was reduced. However for the other tractors those are not registered these safety arcs or cabins are not obligatory and therefore the number of deaths in working accidents was not reduced. Most of the tractors that were involved in worst accidents were without the safety arc or cabin and in many cases not properly technically equipped.

Based on reports and notes about working accidents we were trying to found some the most frequent circumstances or causes causing the accident. In many times this was a difficult task, because there were a lot of various factors that contribute the overturning of the tractor that is the most common reason for deaths of tractor drivers. Most of the tractor drivers lost his life specially because of direct overturning of the tractor that is consequence of three circumstances. The most reasons for overturning are incautious at driving over the edge, bad estimation of the slope and incorrect gear at driving downhill, overloading of the trailer or unsuitable brakes on the trailer that push the tractor and overturn it. The problem of choosing the incorrect gear at driving downhill occurred in the past (nowadays only at technologically obsolete tractors) where transmissions gears were not synchronised and where it was impossible to change to a lower gear. Also the examples that the trailer pushed the tractor were typical in the past when tractors were lighter. Nowadays tractors are heavier but also more powerful and therefore drivers load them more and this also lead to the accident. Altogether is not regarding the basic circumstances for accidents in 75% of accidents the overturning the reason for bad injury or deaths.

The data about the number of deaths in accidents with agriculture and forestry tractors divided by reasons for accidents were obtained on the Ministry of the interior. In these data there are some difficulties. First, by years the structure of the database for accidents were changing and with this development also the distribution by causes was changing by the number and by the content. By years the number of causes was increasing. The second problem that occurs here is the cause named "other". In this rubric was installed a big number of accidents (in the period 2002 – 2005 almost 47%), that a little bit spoil the picture of distribution of accidents by causes. The most likely is this the inconsequentiality of the police at the evaluation of the causes for accidents and for not enough of the attention for the accidents respectively. This confirms also the comparison of the reports of the accidents that are written by the Slovene police officers and those written by the Dutch officers. In the Netherlands is every such report like an expertise with very accurate description of the situation and the research of the causes for the accident while is in the Slovenia very short document.

The most accident happen when the driver bad estimate the driving surface he drives or work on and therefore too big leaning happen the slip and finally overturning of the tractor. Slips occurs especially on wet and soaked driving surface or on dry grass by haymaking.

Second often circumstance is overturning of the tractor caused by incautious driving on edges of meadows, fields and forests where not hardened driving surface do not hold out the weight of the tractor or the drivers drive over steep edge. Especially in last few years there were a lot of accidents with deaths caused by overturning of the tractor over the edge of the road or at driving backwards. At these overturnings there is no other circumstances, high speed or heavy trailers the appropriate safety cabin would reliably protect the driver of the tractor.

Third often circumstance is overturning of the tractor caused by too fast driving or inappropriate choose of the gear or overloading of the trailer that caused that driver could not stop the tractor. Drivers do not take into consideration that in many tractors while driving from the hill is not possible to change to lower gear because they could not stop the tractor. Reasons for overturning are also on inappropriate attaching of the trailer or working machine to the tractor when driving up to the hill the trailer because of the too high connecting point lift the front part of the tractor and overturn it back.

4.2 Causes in Some other European Countries

In Germany there is only for 20% of all deaths with agriculture and forestry tractors reason on turning, starting or breaking the tractor. These are of course that circumstances in tractor driving that the possibility of overturning is the highest. We could see hear the influence of the technical legislation that was in use already in year 1910 and that reached that only technical proper and safe tractors were in use. In United Kingdom the overturning and hitting with the vehicle represents 20% of all accidents with deaths. This is the biggest percentage of the accidents with deaths.

Table 2: *Reasons and circumstances that causes the accidents between the tractor drivers and others in traffic in Slovenia (period 1986 – 2002)*

year	86	87	88	89	90	91	92	93	94	95	96	97	98	99	00	01	02	SUM
reason	deaths																	
incautious driving	4	3	1	2	0	0	2	2	4	4	0	1	5	5	5	4	1	43
bad estimation of the surface, slip - overturning	3	5	5	6	5	4	2	9	6	3	2	3	7	4	4	2	4	74
driving over the edge - overturning	2	1	5	2	4	3	9	5	7	1	1	6	5	8	4	3	0	66
incorrect gear, speed	4	4	3	8	2	3	3	3	1	3	1	1	1	3	3	4	0	47
jump on moving tractor	0	0	1	2	1	0	2	1	1	1	2	4	1	0	3	0	1	20
fall from the tractor or trailer	0	1	0	2	1	1	0	0	1	2	3	1	1	1	1	2	1	18
unprotected conectors and shaft	0	0	1	0	2	3	1	0	1	0	2	3	0	0	2	1	3	19
other	2	2	0	1	1	3	0	1	6	0	1	2	3	1	3	1	5	32

In Portugal is 34.5% of traffic accidents with agriculture and forestry tractors caused by too high speed or by changing the direction of the driving. These are again those circumstances in tractor driving that the possibility of overturning is the highest.

In Switzerland 989 people died as a result of tractor traffic accidents between 1976 and 2005, and 519 of them because of overturning. These accidents represent 52.4 % of all deaths that is understandable according to the geographic structure of the country despite of long use of the legislation on this field.

In Serbia is the tractor first and the biggest reason for accidents on farms and causes are at:

- non professional use (driving the tractor with not correct technique and speed on slope surface, overturning, …),
- non professional maintenance (various repairing or interventions, changing of wheels, filling with the gasoline, …).

The overturning of the tractor is the reason for 40% of all accidents with tractors.

5 FINAL CONCLUSIONS

Based on written we could establish that the overturning of the tractor is the most often reason for accident with agriculture or forestry tractor in road traffic. In many of the studies is this reason on the first place. Similar result gives us also the research studies in various countries that we obtained the data. Therefore we could conclude that if we would like to do the traffic and work with these vehicles safer and prevent unnecessary deaths we have to work especially on two areas.

On area of agriculture or forestry tractors is necessary to act in a direction that these vehicles become safer. Regarding conformity assessment of tractors and prescriptions for offering to the market a lot is already done because the type approval prescriptions for safety constructions (the roll-over protection structures) and for safety belts for drivers are already in place. Furthermore there is necessary to assure that the roll-over protection structures for

Table 3: *Reasons and circumstances that causes the accidents between the tractor drivers and others in traffic in Slovenia (period 2003 - 2005)*

	sum	2003	2004	2005
sum	51	18	22	11
alcohol, drugs	1	0	0	1
incorrect side / direction of driving	4	1	2	1
abnormality on the tractor	1	0	1	0
incorrectnes of the pedestrian	1	1	0	0
inappropriate speed	5	1	4	0
unconsideration of rules	6	2	1	3
unusing of protectiv equipment	4	0	3	1
movement of the tractor	1	0	1	0
other	24	11	9	4
rest	3	1	1	1
unknown	1	1	0	0

Table 4: *Reasons and circumstances that causes the accidents between the tractor drivers and others in traffic in Slovenia (period 2005 – 2006)*

traffic accidents	reason for traffic accident	sum			2005			2006		
			death	personal		death	personal		death	personal
		sum	result	injury	sum	result	injury	sum	result	injury
with at least 1	sum	132	10	122	67	6	61	65	4	61
causer that is										
the tractor driver	incorrect side / direction of the driving	8	-	8	5	-	5	3	-	3
	inappropriate overtaking	3	-	3	1	-	1	2	-	2
	irregularity on the road	1	-	1	1	-	1	-	-	-
	irregularity on the load	4	-	4	3	-	3	1	-	1
	inappropriate speed	5	-	5	3	-	3	2	-	2
	unconsideration of the rules of the priority	24	2	22	9	1	8	15	1	14
	inappropriate safety distance	2	-	2	2	-	2	-	-	-
	movement of the vehicle	17	-	17	9	-	9	8	-	8
	psyhophisical condition of the causer	31	8	23	21	5	16	10	3	7
	inexperience of the									
	causer	22	-	22	6	-	6	16	-	16
	other	15	-	15	7	-	7	8	-	8
with at least 1 participant that is tractor	sum	200	10	190	107	6	101	93	4	89
	incorrect side /	15	-	15	9	-	9	6	-	6

driver	direction of the driving	12	-	12	7	-	7	5	-	5
	inappropriate overtaking	4	-	4	3	-	3	1	-	1
	irregularity on the load	19	-	19	11	-	11	8	-	8
	inappropriate speed	25	1	24	10	1	9	15	-	15
	unconsideration of the	6	-	6	4	-	4	2	-	2
	rules of the priority	18	-	18	10	-	10	8	-	8
	inappropriate safety distance	45	9	36	31	5	26	14	4	10
	psyhophisical condition of the	37	-	37	12	-	12	25	-	25
	causer	19	-	19	10	-	10	9	-	9

protecting drivers will be mounted also on the old tractors that are still in use. This could be assured with the prescriptions on the obligatory equipment for these vehicles and control on periodical technical inspections of the tractors. Type-approval legislation also regulate other parts of the tractor that contribute to the higher safety. The example of choosing the incorrect gear at driving downhill has been solved with the prescription that all transmission gears have to be synchronised. With the comparison between countries is obviously that in those countries where the legislation is in use for a long period also the number of deaths in accidents with such vehicles is lower. Moreover it is also possible to ensure with some constructional solutions that tractors will be also in exceptional situations still enough stable. These are various solutions from simple with additional weights to constructions for moving weights and modifications of the wheel suspensions.

Another area is of course the area of drivers. They have to be well educated that will know what is the proper use of these vehicles, where are their limits of use and how to recognise the moments where is only one step to the tragedy. And this step is very short because the studies shows us that the tractor could overturn when it is lifted for an angle of 75°. This angle is known as a point of no return. This angle could be reached already in 0.75 seconds. And this is in any case the time in which the driver could not react.

6 REFERENCES

[1] The Council for prevention and education in the traffic: Accidents at driving and work with tractors for the period 1981 – 2002.

[2] Hribernik, F., The prevention of traffic and working accidents in agriculture, Association of organisations for the technical education of Slovenia, Ljubljana, december 1995,

[3] Evans, L., Traffic Safety and the driver, New York, Van Nostrand Reinhold, 1991.

[4] Culpin, C., Farm machinery, 12th edition, Cambridge, Blackwell Scientific Publications, 1992

[5] Srivastava, A. K., Goering, C., E. Rohrbach, R.P.; Engineering principles of agricultural machines, American Society of Agricultural Engineers, 1993.

[6] Inić, M. Safety of the agriculture traffic, Beograd, Savremena administracija, 1987

[7] Oljača, V.M., Raičević, N.L., Radoja, L., Accidents with tractor drivers in public transport in Serbia, JUMTO 2004, 03.12.2004, Novi Sad.

[8] Bernik, R. The technik in agriculture, tractor, Ljubljana, Biotechnical faculty, Agronomy department, 2004.

[9] Fidler, S. Safe work with the tractor and its mechanisations, Zveza organizacij za tehnično kulturo Slovenije (Asociation of organisations for the technical education of Slovenia), Kmetijsko tehniška komisija (Commission for agriculture technik), Ljubljana, 1987.

[10] Schiling, E. Agriculture mechanisations, Text book and hand book for agriculture mechanisation construction, Koeln, 1960

[11] Murphy, D. J. Tractor overturn hazards, The Pennsylvania State University, College of Agriculture Sciences, Cooperative Extension, Agricultural and Biological Engineering, Pennsylvania, ZDA.

[12] National Agriculture Safety Database (NASD), Farm Safety Association: A guide to safe farm tractor operation, Review 04/2002, Guelph, Ontario, Canada.

[13] EU–database CARE (Community database on accidents on the roads in Europe)http://europa.eu.int/comm/transport/care.

Strojniški vestnik - Journal of Mechanical Engineering 54(2008)7-8, 565-573
UDC 656.088:621.879.324
Paper received: 24.08.2007
Paper accepted: 19.12.2007

Improving Repair Management of Bucket Wheel Excavator SRs1200 by Application of Project Management Concept

Brane Semolič[1,*] - Petar Jovanović[2] - Sava Kovačev[3] - Vladimir Obradović[2]
[1] Faculty of Logistics, Celje, Slovenia
[2] University of Belgrade, Belgrade, Serbia
[3] Kolubara Metal, Lazarevac, Serbia

The losses resulting from the defect or breakdown of equipment amount to incredible sums, often far higher than the cost of maintenance, repair or reconstruction. It is for this reason that a large number of methods for maintenance and repair of industrial and other plants have been developed. Elaborated in much detail, these methods nevertheless leave a lot of space for improvement. The improvement is primarily viewed in the context of the management of time, resources and costs of such enterprises. This paper presents a certain concept of project management the implementation of which may improve the maintenance and repair projects. The concept was tested in practice and confirmed in the project of revitalizing of the bucket wheel excavator SRs1200 at MB Kolubara, one of the most complex projects of the kind in the region recently, in terms of technical complexity of reconstruction, the number of participants, the number of activities, cost and time of realization, as well as other elements of the project. The application of this concept allowed for achieving significant results in the technical and financial fields, which will further be analyzed in detail.

Keywords: bucket wheel excavators, maintance management, reapair management, project management

0 INTRODUCTION

Simple consumer items such as small electronics, small appliances, and mechanical devices are expected to work without fail. For more complex items such as PCs, communications devices, and even automobiles, most consumers will tolerate very few failures. For some very complex systems such as nuclear power plants and rocket propulsion systems, failures can be disastrous and very high reliabilities are required [1].

Therefore, proper maintenance and repair in terms of time, cost and quality is of utmost importance.

The result of ineffective maintenance management in the USA only represents a loss of more than $60 billion each year. The losses of production time and product quality that result from poor or inadequate maintenance management have had a dramatic impact on the US industries' ability to compete with Japan and other countries that have implemented more advanced manufacturing and maintenance management philosophies [2].

Smaller countries have to pay even more attention to the efficient maintenance and repair management of the big industrial systems, since their competitive position is far more difficult and losses could have substantial influence on the country's economy and stability as a whole.

Traditional approaches of maintenance and repair management could give acceptable results but they have to be combined with contemporary management disciplines. Modern, specialized management approaches, such as change management, innovation management, risk management, project management are in a process of exploring and developing new possibilities and ways of application.

Various methods and techniques of project management, if adopted properly, could substantially improve processes of maintenance and repair of industrial and other big pieces of equipment.

1 THEORY REVIEW

Industrial and process plants typically employ several types of maintenance anagement [2]:

a. run-to-failure

When a machine breaks down, fix it. This is a reactive, the most expensive method of

*Corr. Author's Address: University of Maribor, Faculty of Logistics, Mariborska 7, 3000 Celje
brane.semolic@siol.net

maintenance management. The major expenses associated with this type of maintenance management are high spare parts inventory cost, high overtime labor costs, high machine downtime, and low production availability. To minimize the impact on production created by unexpected machine failures, maintenance personnel must also be able to react immediately to all machine failures [2].

Breakdown maintenance was practiced in the early days of production technology and was reactive in nature. Equipment was allowed to run until a functional failure occurred. Secondary damage was often observed along with a primary failure [3].

b. preventive maintenance

Maintenance tasks are based on elapsed time or hours of operation. All preventive maintenance management programs assume that machines will degrade within a time frame typical of their particular classification. The normal result of using statistics to schedule maintenance is either unnecessary repairs or catastrophic failure [2].

Some of the preventive maintenance procedures have been developed; however, they lack details to make them efficient and safe, and to reinforce sound maintenance practices [4].

c. predictive maintenance

Predictive maintenance is monitoring the vibration of rotating machinery in an attempt to detect incipient problems and to prevent catastrophic failure [2].

d. Total Productive Maintenance (TPM)

The concept was developed by Deming in the late 1950s. It is a program of zero breakdowns and zero defects aimed at improving or eliminating the following six crippling shop-floor losses [2]:

- equipment breakdowns
- setup and adjustment slowdowns
- idling and short-term stoppages
- reduced capacity
- quality-related losses
- startup/restart losses

e. Reliability-Centered Maintenance

If machinery and plant systems are properly designed, installed, operated, and maintained, they will not fail, and their useful life is almost infinite. Few, if any, catastrophic failures are random, and some outside influence, such as operator error or improper repair, causes all failures [2].

These and other traditional ways of maintenance and repair management have significant drawbacks. Various issues could emerge as a reason why these strategies do not give best results in terms of objectives, costs, time and quality. If we focus on these elements: objectives, costs, time and quality, it is more than obvious that tools and techniques, as well the process of project management should be applied in order to improve repair and maintenance management as a whole [5].

Even though, many authors recognize engineering and maintenance as specific projects [6], project management methodology is not applied at all or at least not in a proper way in these areas in transition economies.

This process of project management is intended to guide project managers and project teams in effectively performing key process steps, such as identifying the true need defining the project objective, creating an execution schedule, and maintaining control throughout the entire project [7].

Project management is the application of knowledge, skills, tools, and techniques to project activities to meet project requirements [8].

Planning and scheduling major maintenance projects using computer supported Critical Path Method (CPM) techniques was one of the earliest applications of computers in support of the maintenance function. The central idea behind development and use of such systems was to identify opportunities for parallel execution of tasks associated with a turnaround project so that available manpower and resources may be utilized as efficiently as possible to minimize equipment downtime [9].

Typically, the well-designed CPM system produces reports which show how limited resources may be used to complete a project in the shortest possible time. Alternatively, the system may show the manpower necessary for completion of a project in a given length of time [9].

In spite of the CPM system's "head start" in use by maintenance groups, this potentially profitable tool soon was abandoned by a surprisingly large number of plants and companies.

Most companies said the available CPM systems were too complex or too cumbersome for effective use in maintenance turnaround projects

or small construction jobs [9].

There are two major issues for abandoning of the CPM techniques.

First of all CPM is not a project management.

Even though project management has been in existence for more than 40 years, there are still different views and misconceptions about what project management really is. Textbooks on operations research or management science still have chapters entitled "Project management" that discuss only PERT (and CPM) scheduling techniques. A textbooks on organizational design recognized project management as simply another organizational form [10].

Every day engineers, salespeople, technicians, and countless others are thrust into the role of project manager. They're very good at what they do. In fact, they're typically the most technically knowledgeable engineers or the most successful salespeople [7].

Industrial and mechanical engineers usually posses substantial technical knowledge regarding the industry and equipment that they are involved with, but not the knowledge of project management as a process.

The art of project management relates to the fact that projects are really about people getting things done. Project management requires a keen knowledge of human behavior and the ability to skillfully apply appropriate interpersonal skills. The second aspect involves the knowledge, understanding, and skillful application of a prescribed project management process [7].

The customer satisfaction is another very important issue in project management. Customer satisfaction, connected with the criteria for successful project objectives realization, is the basic starting point for the introduction of project excellence [18].

The project management is a scientifically based and practically confirmed concept that uses appropriate methods of organization, planning and control in order to rationally coordinate all the necessary resources and activities in order that a certain project be executed in a most efficient manner [11].

There is a number of approaches to project management, the best known and the most largely accepted of which are certainly those proposed by the International Project Management Association (IPMA) and the Project Management Institute (PMI).

To the purpose of the maintenance and repair of industrial equipment project in Serbia, we propose the project devised by Jovanović [11], which in turn sublimes the elements of other proposed project management models. According to this concept, it is necessary to primarily identify the basic elements of the execution of any project to be planned, monitored and controlled, and these are: time, resources and costs. Therefore this concept of project management includes three basic modules – time management, resources management and project execution costs management, as shown in Figure 1. Planning, monitoring and control over time, resources and costs of the project execution help achieve the basic objectives of the project, i.e., meeting the planned deadlines for the project completion within the planned costs [11].

According to all previously mentioned, we have come to the following hypothesis: the application of project management and the general concept mentioned above, with specific procedures adjusted for this purpose, could substantially contribute to the time and cost reduction in maintenance and repair projects.

In order to prove the above stated hypothesis, we applied the project management concept to one of the biggest repair projects in Serbia.

2 CONCEPT APPLICATION

After the breakdown of the bucket wheel excavator SRs 1200x 24/4 at the surface excavation area "Field D" in the Mining Basin Kolubara, Serbia, which burned away and was cut off from exploitation, which has in years caused a significant delay in the production at strip mines, and consequently the coal tailings, the Electric Power Industry of Serbia decided to reerect - revitalize the excavator to which aim they announced an international tender for the bucket wheel excavator revitalizing project realization, to be funded by a cheap credit provided by the Government of the Federal Republic of Germany through the "Kreditanstalt für Wiederaufbau" bank for reconstruction of Frankfurt.

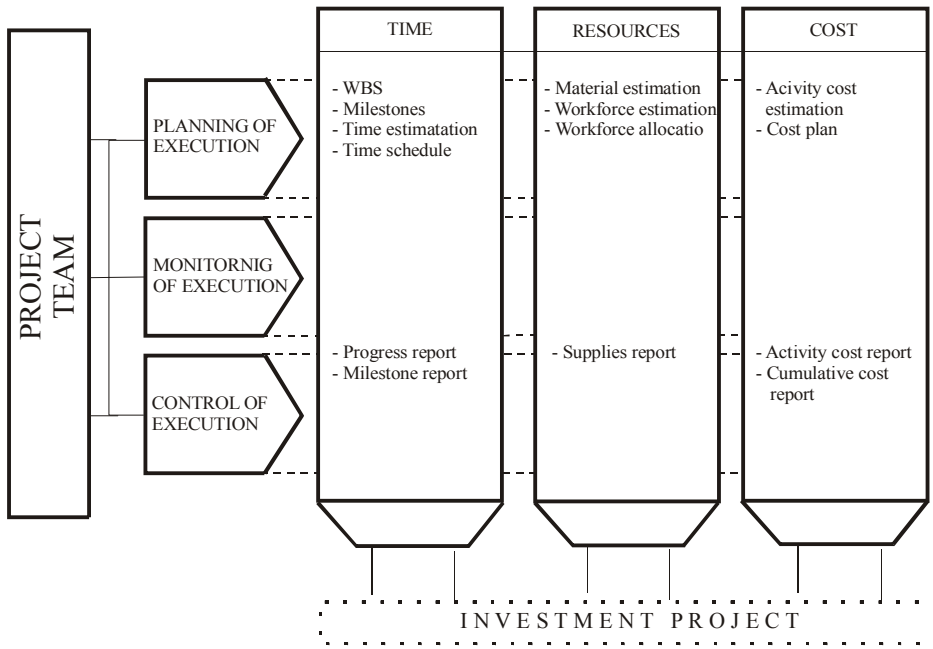

Fig. 1. *A General project management concept*

The tender was announced and carried out aided and conveyed by the consultants VEAG Power Consult of Cottbus, Germany. The tender was won by a German company FAM of Magdeburg, representing the consortium including Kolubara Metal (hereinafter KM) of Vreoci, Serbia, as main subcontractor for machinery equipment and a complete assembly and installment and ABB of Cottbus, Germany, as main subcontractor for electric equipment.

The basic objective of the project was to reduce the lagging in the strip mines in the Mining Basin of Kolubara, which will directly affect the coal stock balance to be delivered by the MB Kolubara to the Steam Power Plant "Nikola Tesla" at Obrenovac. In order to achieve this basic objective, it was the obligation of the FAM/ABB/KM consortium with their subcontractors and suppliers in the realization of the scope of deliveries and services in the contracted period and for the anticipated – contracted (fixed) value of the transaction, to complete the revitalizing and launch the bucket wheel excavator SRs 1201 destroyed in the fire.

The resulting sub objectives are the following:

- The realization of the first revitalizing of the bucket wheel excavator in the MB Kolubara, which in turn will serve as example for the future revitalizations in terms of the method and scope of modernization;
- The modernization from the aspect of the solutions applied both in the machine and in the electric sections, as regards the fact that the original solutions date back to 1968 and that manifold changes meanwhile occurred in the regulations regarding this matter as well as in the applied multidisciplinary technical solutions, so that the constructive and designing measures undertaken in the revitalizing of the bucket wheel excavator resulted in the increase in the excavator capacity from 3450 m^3/h to 4100 m^3/h of loose soil;
- Allowing for further revitalizing by providing a reliable large capacity excavator;
- Technology transfer from German firms to the national ones.

The contracted liability of the KM towards the FAM as the consortium representative includes the following:

- designing (designing detailed engineering for machine equipment);
- malfunction detection (including special purpose tests) and revitalization of

machine equipment and steel structure;
- manufacturing, transport and assembly of the entire revitalizing and new equipment at the assembly site at Zeoke - "Field D"
- participation in functional trials of the assembled tool in the free mode of operation;
- participation in the launching of the excavator in the full load mode of operation.

The contracted value of the transaction of the Kolubara Metal was stipulated at 3,095,000.00 EUR.

Bearing in mind that the key elements of the bucket wheel excavator SRs 1201 revitalizing were the deadline, the budget and the participation in the consortium, the general management of the KM made a firm decision to apply the project management approach with all its elements in this job, primarily on the basis of the proposed project management concept, as well as the project management procedure adapted to the projects of overhauling and revitalizing of heavy machinery equipment as given in [11].

To the purpose of increasing the capacity of the KM in the field of project management the experts from the University of Belgrade and the Serbian Project Management Association (YUPMA), member of the International Project Management Association (IPMA) were recruited.

In accordance with the concept, the project organization structure and the KM project team were formed first, to be engaged in revitalizing work. As there is a large number of participants in the project, the project organization structure is rather complex and is shown in Figure 2.

The project itself was conducted by the KM project team consisting of a number of functionally different experts, so that a multidisciplinary approach could be achieved. The team included the project manager (the team leader), 1 mechanical engineer, an expert in the assembly/dismantling activities, 1 civil engineer, an expert in steel structures, 1 mechanical engineer of machinery equipment, 1 electrical engineer, 1 graduate process engineer for antirust protection, 2 mechanical and 1 electrical technicians, with an occasional inclusion of 1 graduate process engineer specialized in welding. In addition to the mentioned team members, the experts from the Serbian Project Management Association were engaged as consultants and provided professional support in all the phases of project management.

The given project management concept meant that the execution would be planned in detail, so that the plan of the overall project was obtained, which in turn would serve as basis for further management. Devising the project plan meant identification of all activities to be carried out as per contract, devising the WBS (Work Breakdown Structure) and determining the key events.

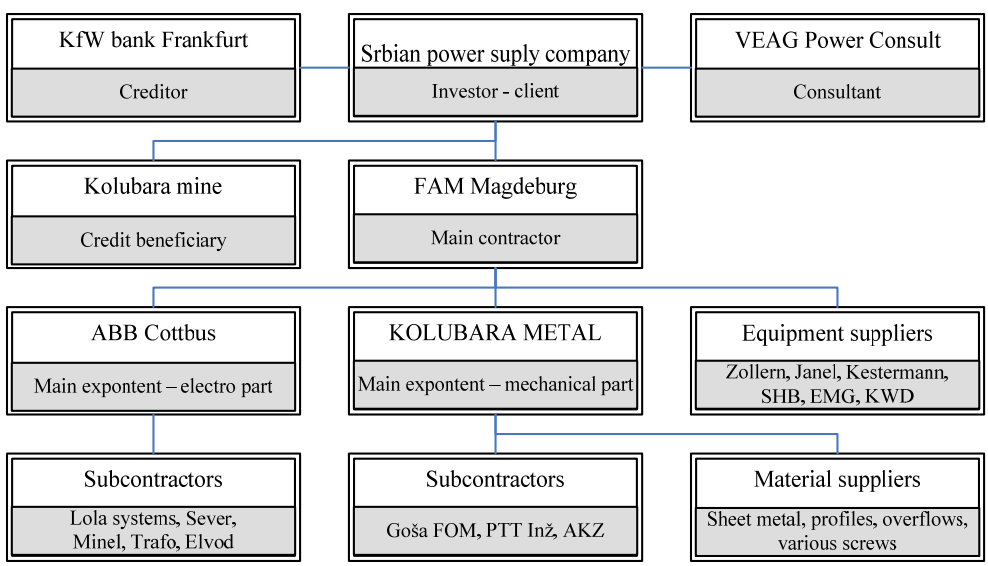

Fig. 2. *The bucket wheel excavator SRs 1201 revitalizing project organization*

A special problem in planning referred to identifying the prospective newly established activities (additional works or supplies caused by a detailed malfunction detection of equipment previously estimated as usable, possible delays in manufacturing by the subcontractors, etc…). On the basis of the detailed plan of activities a time plan and an estimation of the duration of the project were worked out.

The further structuring of the bucket wheel excavator SRs1201 x 24/4 revitalizing was worked out by coordinating individual activities to be carried out with the persons and/or sectors in charge of these activities, as well as responsibility the function bears. It was in this way that the estimate and allocations of workforce, as well as responsibility matrix on the project were determined. In accordance with the concept, the allocation of financial and other resources to particular activities, phases and the project in general was performed, on the basis of which an estimate of resources and costs of the project was accomplished [12].

All the activities related to the project plan were carried out using the project management software tools – MS Project. The master plan scheme is shown in Figure 3.

Due to the complexity of the project, the monitoring and control of the project execution was multilevel. A large number of participants, on one hand, and the demand for high quality of equipment and works performed, strict deadlines for accomplishment individual phases and the project as a whole and over all the project budget that was firmly restricted by the key-in-hand system, on the other hand, required that the approach to management, as well as control of the project execution be consequent [13]. In accordance with the concept adopted, the KM project team decided to do the monitoring of the project execution through the following elements [14]:

- the plan control,
- log,
- receipt control at the manufacturer's and on delivery,
- daily, weekly and other meetings
- various reports and protocols.

A detailed control plan was devised [15] and offered it to the FAM and to the EPS and they accepted it. The plan of control included all the activities in the project that were to be carried out in the KM head office, in the KM workshops and at the site itself.

A log was kept since the opening till the closure of the building site at the assembly site, where all the works and the daily scope were entered and verified by the supervisory board. On receipt of all supplies the receipt control was carried out upon receiving parts or equipment, while in special cases the receipt control was carried out at the manufacturer's, according to the concept adopted.

Daily briefings of the project team took place, during which the members reported what was accomplished the previous day and agreed upon what was to be done next. Also, there were weekly meetings with the representatives of the FAM or the ABB that were ever present at the building site. If necessary, the meetings were organized with all member teams. On all these meetings the official protocol was made. On two-monthly basis the Investor-client organized and the Consultant chaired status meetings, where the project management of the investor and project

ID	WBS	Task Name	Duration
0		**Revitalization project SRs 1201**	**365 days**
1	1	Basic engineering	252 days
3	2	Detailed engineering	234 days
5	3	Technical documentation	126 days
7	4	Revitalization of existing equipment	273 days
9	5	Development and purchase of new equipment	245 days
11	6	Machinery assembly	249 days
13	7	Electric assembly	154 days
15	8	Functional testing	14 days
17	9	Test work	14 days
19	10	Capacity proof	7 days
21	11	Delivery to client	7 days
23	12	Final delivery protocol	0 days

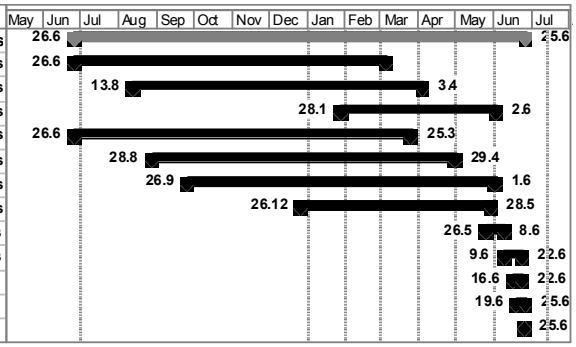

Fig 3. *The project master plan*

managers of all the project teams participated (FAM, ABB, Kolubara Metal).These status meetings were dedicated to the analyses of the progress of the project from the point of view of production, delivery and installment and the accomplished activities were compared with the time-term plan of realization; then the problems were discussed – discrepancies and the method for solving as well as the quality level of the manufactured and installed equipment. Of course, the payment rates to the main contractor were analyzed, as they further affected other payments to other participants in the project.

The project operational monitoring and control were primarily based on the software support of the MS Project. The computer work was carried out when needed, using the mentioned software primarily in the context of time, resources and cost management. The entire system, regarding the space dispersity (3 locations: head office, production and installment) was supported by an appropriate network system.

The project supervision and control were also multilevel. The Investor-client EPS, as mentioned above, formed their own supervision team consisting of the experts from the EPS, Kolubara and the *consultants* from the German firm VEAG Power Consult. On the other hand, the main contractor FAM and the main subcontractors ABB and Kolubara Metal formed their project teams that actually managed the project and controlled the execution. In view of their real position and influence upon the execution of individual phases of the project, the the main contractor's and the main subcontractors' project teams executed an in-depth control over all the elements of the project. This means that their actual impact upon the scope, quality and project realization deadlines was by far greater than that of the Investor. This was supplemented by the need that the contractors' project teams, in addition to their own capacities, were in charge of controlling the performance of their subcontractors and supliers of equipment and production material.

Throughout the execution of the project the KM project team received demands to make certain changes which proved an additional challenge. The demands for change mostly referred to the discrepancies between the EPS teams and the user, the Strip mine Polje D (Field D). The pressure was mainly of technical nature and included, on one side, the demands that larger scale modernization than contracted be made, and, on the other side, that better and more modern solutions be used, which made it impossible to remain within the contracted budget [16]. The Kolubara Metal project team was also under pressure to shorten the previously stipulated deadlines, without all aspects of the project execution being taken into account – for example, supplies, tenders, sub deliverers etc. The best method of managing such change was to keep accurate and complete documentation so as to be able to firmly prove that such demands of the Investor were not appropriately based, and that the demands were excessive.

Despite the cited problems and a striking complexity of the project, the project was successfully brought to an end in accordance with the demands of all project stakeholders. The execution time was 12 instead of the initially planned 14 months, which resulted in significant savings. The technical results and the quality of the project could also serve as an example of good results.

3 RESULTS AND DISCUSSION

Revitalizing of the bucket wheel excavator SRs is of paramount importance for the work of the KM plant and the EPS in general, since it directly affects the production of electricity, and therefore the business operations of a large number of firms in Serbia. Therefore it was of great importance that the revitalizing should be accomplished in as short a time as possible and with the lowest possible costs, so that the losses should be reduced as much as possible.

The project technical results achieved were excellent. After 12 months the project lasted, the total of 1460 t of hardware was installed (including 108 t ballast) as well as approximately 115 t electric equipment, cables (power and optical) and auxiliary structures. The result of this complex job was a bucket wheel excavator SRs 1201x24/4 with substantially improved properties which can be observed in Table 1. Besides these technical results that we can boast of as an outstanding accomplishment in modern practice, as regards their technical specification and the project quality, the financial results of the revitalizing project that are accomplished are also important.

Table 1. *Properties of averaged and reconstructed excavator*

Averaged SRs1200:	Revitalized SRs1201:
• Capacity 3465 m^3/h • Bogie wheel motive power 400 kW	• Capacity 4100 m^3/h • Bogie wheel motive power 630 kW • Circular motion tripple drive of upper construction • Container principle of electric equipment installation • Frequency regulated power

The losses resulting from the bucket wheel excavator breakdown may be classed in two groups: direct losses and indirect losses.

The direct losses refer to the reduced production of coal to be used in the steam power plant, and hence to the reduced production of electricity. The indirect losses are related to the reduced, endangered and inefficient business of numerous commercial and non-commercial organizations dependant on electricity supply. In order to stress the results achieved by the project management application in the bucket wheel excavator revitalizing, we will present the direct benefits resulting from an efficient management of this enterprise.

According to the KM statistical data, conclusion can be drawn that an annual output of the bucket wheel excavator (11 months of exploitation and 1 month routine maintenance) amounts to between 5.5 and 7 million m^3 tailings, which means approximately 550,000 m^3 tailings on monthly basis. As per normative data, the production of 1 ton of coal uses 2.5-3m^3 tailings. This means that the output of the bucket wheel excavator is 200,000 - 230,000 tons of coal monthly, i.e., 2 - 2.3 million tons of coal annually. Furthermore, if taken as an equivalent that 1.5 kg coal produces 1 kWh of electricity, then the monthly output of the bucket wheel excavator amounts to 150 million kWh of electricity, which converted into currency amounts to about 4.5 EUR million per month.

According to the KM and EPS experts estimations, and on the basis of the investigation performed, it is maintained that the indirect losses are three times larger that the direct ones, so that they amount to about 13.5 EUR million per month. On the basis of the technical documentation and the technological method, as well as on the basis of previous experience of the consortium and the YUPMA experts, the designed bucket wheel excavator revitalizing was planned to last 12 months. Experiences regarding such projects show that the usual delays are 3 – 6 months as regards the planned period.

The application of the project management concept in the planning and execution of this project, allowed for the project to be accomplished within 12 months, thus directly saving at least two months or 9 EUR million of direct costs. If direct losses be included, then the savings obtained by the application of project management are even larger and amount up to 36 EUR million.

Very good results were also achieved in the resources and cost management of the project itself, in all its phases and activities. We can freely maintain that the departure from the cost and resources plan devised with the project management methods was almost negligible.

During the one year of the project term the whole KM project team, as well as some representatives of subcontractors, suppliers and other collaborators were subject to a lot of training concerning project management and software tools used as logistic support, which resulted in raising the TM capacity, but also in creating teams of engineers capable, by changing the project management, of promptly and efficiently performing any complex maintenance or repair projects.

Therefore, it can be maintained that the analysis of the results of the revitalising project clearly proves the initial hypothesis and that the results accomplished applying the project management have had great effects in time, costs and resources management in the project, which further resulted in extraordinary savings, as the bucket wheel excavator SRs 1201 was launched again.

4 CONCLUSION

Despite numerous advantages, the traditional methods in the management of maintenance and repair of machinery equipment do have some weaknesses. These weaknesses are mostly related to the time, resources and costs management, however, in managing these enterprises not enough attention has been paid to the human aspects. The paper present a general project management concept which, combined with the traditional methods, may largely improve the existing systems of maintenance and repair management. The application of this concept to the bucket wheel excavator SRs 1201 revitalizing in the MB Kolubara, Serbia, allowed for significant direct and indirect savings resulting from an adequate resources management. These savings are, in the first place, the result of shortening the duration of project execution by two months, thus avoiding the opportunity costs of approximately 36 EUR million. The concept applied clearly achieved the set objectives, but also allowed for its further application in similar projects in this country and in the region.

Further research should certainly be directed towards the elaboration of the concept as regards specific procedures, both in routine maintenance and in emergency cases such as breakdown, thus making it possible to reduce losses and avoid other problems arising from scheduled or unscheduled equipment failure.

5 REFERENCES

[1] Blischke, R. W., Murthy, D. N. Prabhakar. eds. Case Studies in Reliability and Maintenance, *John Wiley & Sons*, New Jersey, 2003.

[2] Mobley, R. Keith An Introduction to Predictive Maintenance, *Elsevier Science - Butterworth - Heinemann*, Burlington, 2002.

[3] Girdhar, Paresh Practical Machinery Vibration Analysis and Predictive Maintenance, *Elsevier*, Oxford, 2004.

[4] Smith, R., Mobley, K. Industrial machinery repair: best maintenance practices pocket guide, *Elsevier Science - Butterworth-Heinemann*, Burlington, 2003.

[5] Graham, R., Englund, R. Creating Environment for Successful Projects, *John Wiley & Sons*, New Jersey, 2004.

[6] Turner, R. The handbook of project based management, *McGraw-Hill*, Berkshire, 1999.

[7] Heerkens, G. Project Management, *McGraw-Hill*, New York, 2002.

[8] A Guide to the Project Management Body of Knowledge (PMBOK guide), *Project Management Institute*, Newtown Square, 2000

[9] Geitner, K. F., Bloch, P. H. Machinery component maintenance and repair, *Gulf Publishing Company*, Houston, 1990.

[10] Kerzner, H. Advanced Project Management – Best Practises on Implementation, *John Wiley & Sons*, New Jersey, 2004.

[11] Jovanović, P. Project Management, *Faculty of Organizational Sciences*, Belgrade, 2006.

[12] Higgins, R. L., Mobley R. K., Smith, R. Maintenance Engineering Handbook, *McGraw-Hill*, New York, 2002.

[13] Geitner, K. F., Bloch, P. H. Major Process Equipment Maintenance and Repair, *Gulf Publishing Company*, Houston, 1997

[14] Kovačev, S. Revitalizacija rotornog bagera SRS1201, *Projektno upravljanje organizacijama*, Zalitibor, 15-17. maj 2006, (In Serbian).

[15] Jovanović, P. Investment Project Decision making Methodology in Serbia, *Project Management Journal* 2 2005.

[16] Jovanović, P., Contemporary management practice in transition countries, *European business Journal*, vol. 15, no.2, 2003.

[17] Semolic, B., Šostar, A., Network Organizations – a new paradigm of the 21st century, Journal of Mechanical Engineering, vol. 53, no. 503, 2007.

[18] Semolic, B. and Kovac, J. Starting points of project excellence, Project management review, vol. 2, 2007.

Corrigendum

Product Family Modelling in Conceptual Design Based on Parallel Configuration Grammars

Eugeniu-Radu Deciu, Egon Ostrosi, Michel Ferney, Marian Gheorghe
Strojniški vestnik – Journal of Mechanical Engineering, vol. 54(2008), no.6, p.398-412

The equation 7 on page 408 of the above mentioned article has to be corrected. The corrected form of the equation :

$$P_1^{add}: \left| \begin{array}{c} \left[\langle CONICAL\_THREAD\_AREA \rangle \rightarrow \langle CYL\_THREAD\_AREA \rangle \langle CONICAL\_AREA \rangle \right] \\ \left[\langle PlaneConnection \rangle \rightarrow \langle ExtPlaneFace_1 \rangle \langle ExtPlaneFace_1 \rangle \right] \\ \left[\begin{array}{c} \langle ExtThread \rangle \rightarrow \langle ExtThread \rangle \langle 0 \rangle \\ \langle ExtPlaneFace_2 \rangle \rightarrow \langle 0 \rangle \langle ExtPlaneFace_2 \rangle \\ \langle KeyGroove \rangle \rightarrow \langle 0 \rangle \langle KeyGroove \rangle \\ \langle ConicalLatFace \rangle \rightarrow \langle 0 \rangle \langle ConicalLatFace \rangle \end{array} \right] \end{array} \right|$$

Understanding the Mechanical Properties of Self-Expandable Stents: A Key to Successful Product Development

Daisuke Yoshino - Katsumi Inoue - Yukihito Narita
Strojniški vestnik – Journal of Mechanical Engineering, vol. 54(2008), no.6, p. 471-485

In the footnotes of the above mentioned article there has been a mistake. Above there is the corrected title. The wrong form of the title appeared in the footer of the pages (473/475/477/479/481/483/485).

Instructions for Authors

From 2008 Journal of Mechanical is published only in English language with Slovenian abstracts. Authors are entirely responsible for language correctness. If reviewer estimates that language is poor, Editorial can require native English proof-reading with certificate from the author once again.

Papers can be submitted electronically on Editorial's e-mail or by post.

Papers submitted for publication should comprise:

- Title, Abstract, Keywords,
- Main body of text
- Tables and Figures (graphs, drawings or photographs) with captions,
- List of References and
- Information about the authors, corresponding author and his full address.

For papers from abroad (in case that none of authors is Slovenian) Editorial will provide Slovenian translation of the Abstract.

Papers should be short and should comprehend 8 to 12 pages.

THE FORMAT OF THE PAPER

The paper should be written in the following format:

- A Title, which adequately describes the content of the paper.
- An Abstract, which should be viewed as a mini version of the paper and should not exceed 250 words. The Abstract should state the principal objectives and the scope of the investigation, the methodology employed, summarize the results and state the principal conclusions.
- An Introduction, which should provide a review of recent literature and sufficient background information to allow the results of the paper to be understood and evaluated.
- A Theory or experimental methods used.
- An Experimental section, which should provide details of the experimental set-up and the methods used for obtaining the results.
- A Results section, which should clearly and concisely present the data using figures and tables where appropriate.
- A Discussion section, which should describe the relationships and generalizations shown by the results and discuss the significance of the results making comparisons with previously published work. (Because of the nature of some studies it may be appropriate to combine the Results and Discussion sections into a single section to improve the clarity and make it easier for the reader.)
- Conclusions, which should present one or more conclusions that have been drawn from the results and subsequent discussion and do not duplicate the Abstract.
- References, which must be numbered consecutively in the text using square brackets [1] and collected together in a reference list at the end of the paper.

THE LAYOUT OF THE TEXT

Texts should be written in Microsoft Word format. Paper must be submitted in electronic version by e-mail or by post on CD.

Do not use the LaTeX text editor, since this is not compatible with the publishing procedure of the Journal of Mechanical Engineering.

Equations should be on a separate line in the main body of the text and marked on the right-hand side of the page with numbers in round brackets.

Units and abbreviations

Only standard SI symbols and abbreviations should be used in the text, tables and figures. Symbols for physical quantities in the text should be written in italics (e.g. v, T, n, etc.). Symbols for units that consist of letters should be in plain text (e.g. ms-1, K, min, mm, etc.).

All abbreviations should be spelt out in full on first appearance, e.g., variable time geometry (VTG).

Meaning of symbols and units belonging to symbols should be explained in each case or quoted in special table at the end of the paper before References.

Figures

Figures must be cited in consecutive numerical order in the text and referred to in both the text and the caption as Fig. 1, Fig. 2, etc. Pictures may be saved in resolution good enough for printing in any common format, e.g. BMP, GIF or JPG. However, graphs and line drawings should be prepared as vector images, e.g. CDR, AI.

All Figures should be prepared in black-and-white technique, without borders and on white grounding. All Figures should be sent separately in their original formats.

When labeling axes, physical quantities, e.g. t, v, m, etc. should be used whenever possible to minimize the need to label the axes in two languages. Multi-curve graphs should have individual curves marked with a symbol. The meaning of the symbol should be explained in the figure caption.

Tables

Tables must be cited in consecutive numerical order in the text and referred to in both the text and the caption as Table 1, Table 2, etc. In addition to the physical quantity, e.g. t (in italics), units (normal text), should be added in square brackets. Each column should have the title line. Tables should not duplicate information that is already noted anywhere in the paper.

Acknowledgement

Acknowledgement for co-operation or help can be included before References. Author should state the research (co)financer.

The list of references

All references should be collected at the end of the paper in the following styles for journals, proceedings and books, respectively:

[1] Wagner, A., Bajsić, I., Fajdiga, M. Measurement of the surface-temperature field in a fog lamp using resistance-based temperature detectors. Strojniški vestnik – Journal of Mechanical Engineering, February 2004, vol. 50, no. 2, p. 72-79.

[2] Boguslawski L. Influence of pressure fluctuations distribution on local heat transfer on flat surface impinged by turbulent free jet. Proceedings of International Thermal Science Seminar II, Bled, June 13.-16., 2004.

[3] Muhs, D. et al. Roloff/Matek mechanical parts, 16th ed. Wiesbaden: Vieweg Verlag, 2003. 791 p. (In German). ISBN 3-528-07028-5

ACCEPTANCE OF PAPERS AND COPYRIGHT

The Editorial Committee reserves the right to decide whether a paper is acceptable for publication, obtain professional reviews for submitted papers, and if necessary, require changes to the content, length or language.

The corresponding author must, in the name of all authors, also enclose a written statement that the paper is original unpublished work, and not under consideration for publication elsewhere.

On publication, copyright for the paper shall pass to the Journal of Mechanical Engineering. The JME must be stated as a source in all later publications.

Editorial does not return submitted materials. Unpublished material is not preserved and is not send anywhere else without author's consent.

Paper prepared for publishing will be send to authors in PDF format. Authors should make minor corrections if needed. With this author confirms paper for publishing.

PUBLICATION FEE

For all papers authors will be asked to pay a publication fee prior to the paper appearing in the journal. However, this fee only needs to be paid after the paper is accepted for publishing by the Editorial Board. The fee is €180.00 (for all papers with maximum of 6 pages), €220.00 (for all paper with maximum of 10 pages) and €20.00 for each addition page. Publication fee includes 25 separates of each paper send to corresponding author.

Vsebina

Strojniški vestnik - Journal of Mechanical Engineering
letnik 54, (2008), številka 7-8
Ljubljana, avgust 2008
ISSN 0039-2480

Izhaja mesečno

Povzetki razprav

Osebne vesti

Strojniški vestnik - Journal of Mechanical Engineering 54(2008)7-8, SI 83
UDK 681.786
Prejeto: 02.06.2008
Sprejeto: 07.07.2008

Laserski večlinijski triangulacijski sistem za hitro merjenje 3-D oblike prsnega koša med dihanjem

Matija Jezeršek[1,*], Matjaž Fležar[2], Janez Možina[1]
[1] Univerza v Ljubljani, Fakulteta za strojništvo, Slovenija
[2] Univerzitetna klinika Golnik, Golnik, Slovenija

Opisan je optični sistem za 3-D merjenje oblike prsnega koša med dihanjem. Sistem temelji na laserski triangulaciji z večlinijskim osvetljevanjem. Sestoji iz CCD kamere in laserskega projektorja, ki na merjeno telo sočasno projicira 33 svetlobnih ravnin. Natančnost znaša ±0.5 mm, merilno območje je 400x600x500 mm in meri s frekvenco 80 Hz. Učinkovitost sistema je bila testirana na odraslem prostovoljcu, ki je dihal v dveh režimih: s pomočjo prsnega koša ter s pomočjo trebušnih mišic oziroma abdominalno. Rezultati vzorcev dihanja so prikazani v grafičnem in numeričnem načinu.

Ključne besede: meritve dihanja, prsni koš, laserska triangulacija, 3-D merjenje

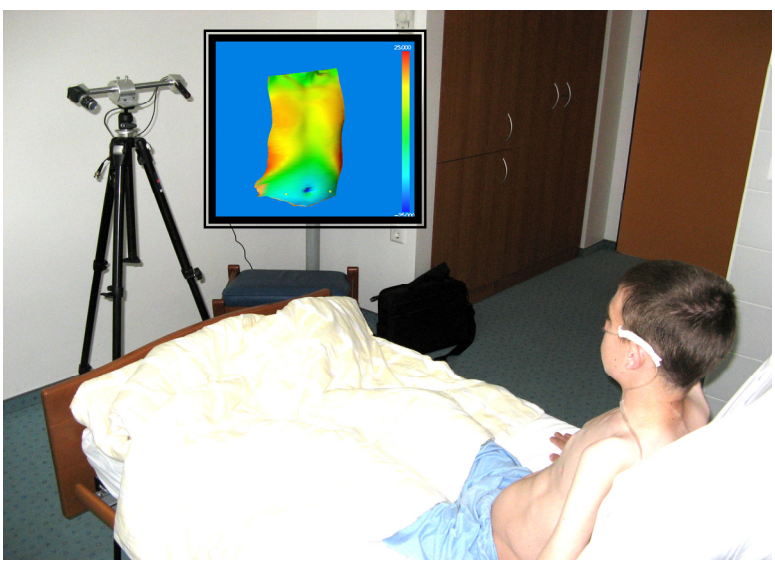

Slika 1. *Laserski večlinijski triangulacijski sistem za hitro merjenje 3-D oblike prsnega koša med dihanjem*

[*]Naslov odgovornega avtorja: Univerza v Ljubljani, Fakulteta za strojništvo, Aškerčeva 6, SI-1000 Ljubljana, Slovenija, matija.jezersek@fs.uni-lj.si

Strojniški vestnik - Journal of Mechanical Engineering 54(2008)7-8, SI 84
UDK 678
Prejeto: 03.04.2007
Sprejeto: 15.05.2008

Oblikovanje funkcionalnosti in trajnosti polimernih izdelkov s spremembami v tehnologiji predelovanja

Urška Florjančič [1,*] - Igor Emri [1,2]
[1] Center za eksperimentalno mehaniko, Univerza v Ljubljani, Slovenija
[2] Institute for Sustainable Innovative Technologies, Ljubljana, Slovenija

Delo obravnava nove možnosti spreminjanja funkcionalnosti polimernega izdelka s pomočjo spreminjanja strukture materiala v fazi predelovanja in posledično njegovega časovno odvisnega vedenja, ki opredeljuje trajnost končnega izdelka. V prvem delu prispevka poročamo o razlikah v strukturi materiala na atomskem nivoju, ki so nastale kot posledica razlik v tehnologiji predelovanja polimernega izdelka. Podan je kratek pregled trenutnega stanja na področju raziskav, ki obravnavajo pojav večdimenzionalnih interakcij v procesu formiranja strukture materiala. Obenem so predlagane eksperimentalne metode, s katerimi je mogoče raziskovati in analizirati vpliv procesnih parametrov na formiranje strukture materiala ter posledično na makroskopske lastnosti končnega polimernega izdelka.

V drugem delu prispevka iščemo odgovore na dvoje vprašanj: (i) ali je mogoče z obstoječo opremo za procesiranje polimerov v industrijskem okolju (v našem primeru ekstrudiranje) ustvariti pogoje, pri katerih se pojavijo nelinearni procesi med formiranjem strukture materiala, in (ii) kolikšne spremembe strukture in posledično mehanske in druge lastnosti končnega polimernega izdelka lahko dosežemo v industrijskem okolju s spremembami v tehnologiji (t.j., s spremembo procesnih parametrov).

V delu je demonstrirana možnost spreminjanja funkcionalnosti polimernih izdelkov preko spreminjanja strukture materiala, ki jo dosežemo z izbiro ustreznih procesnih parametrov. Rezultati raziskave so pokazali, da lahko tehnološke pogoje v območju temperatur in tlakov, tipičnih za ekstrudiranje polimerov v industrijskih razmerah, spremenimo tako, da pomembno vplivamo na formiranje strukture in posledično na časovno odvisne mehanske lastnosti materiala in s tem na funkcionalnost končnega izdelka. Izkazalo se je, da je s spremembami procesnih parametrov v območju industrijskih pogojev možno izboljšati trajnost za več velikostnih razredov! To odpira nove možnosti na področju spreminjanja funkcionalnosti polimernih izdelkov in s tem povečevanje njihove konkurenčne sposobnosti na svetovnem trgu.

Ključne besede: polimeri, strukturne spremembe, funkcionalnost, trajnost

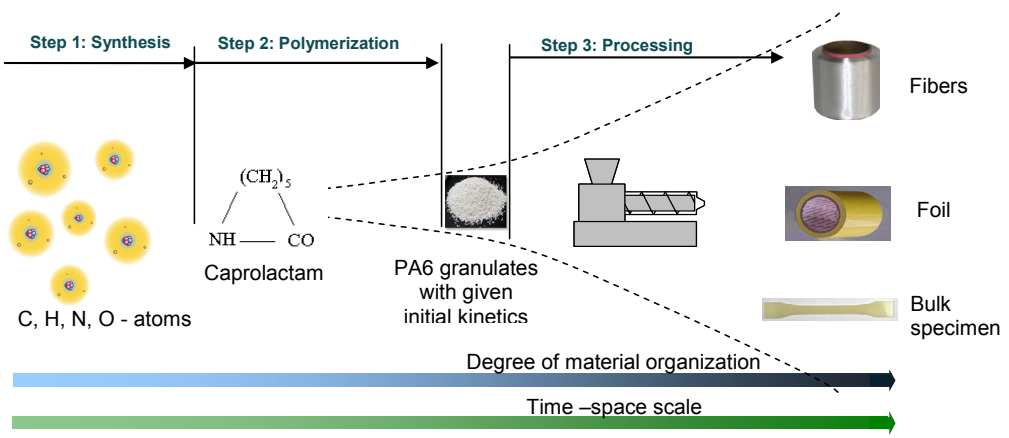

Slika 1. *Različne faze oblikovanja polimerne strukture [1]*

[*]Naslov odgovornega avtorja: Urška Florjančič, Center za eksperimentalno mehaniko, Univerza v Ljubljani, Cesta na Brdo 85, SI-1000 Ljubljana, Slovenia, urska.florjancic@fs.uni-lj.si

Strojniški vestnik - Journal of Mechanical Engineering 54(2008)7-8, SI 85
UDK 621.91
Prejeto: 06.11.2007
Sprejeto: 19.12.2007

Vpliv rezalne sile in podajanja na nastanek nalepka, rezalne sile in površinsko hrapavost pri obdelavi zlitine Aa6351 (T6)

Hasan Gokkaya[1] - Ahmet Taskesen[2,*]
[1] Zonguldak Karaelmas Universitesi Safranbolu Meslek Yuksekokulu, Turkey
[2] Makine Egt. Bolumu, Teknik Egt. Fakultesi, Gazi Universitesi, Ankara, Turkey

V predstavljenem prispevku so eksperimentalno preučeni vplivi parametrov obdelave kot sta rezalna hitrost) in podajanje na nastanek nalepka, glavno rezalno silo in površinsko hrapavost. Določeni so bili optimalni in kritični rezalni parametri. Ugotovljeno je bilo, da mora biti rezalna hitrost pri obdelavi zlitine AA6351 (T6) z neoplaščenimi karbidnimi ploščicami višja od 400-500 m/min, da ne pride do nastanka nalepka. Rezultati raziskave kažejo, da ima največji vpliv na rezalno silo in površinsko hrapavost podajanje. Kot rezultat raziskave sta bila določena optimalna rezalna sila in optimalno podajanje za minimalno površinsko hrapavost obdelovanca.

Ključne besede: obdelovalni postopki, obdelovalni parametri, rezalne sile, hrapavost površin

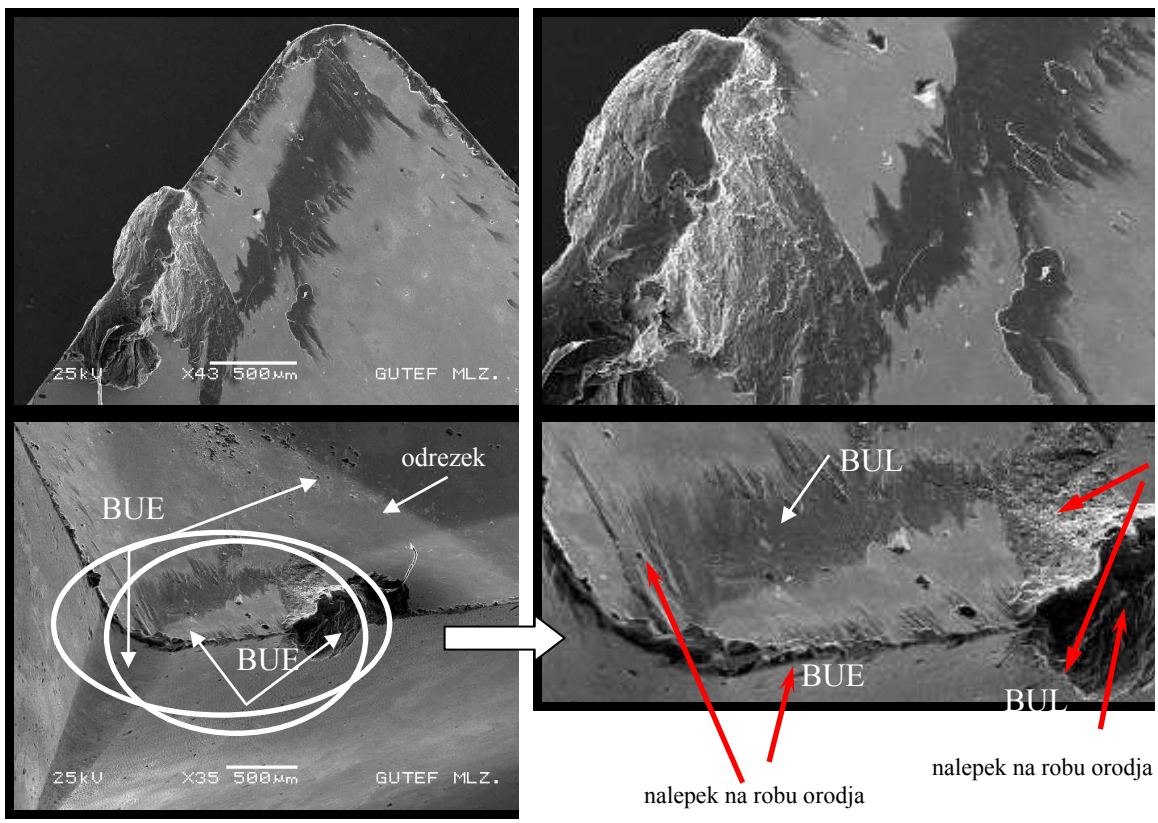

Slika 2. *Posnetek nalepka na neoplaščeni površini ploščice, izdelan z vrstičnim elektronskim mikroskopom, pri 200 m/min in 0,30 mm/vrt.*
a)Posnetek cepilne površine orodja, ustvarjen z vrstičnim elektronskim mikroskopom
b)3D-posnetek, ustvarjen z vrstičnim elektronskim mikroskopom

*Naslov odgovornega avtorja: Makine Egt. Bolumu, Teknik Egt. Fakultesi, Gazi Universitesi, Ankara, Turkey, taskesen@gazi.edu.tr

Strojniški vestnik - Journal of Mechanical Engineering 54(2008)7-8, SI 86 Prejeto: 12.09.2007
UDK 621.9:669.14 Sprejeto: 19.12.2007

Eksperimentalna raziskava odvisnosti glavne rezalne sile in površinske hrapavosti od rezalnih parametrov

Ihsan Korkut[1,*] - Mehmet Boy[2]
[1] Gazi University, Ankara, Turkey
[2] Karabük University,Turkey

Opravljena je bila eksperimentalna raziskava glavnih rezalnih sil na rezalno orodje v odvisnosti od rezalnih parametrov pri obdelavi jekla AISI 1117. Pridobljeni eksperimentalni rezultati so bili primerjani z empiričnimi rezultati. Rezalne sile so bile pri eksperimentalni raziskavi merjene s trokomponentnim (Fc, Ff in Fp) piezoelektričnim dinamometrom Kistler 9257A. Dinamometer je bil povezan z nabojnim ojačevalnikom 5019 B130, priključenim na osebni računalnik s programsko opremo za merjenje sil Kistler Dynoware. Empirični rezultati so bili pridobljeni s Kienzlejevim pristopom. V eksperimentih je bilo uporabljenih pet različnih rezalnih hitrosti, pet različnih podajanj in dve različni globini reza. Ugotovljeno je bilo, da se rezalne sile zmanjšajo s povečanjem rezalne hitrosti oziroma povečajo s povečanjem podajalne hitrosti. Eksperimentalni rezultati kažejo podoben trend kot empirični rezultati. Ob koncu eksperimentov je bilo ugotovljeno, da se kakovost površine izboljša s povečanjem rezalne hitrosti in zmanjša s povečanjem podajanja.

Ključne besede: obdelovalni postopki, jeklo, rezalne sile, hrapavost površin, parametri rezanja

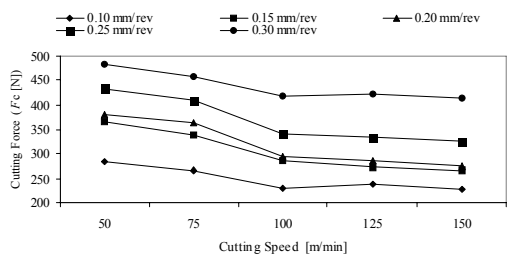

Slika 3. *Odvisnost glavne rezalne sile od rezalne hitrosti pri globini reza 1 mm in neoplaščenem rezalnem orodju*

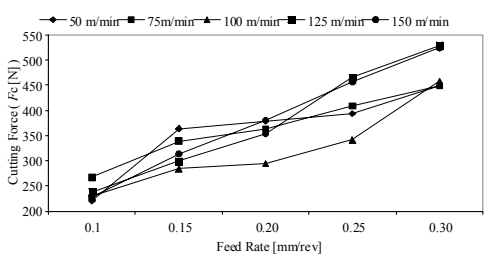

Slika 4. *Odvisnost rezalne sile od podajanja pri globini reza 1 mm in neoplaščenem rezalnem orodju*

*Naslov odgovornega avtorja: Gazi University,Technical Education Faculty, 06500, Besevler, Ankara, Turkey
ikorkut@gazi.edu.tr

Strojniški vestnik - Journal of Mechanical Engineering 54(2008)7-8, SI 87
UDK 681.586, UDK 621.38
Prejeto: 20.07.2007
Sprejeto: 19.12.2007

Modeliranje in analiza mikro elektro-mehanskega sistema

Maja Atanasijević-Kunc[1,*] - Vinko Kunc[2] - Janez Diaci[3] - Rihard Karba[1]
[1] Univerza v Ljubljani, Fakulteta za elektrotehniko, Ljubljana, Slovenija
[2] IDS Integrirani in diskretni sistemi, d.o.o., Ljubljana, Slovenija
[3] Univerza v Ljubljani, Fakulteta za strojništvo, Ljubljana, Slovenija

Modeliranje mikro-mehanskih sistemov, ki delujejo v kombinaciji z integriranimi elektronskimi vezji, je dokaj zahtevna naloga, ki zahteva poznavanje načrtovanja sistemov z obeh področij v kombinaciji z matematičnim modeliranjem, kar je še posebej pomembno, kadar želimo proučiti nove možnosti delovanja obravnavanega procesa in njegove lastnosti. Tovrstno modeliranje postaja vse pomembnejše, saj vse hitreje narašča uporaba tako imenovanih "pametnih senzorjev", ki temeljijo na mikro-mehanskih sistemih. Naša naloga je bila načrtati zanesljiv model mikro elektro-mehanskega senzorja pospeška, ki uporablja ekstremno majhen mehanski sistem, katerega proizvodnja je nezahtevna. Vpeta masa in izhodni signal tega senzorja sta za velikostni razred manjša od obstoječih sistemov. Opisani model smo nadalje uporabili pri razvoju mehaničnega in električnih delov sistema. Pri razvoju modela smo uporabili tudi meritve prototipnih naprav, s pomočjo katerih smo preverjali statične lastnosti, pri odzivu na stopničasta testna vzbujanja pa tudi dinamične. Ob upoštevanju poznanih fizikalnih zakonitosti in ravnotežnih razmerij smo razvili predstavljeni model, ki se zelo dobro ujema z izvedenimi meritvami.

Ključne besede: mikromehanski sistemi, **modeliranje, senzorji pospeška, kontrolni sistemi**

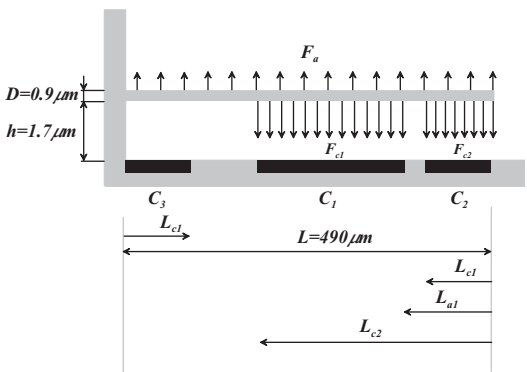

Slika 1. *Prerez mikro-mehanskega sistema*

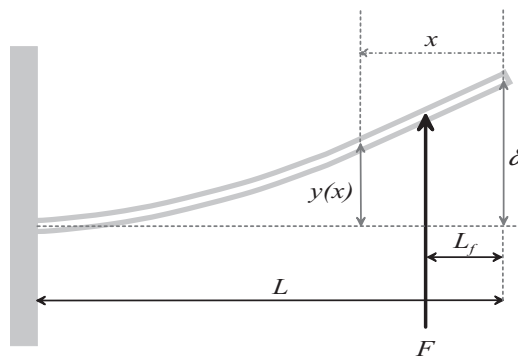

Slika. 2. *Upogib konzole*

*Naslov odgovornega avtorja: Univerza v Ljubljani, Fakulteta za elektrotehniko, Tržaška c. 25, 1000 Ljubljana, Slovenija, maja.atanasijevic@fe.uni-lj.si

Strojniški vestnik - Journal of Mechanical Engineering 54(2008)7-8, SI 88
UDK 696.135, UDK 628.3
Prejeto: 06.12.2007
Sprejeto: 12.03.2008

Eksperimentalne raziskave poroznosti in prepustnosti kosmov v suspenzijah iz biološke čistilne naprave

Boštjana Žajdela[1], Matjaž Hriberšek[2], Aleš Hribernik[2]
[1] Regionalna razvojna agencija Mura, Slovenija
[2] Univerza v Mariboru, Fakulteta za strojništvo, Slovenija

Prispevek obravnava gibanje kosmov v suspenziji, ki je delovna zmes na biološki čistilni napravi (BČN). Podane so osnovne enačbe za rešitev problema in analiza odpadne vode BČN Lendava z vzorčenjem. V eksperimentalnih raziskavah je največja pozornost namenjena geometrijskim in sedimentacijskim sposobnostim kosmov, ki so ključni parametri pri razvoju numeričnega postopka za simulacijo gibanja kosmov. Predstavljene so obsežne analize oblike kosmov, velikosti primarnih delcev ter kosmov, poroznosti ter prepustnosti kosmov in gostote kosmov. Na osnovi rezultatov eksperimentalnih raziskav so definirani in izračunani fizikalni parametri kosmov ob upoštevanju njihove poroznosti.

Ključne besede: čiščenje odpadnih voda, biološke čistilne naprave, sedimentacija, poroznost

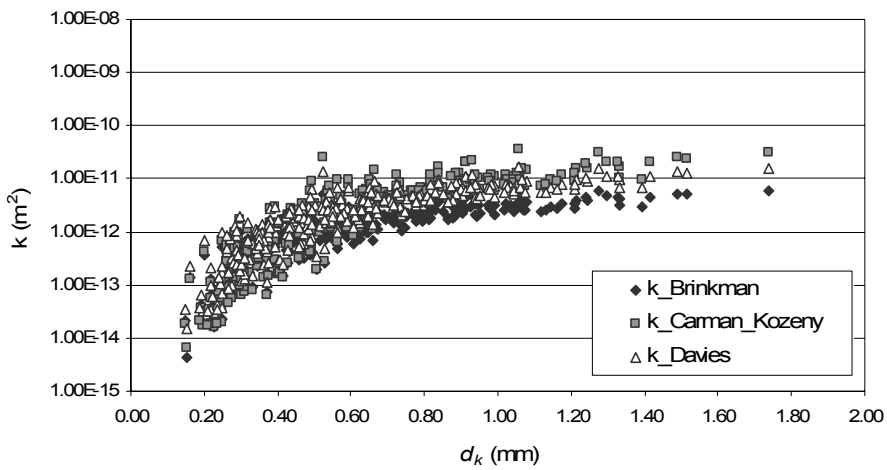

Slika 8. *Permeabilnost kosmov po modelih Brinkman, Carman-Kozeny in Davies*

*Naslov odgovornega avtorja: Boštjana Žajdela, Regionalna razvojna agencija Mura, Slovenia
bostjana.zajdela@rra-mura.si

Strojniški vestnik - Journal of Mechanical Engineering 54(2008)7-8, SI 89
UDK 614.86:631.372
Prejeto: 13.08.2007
Sprejeto: 19.12.2007

Raziskava števila nesreč s kmetijskimi in gozdarskimi traktorji v evropi in najpogostejši vzroki zanje

Rajko Bernik[1], Robert Jerončič[2,*]

[1]Univerza v Ljubljani, Biotehniška Fakulteta, Ljubljana, Slovenija
[2] Ministrstvo za promet, Direktorat za promet, Ljubljana, Slovenija

Kmetijski in gozdarski traktorji predstavljajo veliko potencialno nevarnost za prometno ali delovno nesrečo. Zaradi svoje konstrukcije ima traktor visoko težišče in je zaradi tega zelo nestabilno vozilo. V Sloveniji je od leta 1981 do leta 2005 umrlo 773 ljudi. Na srečo pa je število mrtvih vsako leto manjše. Najpogostejši vzrok za nesreče s kmetijskimi in gozdarskimi traktorji je prevračanje vozila. To velja tako za Slovenijo kot tudi za večino ostalih držav po svetu. Podatki o mrtvih v nesrečah s kmetijskimi in gozdarskimi traktorji so bili pridobljeni s pomočjo tujih homologacijskih in registracijskih organov.

Ključne besede: kmetijska mehanizacija, traktorji, prometne nesreče

Table 1: *Podatki o smrtih v prometnih nesrečah s kmetijskimi in gozdarskimi traktorji*

	1990	1991	1992	1993	1994	1995	1996	1997	1998	1999	2000	2001	2002	2003	2004	2005
Slovenija	18	8	11	12	13	8	6	9	7	6	5	10	4	4	9	2
Finska	-	2	7	3	1	5	5	4	1	3	4	2	2	3	1	0
Avstrija	-	24	13	18	20	20	15	7	13	12	19	15	12	10	7	8
Nizozemska	-	7	1	5	3	1	2	2	2	4	3	1	2	5	5	5
Švedska	-	5	4	2	1	5	0	3	3	6	4	0	3	2	5	1
Nemčija	-	-	115	112	94	107	134	112	101	106	95	96	104	110	87	-
Luksemburg	-	0	0	0	0	0	0	1	1	0	2	0	0	0	0	0
Velika Britanija	-	2	2	2	0	0	1	1	1	2	7	3	1	11	7	0
Portugalska	-	57	58	55	36	38	36	35	33	30	38	32	31	26	35	33
Estonija	32	23	12	14	17	9	4	4	9	1	2	7	4	2	-	2
Latvija	-	-	-	-	-	14	7	12	15	10	7	10	9	11	10	-
Poljska	175	123	115	111	93	98	68	84	82	72	72	62	47	61	57	67
Švica	-	-	-	-	-	-	27	26	26	24	28	23	20	25	18	13
Srbija	107	94	80	69	74	66	72	106	81	55	58	-	-	-	-	-
Belgija	0	4	2	1	2	4	3	2	3	4	5	0	1	2	3	1
Danska	-	3	3	3	4	2	0	0	3	2	3	1	0	0	0	3
Francija	-	43	37	28	32	32	36	35	22	20	26	12	20	25	13	12
Grčija	-	114	93	79	99	81	44	80	61	71	54	72	43	46	37	26
Italija	-	51	40	42	47	30	38	31	23	38	28	24	23	24	23	23
Španija	-	43	40	23	26	30	36	33	30	32	35	28	16	23	40	26
Hrvaška	-	-	-	-	-	-	20	14	8	3	10	13	14	8	10	13

[*]Naslov odgovornega avtorja: Ministrstvo za promet, Direktorat za promet, Langusova 4, 1535 Ljubljana, Slovenija, robert.jeroncic@gov.si

Strojniški vestnik - Journal of Mechanical Engineering 54(2008)7-8, SI 90
UDK 656.088:621.879.324
Prejeto: 24.08.2007
Sprejeto: 19.12.2007

Izboljšava sistema vzdrževanja in popravil bagra za dnevni kop SRs1200 z uporabo pristopa projektnega managementa

Brane Semolič[1,*] - Petar Jovanović[2] - Sava Kovačev[3] - Vladimir Obradović[2]
[1] Fakulteta za logistiko, Celje, Slovenija
[2] Univerza v Beogradu, Beograd, Srbija,
[3] Kolubara Metal, Lazarevac, Srbija

Stroški poškodb strojev in naprav so zelo veliki, velikokrat celo precej večji kot stroški vzdrževanja, popravil ali rekonstrukcij. Zaradi tega razloga se razvijajo različne metode vzdrževanja in popravil industrijskih ter ostalih strojev in naprav. Podrobnejše proučevanje omenjenih metod daje veliko možnosti za njihove izboljšave. Omenjene izboljšave so najbolj vidne na področju managementa časa, virov in stroškov takšne organizacije. Pričujoči prispevek predstavlja izboljšavo sistema vzdrževanja in popravil opreme s pomočjo uporabe metod in tehnik projektnega managementa. Predstavljene metode dela so bile preizkušene v praksi na primeru projekta revitalizacije bagrov za dnevni kop SRs1200, v podjetju MB Kolubara, in sicer na enem izmed najkompleksnejših tovrstnih projektov v tej regiji. Kompleksnost projekta je bila izražena v kompleksnosti tehniških zahtev rekonstrukcije bagra, v številu aktivnosti projekta, številu sodelujočih posameznikov in organizacij, kakor tudi stroških ter omejenosti razpoložljivega časa za izvedbo projekta. Uporaba opisanega načina dela je pomembno vplivala na uresničitev nadpovprečnih rezultatov na tehničnem in finančnem področju uresničitve ciljev projekta.

Ključne besede: žlični bagerji, vzdrževanje, popravila strojev, projektno vodenje

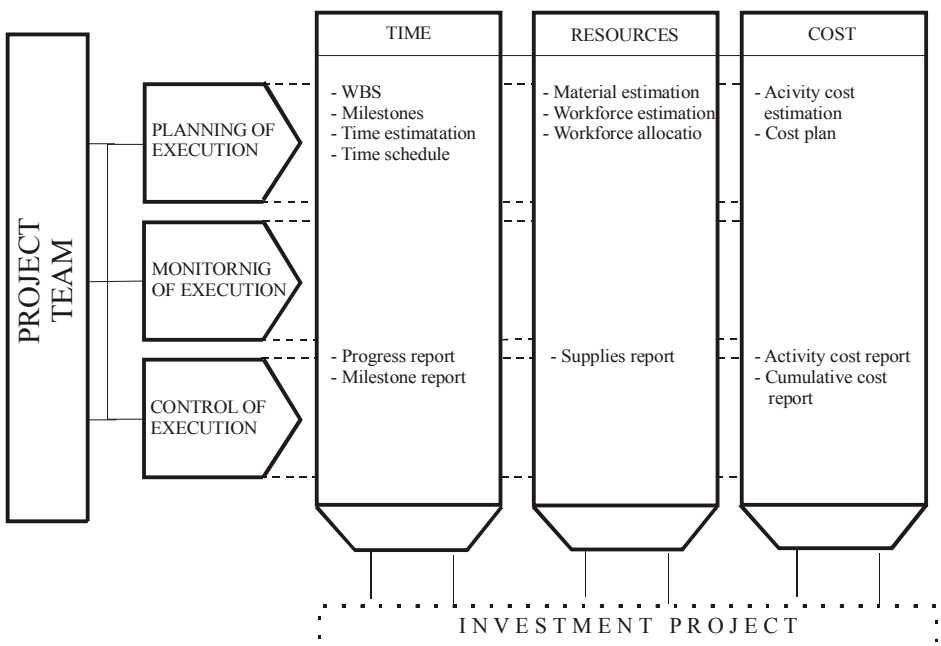

Slika 1. *Splošen koncept projektnega managementa*

[*]Naslov odgovornega avtorja: Univerza v Mariboru, Fakulteta za logistiko, Mariborska 7, 3000 Celje, brane.semolic@siol.net

Osebne vesti

Prof. dr. Matija Tuma, 70 letnik

Prof. dr. Matija Tuma se je rodil 17. 7. 1938 v Ljubljani, kjer je obiskoval osnovno šolo in klasično gimnazijo. Leta 1956 je maturiral in se nato vpisal na Fakulteto za strojništvo v Ljubljani. Že med študijem ga je mikalo področje energijskih pretvorb in termodinamike, zato si je za mentorja pri diplomskem delu izbral prof. Ranta. Diplomiral je leta 1962. Iz razširjene diplome je v Strojniškem vestniku objavil svoj prvi znanstveni članek v katerem raziskuje vpliv temperature predgretega zgorevalnega zraka in vrste goriva na eksergijski izkoristek parnih kotlov. Kot mlad diplomirani inženir strojništva se je po služenju vojaškega roka zaposlil v tovarni Rog, kjer je oral ledino na področju konstruiranja transportnih naprav v proizvodnji. Leta 1966 se je z ženo in sinom preselil v Švico, kjer se je zaposlil v koncernu ABB v Badnu kot projektant na oddelku za velike parne turbine. Svojo kariero v tem koncernu je končal kot vodja skupine za tehniko postrojenj. V tistem času so v Sloveniji gradili JE Krško, zato se je želel vrniti domov in sodelovati pri izgradnji. Krška jedrska elektrarna je njegovo prošnjo za zaposlitev zavrnila. Zanj je bila to sreča v nesreči saj je zaradi zavrnitve odšel v službo na Zvezno tehniško visoko šolo, ETH v Zuerichu v ustanovo, ki se ponaša s 14 Nobelovimi nagrajenci. Tu je delal kot višji asistent in kljub pedagoškim obveznostim in leta 1978 doktoriral s področja termodinamike in prenosa toplote.

V Švici se je zakoncema Tuma rodil še en sin. Tu se je družil z slovenskimi izseljenci in pomagal pri ustanovitvi fundacije "Pro cultura slovenica". Matija je fundaciji dal ime in napisal pravila v skladu s švicarskimi zakoni. Fundacija, ki finančno podpira šolanje zamejskih Slovencev v materinem jeziku, obstoja še danes. V tistem času je aktivno spremljal dogajanja med Slovenci v Avstriji, Italiji in na Madžarskem ter v bran rojakov pisal članke v zamejske, slovenske in švicarske časopise. Bil je med ustanovitelji slovenskega dopolnilnega pouka za otroke v Zürichu.

Rad je hodil v hribe. Ljubezen do planin je podedoval po svojem starem očetu dr. Henriku Tumi, znanem gorniku, zavednem Slovencu in buditelju narodne zavesti. Bil je zelo povezan z dejavnostjo slovenskega izseljeniškega planinskega društva Triglav. Povzpel se je na 19 štiritisočakov, tudi na Mont Blanc, Monte Roso in Matterhorn. Nekatere vzpone je opisal in svoja doživetja objavil v Planinskem vestniku v člankih "Kako me je osvojil štiritisočak" in "Grozo izzivam, v dušo jo vabim". Zanimivi so tudi njegovi članki z opisi gora, ki nosijo enako ime kot je njegov priimek. To je gora Piz Tuma v Švici in Torre Tuma v Argentini, ki je dobila ime po njegovem starem očetu.

Prišel je čas, ko se je bilo treba odločiti za povratek v domovino, kjer je najprej dobil zaposlitev v tovarni Lek. Konec leta 1982 se je Matija zaposlil kot izredni profesor na Fakulteti za strojništvo. Po prihodu na fakulteto je s svojim delom markantno zaznamoval razvoj Katedre za energetsko strojništvo, Fakultete za strojništvo in tudi celotne energetike v Sloveniji. Leta 1986 je postal predstojnik Katedre za energetsko strojništvo in to, s kratkimi presledki, ostal vse do upokojitve. Leta 1993 je bil izvoljen v naziv redni profesor. Bil je dekan fakultete od leta 1995 do leta 1997. Leta 1994 je postal član Sveta za visoko šolstvo vlade Republike Slovenije, 1995 nacionalni koordinator za področje Energetika pri ministrstvu za znanost in tehnologijo in leta 2000 član Sveta za znanost in tehnologijo Republike Slovenije. Bil je član nadzornih svetov v več podjetjih in v tujini tudi član Znanstvenega sosveta VGB, Nemčija.

Upokojil se je 30.9.2004 po skoraj dvainštiridesetih letih delovne dobe. Kljub upokojitvi je še vedno aktivno deloval na področju termoenergetike. V njegovem COBISS-u se je od upokojitve do danes število enot povečalo za štirideset. Postal je tudi član

Terminološke komisije pri Slovenski akademiji znanosti in umetnosti.

V času aktivnega delovanja je prof. Tuma bogato prispeval na pedagoškem, raziskovalnem in strokovnem področju energetskega strojništva. Njegovi sodelavci smo občudovali njegovo predanost, saj delovnega časa sploh ni poznal. Predaval je na diplomskem in podiplomskem študiju, bil je mentor šestim doktorjem, trinajstim magistrom in sedeminosemdesetim diplomantom. Dva njegova kandidata sta dobila Prešernovo nagrado. Spisal je dva univerzitetna učbenika, ki sta izšla v več izdajah. Širše področje njegovega raziskovalnega in strokovnega dela je bilo pretvarjanje energij, ožje pa klasične in jedrske elektrarne, plinske in parne turbine ter racionalna raba energije v industriji. Objavil je petinpetdeset znanstvenih člankov, od tega petintrideset v tujih revijah in štiriindvajset v revijah s faktorjem vplivnosti, veliko število strokovnih člankov, ter znanstvenih in strokovnih referatov, do upokojitve skupno stoosemnajst člankov in referatov.

Obseg njegovega strokovnega dela je izjemen. Sodeloval je z vsemi slovenskimi termoelektrarnami, s številnimi podjetji, ki imajo energetsko intenzivno proizvodnjo ter z vladnimi inštitucijami. Njegovo delo na strokovnem področju obsega stooseminsedemdeset poročil. V COBISS-u danes izkazuje preko petstoosemdeset enot, med katerimi je, razen že naštetih del, tudi preko petdeset nestrokovnih člankov, več intervjujev, polemike, itd.

Sodelavci smo ga osebno, kot človeka, doživljali predvsem kot vodjo Laboratorija za termoenergetiko, predstojnika Katedre za energetsko strojništvo in vodjo raziskovalne skupine. Njegov prirojeni čut za sodelovanje in pravičnost je omogočal ustvarjalno klimo v skupinah, ki jih je vodil. Ko je leta 1986 prevzel predstojništvo katedre, so bili na katedri štirje doktorji znanosti, ob njegovem odhodu v pokoj jih je bilo enajst, od tega sedem visokošolskih učiteljev. Spomniti se moramo na izrazito človeško plat njegovega vodenja katedre in laboratorija kar je povzročalo pozitivne odnose med sodelavci. To dokazuje tudi dejstvo, da v praktično dvajsetih letih njegovega vodenja katedre, niti enkrat ni prišlo do osebnih trenj ali napetosti med člani. Kot vodja raziskovalne skupine je omogočil v skupini oblikovati okolje nadpovprečne ustvarjalnosti.

Njegovi bivši sodelavci Laboratorija za termoenergetiko se iskreno veselimo njegovih obiskov na fakulteti v vlogi upokojenca in prav radi prisluhnemo njegovim nasvetom, ki nam jih predstavi na osnovi svojih izkušenj. Veseli smo, da je v upokojitvi našel nove cilje in izzive, ter jih koristno uporabil v svoje zadovoljstvo.

Ob življenjskem jubileju mu iskreno čestitamo, ne le kolegi in prijatelji, temveč želje izrekamo tudi v imenu njegovih študentov, diplomantov, podiplomcev in vseh nekdanjih sodelavcev. Želimo mu obilico zdravja, še mnogo zadovoljnih in plodnih let ter veliko, veliko osebne sreče.

prof. dr. Janez Oman

Doktorata, magisteriji, specializaciji in diplome

DOKTORATA

Na Fakulteti za strojništvo Univerze v Ljubljani sta z uspehom zagovarjala svoji doktorski disertaciji:

dne *16. junija 2008*: **Alen Šarlah** z naslovom: "Termohidravlične lastnosti regeneratorjev toplote v magnetnem hladilniku" (mentor: prof. dr. Alojz Poredoš);

V doktorskem delu so predstavljene raziskave kompaktnih regeneratorjev toplote in aktivnih magnetnih regeneratorjev s stališča termohidravličnih karakteristik in magnetnih lastnosti. Izpeljan je brezdimenzijski numerični model za določitev toplotne prestopnosti ter preverjen z uporabo analitičnih metod. Model je bil skupaj z rezultati eksperimenta uporabljen za oceno šestih različnih geometrij regeneratorjev toplote, pri čemer so bili ocenjevalni parametri toplotna prestopnost, padec tlaka in toplotna učinkovitost.

Obstoječ numerični model je v nadaljevanju nadgrajen z vplivom magnetnih lastnosti materialov in karakteristikami delovanja aktivnega magnetnega regeneratorja. Pri tem so magnetne lastnosti dobljene z uporabo molekularne aproksimacije magnetnega polja. Model je bil testiran s stališča termodinamične konsistentnosti in preverjen z uporabo razpoložljivih eksperimentalnih rezultatov. Na koncu je predstavljenih nekaj rezultatov numerične simulacije delovanja aktivnega magnetnega regeneratorja za testirane geometrije. Primerjava je narejena na osnovi dosežene temperaturne razlike in hladilnega števila. Numerični model predstavlja vsestransko orodje za napoved delovanja aktivnih magnetnih regeneratorjev in oceno ustreznosti različnih oblik regeneratorjev.

dne *26.junija 2008*: **Boštjan Veber** z naslovom: " Modeliranje vpliva popravil na zdržljivost izdelkov v razvoju" (mentor: prof. dr. Matija Fajdiga);

Postavljena je metodologija za napovedovanje zdržljivosti popravljivih izdelkov že v zgodnejših fazah razvojnega postopka. Celovit postopek za izračun zdržljivosti popravljivega izdelka vključenje eksperimentalno modeliranje vgrajene zanesljivosti, učinkovitosti popravil in modeliranje obnovitvene funkcije splošnega obnovitvenega procesa. Z odpravo okvare lahko pri izdelku vzpostavimo stanje 'dober kot nov', 'slab kot star' ali boljši kot star, toda slabši kot nov'. Predstavljena sta dva pristopa za opis vpliva popravila na vgrajeno zanesljivost izdelka. Učinkovitost popravila modeliramo z vpeljavo navidezne dobe delovanja izdelka. Jedro zgrajenega modela je pogojna kumulativna porazdelitvena funkcija verjetnosti časa delovanja do naslednje okvare, ki je modelirana z mešanico Weibullovih porazdelitev. V razvojnem postopku je na voljo le omejena količina podatkov o okvarah, zato proste parametre splošnega obnovitvenega procesa ocenimo z metodo največje verjetnosti. pripadajoče enačbe rešimo z uporabo algoritma matematičnega pričakovanja in genetskega algoritma. Zdržljivost popravljivega izdelka nato določimo z Monte Carlo simulacijo ocenjenega modela splošnega obnovitvenega procesa.

MAGISTERIJI

Na Fakulteti za strojništvo Univerze v Ljubljani je z uspehom zagovarjal svoje magistrsko delo:

dne *9. junija 2008* **Jože Jenkol**e z naslovom: "Informacijska podpora odločanju v adaptivnih distribuiranih delovnih strukturah" (mentor: izr. prof. dr. Alojz Sluga)

Na Fakulteti za strojništvo Univerze v Mariboru sta z uspehom zagovarjala svoji magistrski deli:

dne *9. junija 2008* **Boštjan Slapnik** z naslovom: "Sistemski model računalniško povezane proizvodnje ročnega orodja" (mentor: prof. dr. Jože Balič).

dne *12. junija 2008* **Damjan Osrajnik** z naslovom: "Načrtovanje in vzdrževanje komunalnih čistilnih naprav" (mentor: prof. dr. Boris Aberšek)

SPECIALIZACIJI

Na Fakulteti za strojništvo Univerze v Mariboru sta z uspehom zagovarjala svoji specialistični deli:

dne *9. junija 2008* **Sebastjan Kotnik** z naslovom: "Optimizacija tehnoloških postopkov injekcijskega brizganja sintetičnih mas" (mentor: prof. dr. Jože Balič).

dne *10. junija 2008* **Matej Kuhar** z naslovom: "Računalniško podprto vodenje proizvodnje svetlobne opreme vozil" (mentor: izr. prof. dr. Borut Buchmeister).

DIPLOMIRALI SO

Na Fakulteti za strojništvo Univerze v Ljubljani so pridobili naziv univerzitetni diplomirani inženir strojništva:

dne *26. junija 2008*: Tomaž BEVK , Gregor LAPUH, Marc TOSQUELLA TOBELLA.

dne *27. junija 2008*: Matija GREGORC, Lovro KUŠČER, Vid NOVAK, Uroš ŠAJN, Iztok SKOK, Miha ZIBELNIK.

dne *30. junija 2008*: Guillermo Acebal FERNÁNDEZ, Boštjan KASTELIC, Jani KENDA, Marko SKUBE, Luka TAVČAR, Gregor VERŽUN.

Na Fakulteti za strojništvo Univerze v Mariboru so pridobili naziv diplomirani inženir strojništva:

dne *19. junija 2008*: Marin RADOŠ, Peter SEVER.

dne *26. junija 2008*: Marjan GRANFOL, Blaž VAJDA.

*

Na Fakulteti za strojništvo Univerze v Ljubljani so pridobili naziv diplomirani inženir strojništva:

dne *3. junija 2008*: Matej ERMAN, Andrej FIORELLI, Žiga SEVŠEK, Aleš SVETINA, Luka TURK.

dne *18. junija 2008*: Nejc CESTNIK, Matej KEBER, Marko LAH, Miran LONGAR, Irena RUPNIK, Omer DEMIROVIĆ, Dejan ERJAVEC, Jože HREN, Stanislav HRIBAR, Klemen KOSMAČ.

dne *20. junija 2008*: Gregor GOLOB, Tomaž LAHAJNAR, Matej KRAJNC, David NOVAK, Luka ŽNIDAR.

Na Fakulteti za strojništvo Univerze v Mariboru so pridobili naziv diplomirani inženir strojništva:

dne *26. junija 2008*: Janez BLATNIK, Dejan CEBE, Bojan ČRV, David GREIFONER, Janez KERN, Matej LAH, Robert OCEPEK, Igor ZVER.

Navodila avtorjem

Članki so v Strojniškem vestniku od leta 2008 objavljeni samo v angleškem jeziku s slovenskim naslovom, povzetkom ter sliko s podnaslovom v dodatku. Avtorji so v celoti odgovorni za jezikovno lektoriranje članka. V kolikor recenzent oceni, da jezik ni dovolj kakovosten, lahko uredništvo zahteva ponovno lektoriranje usposobljenega lektorja ter potrdilo o opravljenem lektoriranju.

Članki morajo vsebovati:

- naslov, povzetek, ključne besede,
- besedilo članka,
- preglednice in slike (diagrami, risbe ali fotografije) s podnaslovi,
- seznam literature in
- podatke o avtorjih, odgovornega avtorja in njegov polni naslov.

Članki naj bodo kratki in naj obsegajo približno 8 do 12 strani.

Člankom so lahko priložene tudi dodatne računalniške simulacije ali predstavitve, pripravljene v primerni obliki, ki bodo bralcem dostopne na spletni strani revije.

VSEBINA ČLANKA

Članek naj bo napisan v naslednji obliki:

Naslov, ki primerno opisuje vsebino članka.

- Povzetek, ki naj bo skrajšana oblika članka in naj ne presega 250 besed. Povzetek mora vsebovati osnove, jedro in cilje raziskave, uporabljeno metodologijo dela, povzetek rezultatov in osnovne sklepe.
- Uvod, v katerem naj bo pregled novejšega stanja in zadostne informacije za razumevanje ter pregled rezultatov dela, predstavljenih v članku.
- Teorija.
- Eksperimentalni del, ki naj vsebuje podatke o postavitvi preskusa in metode, uporabljene pri pridobitvi rezultatov.
- Rezultati, ki naj bodo jasno prikazani, po potrebi v obliki slik in preglednic.
- Razprava, v kateri naj bodo prikazane povezave in posplošitve, uporabljene za pridobitev rezultatov. Prikazana naj bo tudi pomembnost rezultatov in primerjava s poprej objavljenimi deli. (Zaradi narave posameznih raziskav so lahko rezultati in razprava, za jasnost in preprostejše bralčevo razumevanje, združeni v eno poglavje.)
- Sklepi, v katerih naj bo prikazan en ali več sklepov, ki izhajajo iz rezultatov in razprave.
- Literatura, ki mora biti v besedilu oštevilčena zaporedno in označena z oglatimi oklepaji [1] ter na koncu članka zbrana v seznamu literature.

OBLIKA ČLANKA

Besedilo članka naj bo pripravljeno v urejevalniku Microsoft Word. Članek nam dostavite v elektronski obliki (lahko po elektronski pošti). Ne uporabljajte urejevalnika LaTeX, saj program, s katerim pripravljamo Strojniški vestnik, ne uporablja njegovega formata. Enačbe naj bodo v besedilu postavljene v ločene vrstice in na desnem robu označene s tekočo številko v okroglih oklepajih.

Enote in okrajšave

V besedilu, preglednicah in slikah uporabljajte le standardne označbe in okrajšave SI. Simbole fizikalnih veličin v besedilu pišite poševno (kurzivno), (npr. v, T, n itn.). Simbole enot, ki sestojijo iz črk, pa pokončno (npr. ms-1, K, min, mm itn.).Vse okrajšave naj bodo, ko se prvič pojavijo, napisane v celoti, npr. časovno spremenljiva geometrija (ČSG). Vse veličine morajo biti navedene, ko se prvič pojavijo, v besedilu ali za enačbo.

Slike

Slike morajo biti zaporedno oštevilčene in označene, v besedilu in podnaslovu, kot sl. 1, sl. 2 itn. Posnete naj bodo v ločljivosti, primerni za tisk, v kateremkoli od razširjenih formatov, npr. BMP, JPG, GIF. Diagrami in risbe morajo biti pripravljeni v vektorskem formatu, npr. CDR, AI.

Vse slike morajo biti pripravljene v črno-beli tehniki, brez obrob okoli slik in na beli

podlagi. Ločeno pošljite vse slike v izvirni obliki.

Pri označevanju osi v diagramih, kadar je le mogoče, uporabite označbe veličin (npr. t, v, m itn.). V diagramih z več krivuljami, mora biti vsaka krivulja označena. Pomen oznake mora biti pojasnjen v podnapisu slike.

Preglednice

Preglednice morajo biti zaporedno oštevilčene in označene, v besedilu in podnaslovu, kot preglednica 1, preglednica 2 itn. K fizikalnim veličinam, npr. t (pisano poševno), pripišite enote (pisano pokončno) v oglatih oklepajih.

Zahvala

Zahvala o sodelovanju in pomoči je lahko vključena pred referencami. Navedite (so)financerje raziskave.

Seznam literature

Vsa literatura mora biti navedena v seznamu na koncu članka v prikazani obliki po vrsti za revije, zbornike in knjige:

[1] Wagner, A., Bajsić, I., Fajdiga, M. Measurement of the surface-temperature field in a fog lamp using resistance-based temperature detectors. Strojniški vestnik – Journal of Mechanical Engineering, February 2004, vol. 50, no. 2, p. 72-79.

[2] Boguslawski L. Influence of pressure fluctuations distribution on local heat transfer on flat surface impinged by turbulent free jet. Proceedings of International Thermal Science Seminar II, Bled, June 13.-16., 2004.

[3] Muhs, D. et al. Roloff/Matek mechanical elements, 16th ed. Wiesbaden: Vieweg Verlag, 2003. 791 p. Translation of: Roloff/Matek Maschinenelemente. (v nemščini) ISBN 3-528-07028-5

SPREJEM ČLANKOV IN AVTORSKE PRAVICE

Uredništvo Strojniškega vestnika si pridržuje pravico do odločanja o sprejemu članka za objavo, strokovno oceno recenzentov in morebitnem predlogu za krajšanje ali izpopolnitev ter terminološke korekture.

Avtor mora predložiti pisno izjavo, da je besedilo njegovo izvirno delo in ni bilo v dani obliki še nikjer objavljeno. Z objavo preidejo avtorske pravice na Strojniški vestnik. Pri morebitnih kasnejših objavah mora biti SV naveden kot vir.

Uredništvo prispelih materialov avtorjem ne vrača.

Neobjavljeni material v SV se ne shranjuje, niti ni razposlan drugam brez predhodnega dovoljenja avtorja.

Končno oblikovan članek bo poslan avtorju v PDF formatu. Avtorjeve skrbne korekcije smejo biti najmanjše potrebne. S tem avtor potrdi članek za objavo.

Plačilo objave

Avtorji vseh prispevkov morajo za objavo plačati prispevek v višini 180,00 EUR (za članek dolžine do 6 strani), 220,00 EUR (za članek dolžine do 10 strani) ter 20,00 EUR za vsako dodatno stran. Prispevek se zaračuna po sprejemu članka za objavo na seji Uredniškega odbora. Po objavi prejme avtor članka 25 separatov članka.

IRT3000

innovationr&dtechnology

Indispensible source of information for the professionals


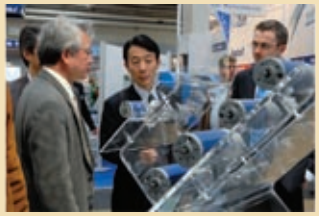


Guide through abundant information from

- metalworking industry
- automation and informatisation
- processing of non-metals
- advanced technologies

EVERY TWO MONTHS ON MORE THAN 140 PAGES

The IRT3000 magazine brings articles about technological and developmental achievements, presents interesting individuals and successful companies, innovative products, advanced projects… Bringing interviews with experts and fair reports, the magazine is an informative and educative media, offering the readers useful information for their profession. The magazine also presents important professional and general economy topics, needed by the companies from listed braches for efficient operations. It is also a forum for idea exchange between academia and industry, at the same time co-creating professional terminology and supporting the networking of science and entrepreneurship as a leading professional magazine.

www.irt3000.com

Contact us for the advertising price list!
e-mail: info@irt3000.si

9 770039 248001
ISSN 0039-2480